POLARIZATION OF ACTIVE GALACTIC NUCLEI AND GRAVITATIONAL LENSED OBJECTS

Luka Č. Popović

Astronomical Observatory, Belgrade, Serbia

Department of Astronomy, Faculty of Mathematics, University of Belgrade, Serbia

AGN&GL Conference

Vrnjacka Banja; July 20-24, 2026

4th AGN&GL conference

Polarization in AGNs

Antonucci & Miller 1985

Sy2=>hidden Sy1

(very important)

Mechanism of polarization

in AGNs

Smith et al. 2004, 2005;
Afanasiev et al. 2014, 2019

Goosmann & Gaskell 2007;
Savic et al. 2019, Marin et al. 2026, Hutsemékers et al. 2026, etc.

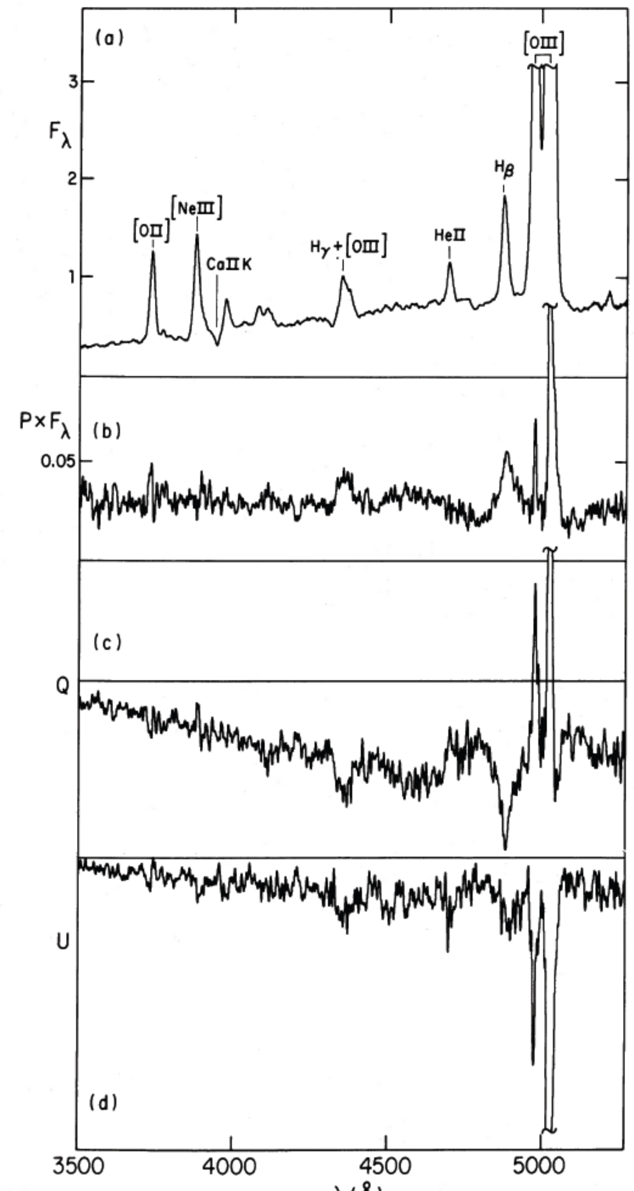

Possible sources of AGN polarization

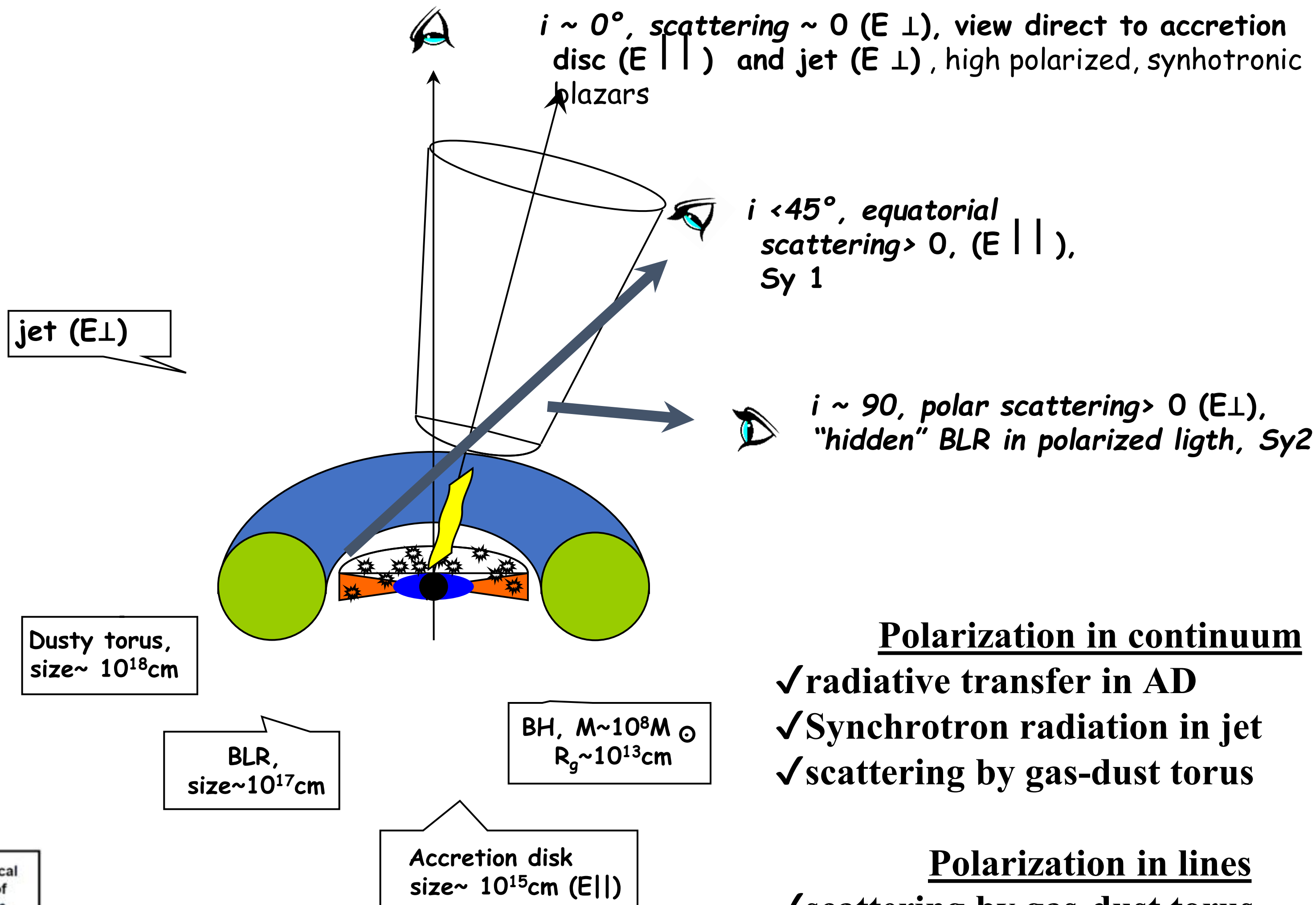

Polarization in continuum

- ✓radiative transfer in AD
- ✓Synchrotron radiation in jet
- ✓scattering by gas-dust torus

Polarization in lines

- ✓scattering by gas-dust torus
- ✓radiative transfer in the BLR

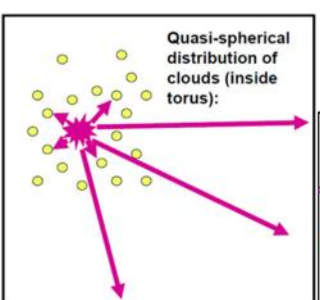

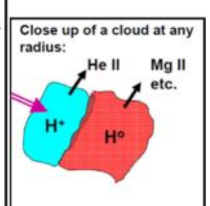

Popovic, Shablovinskaya, Savic, 2022, Astron. Nachr., 343, e21008

Optical emission of AGNs – different emission regions!

The structure can be more complex.
Emission in the optical is coming from different AGN regions + host galaxy

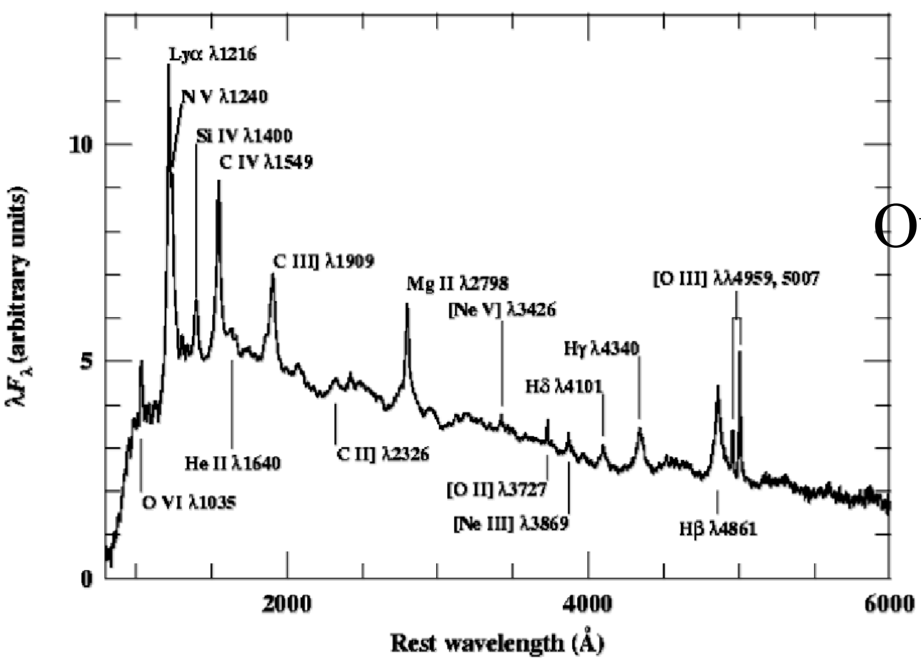

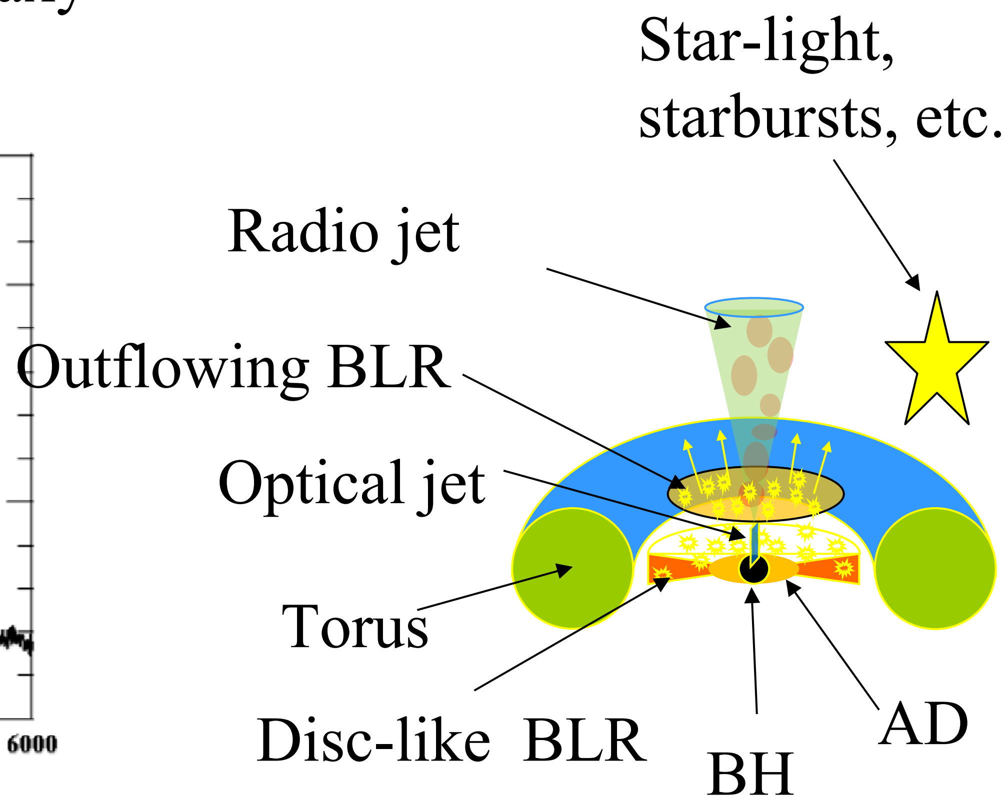

Optical emission of AGNs – different emission regions!

Type 1 or Type 2 AGNs? Very important:

- dust => rate of accretion

- dust distribution with respect to an observer

(Hoenig 2019) =>

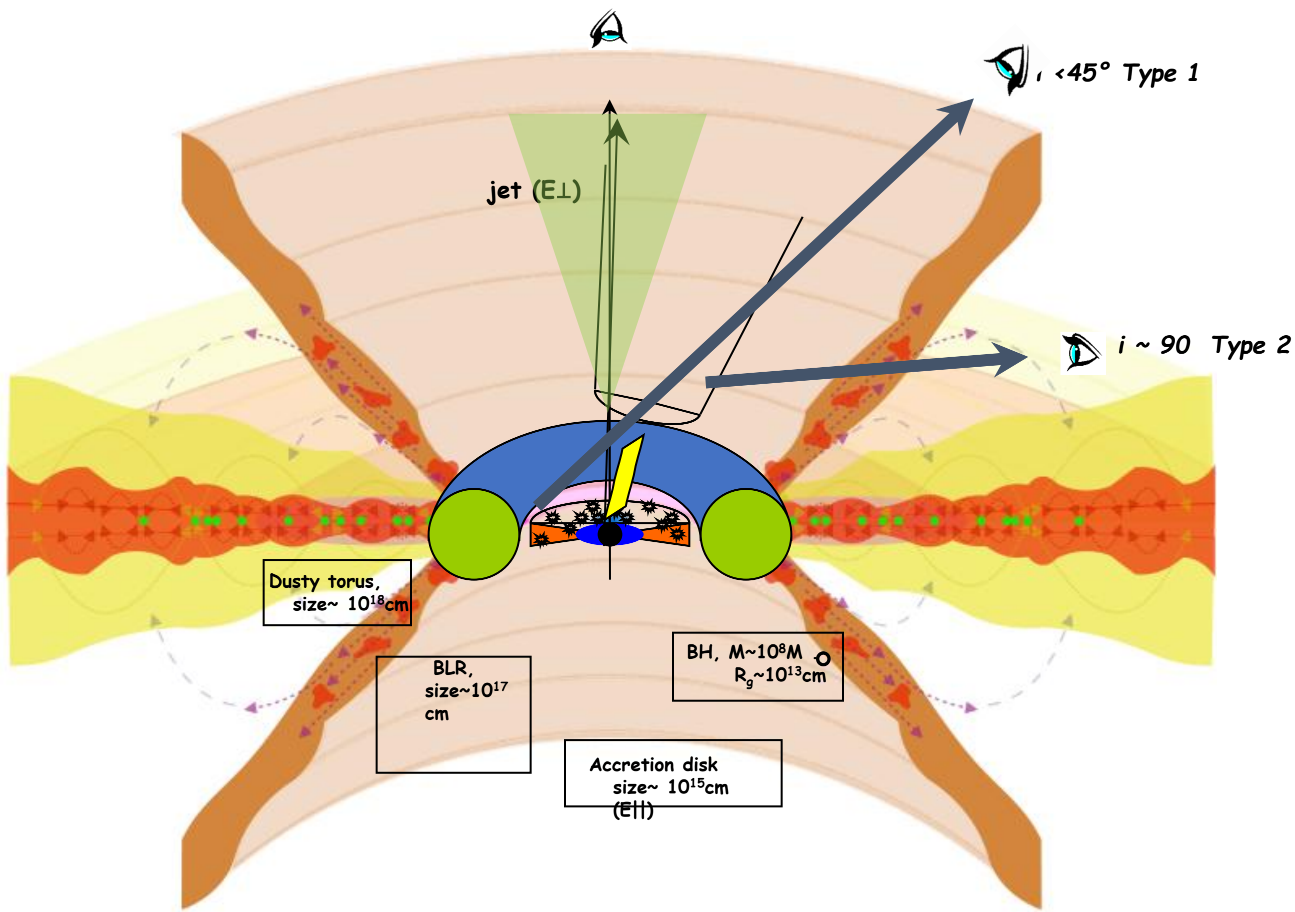

Polarization of AGNs - a simple (UNIFIED) model (e.g. NLS1, see Popovic et al. 2018)

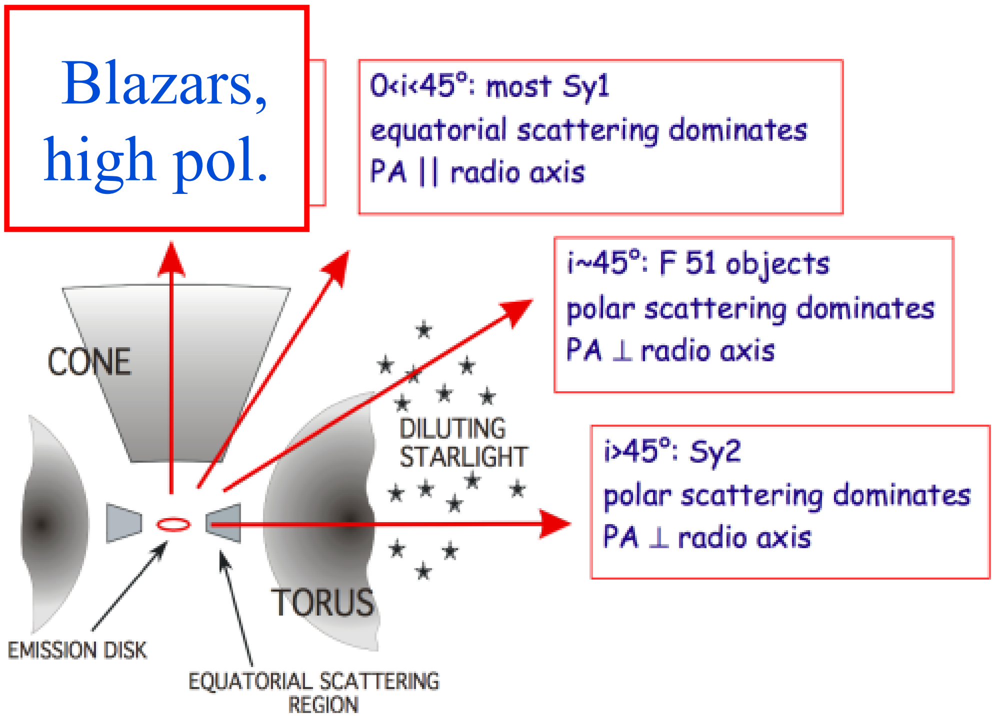

Relation between polarization class and orientation in the generic scattering geometry that broadly explains the optical polarization spectra of Seyfert galaxies Smith et al. (2004)

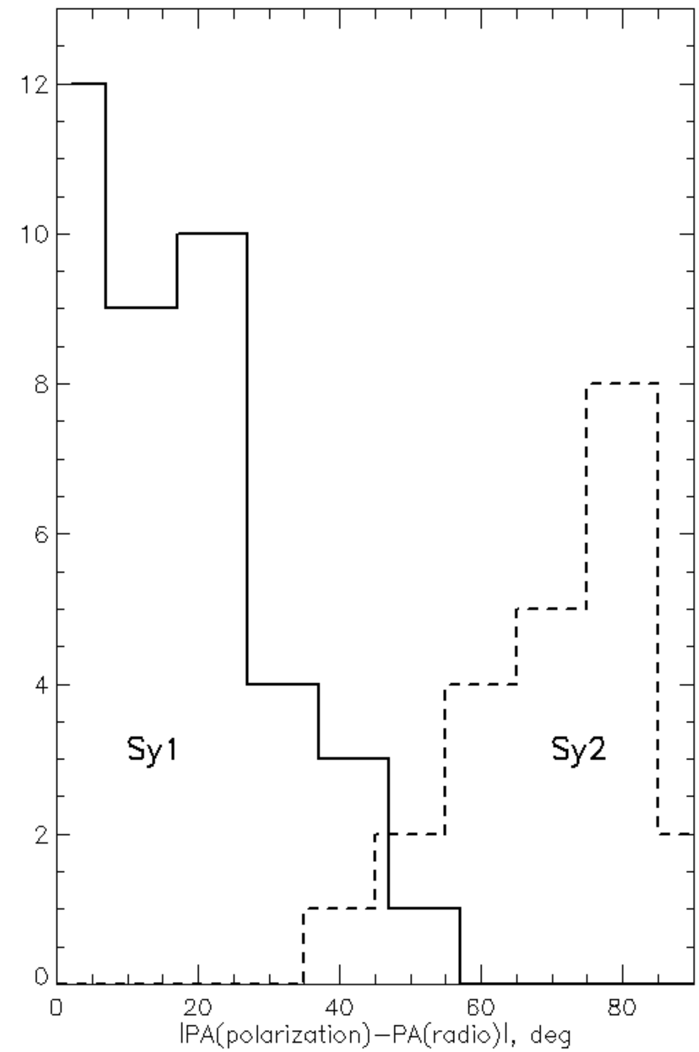

Orientation is important !

Broad line AGNs (Sy 1) – Smith et al. 2004, polar vs equatiorial pol.

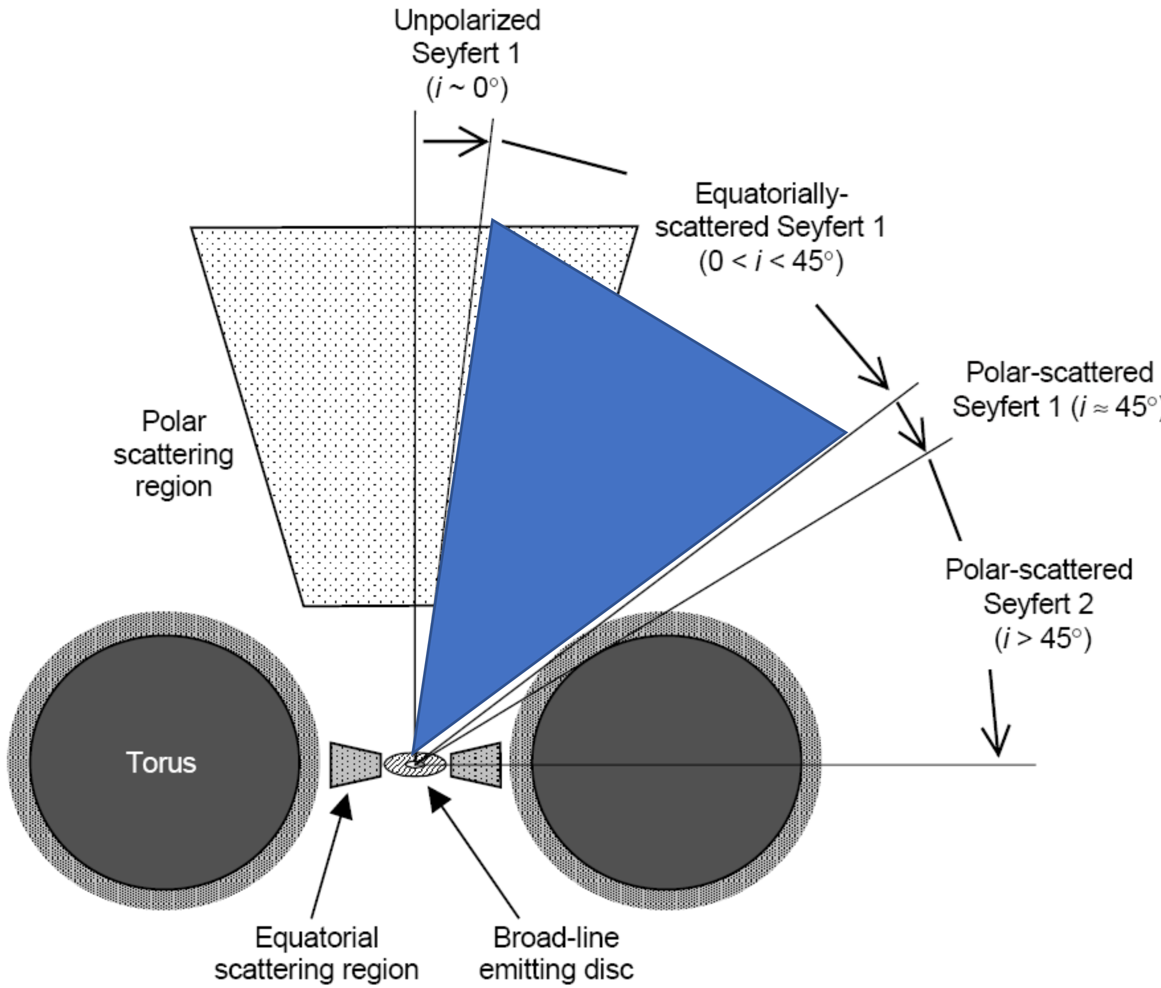

Type 1

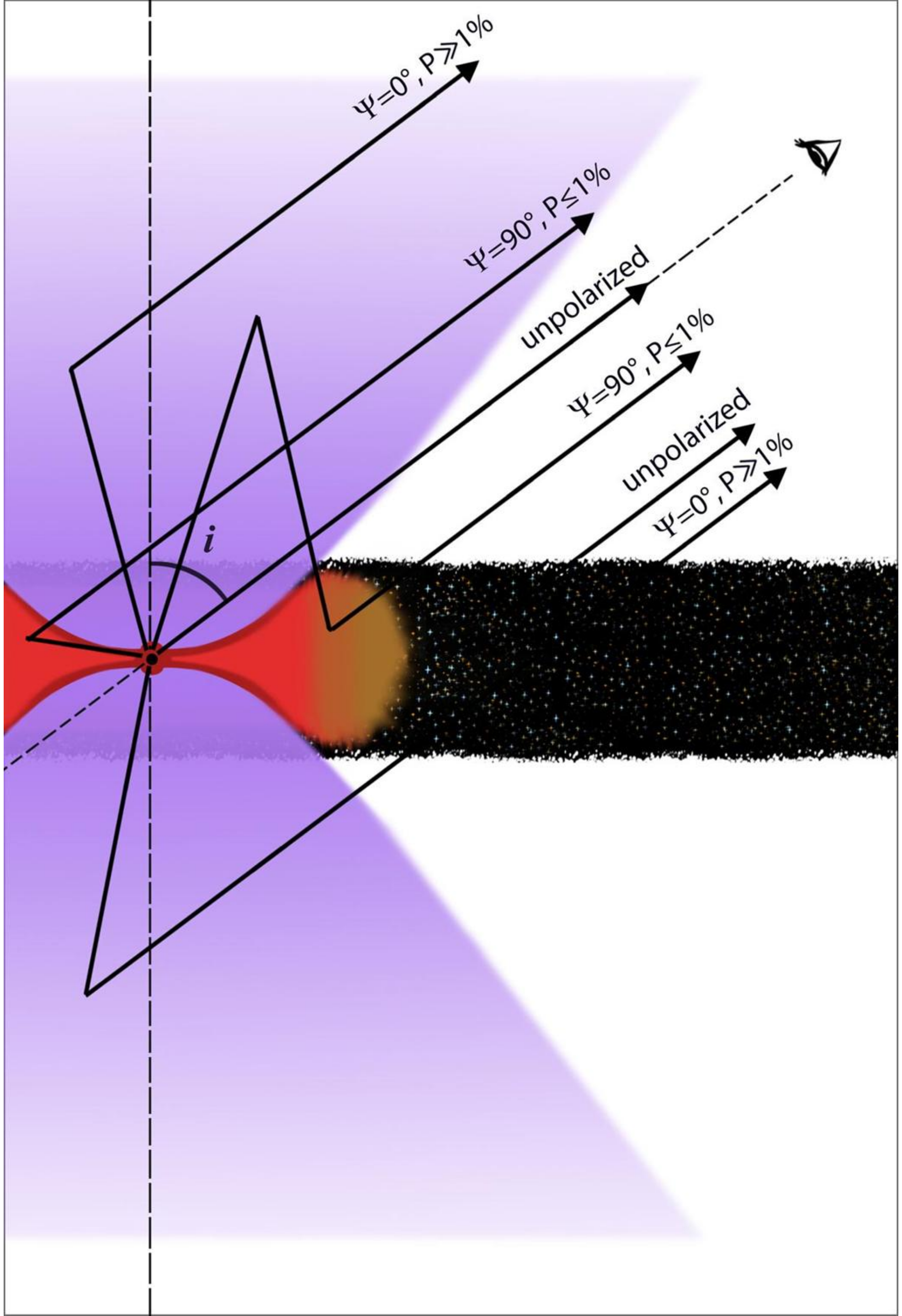

Illustration of the various paths taken by the photons for a typical type 1 viewing angle ($i \sim 45°$). The expected polarization signature of emission or reprocessing regions is indicated. The breaks in the light rays are due to scattering onto electrons or dust grains.

Marin & Hutsemékers 2020, A&A, 636A, 23

Equatorial polarization – Keplerian disk – polarization in the broad line

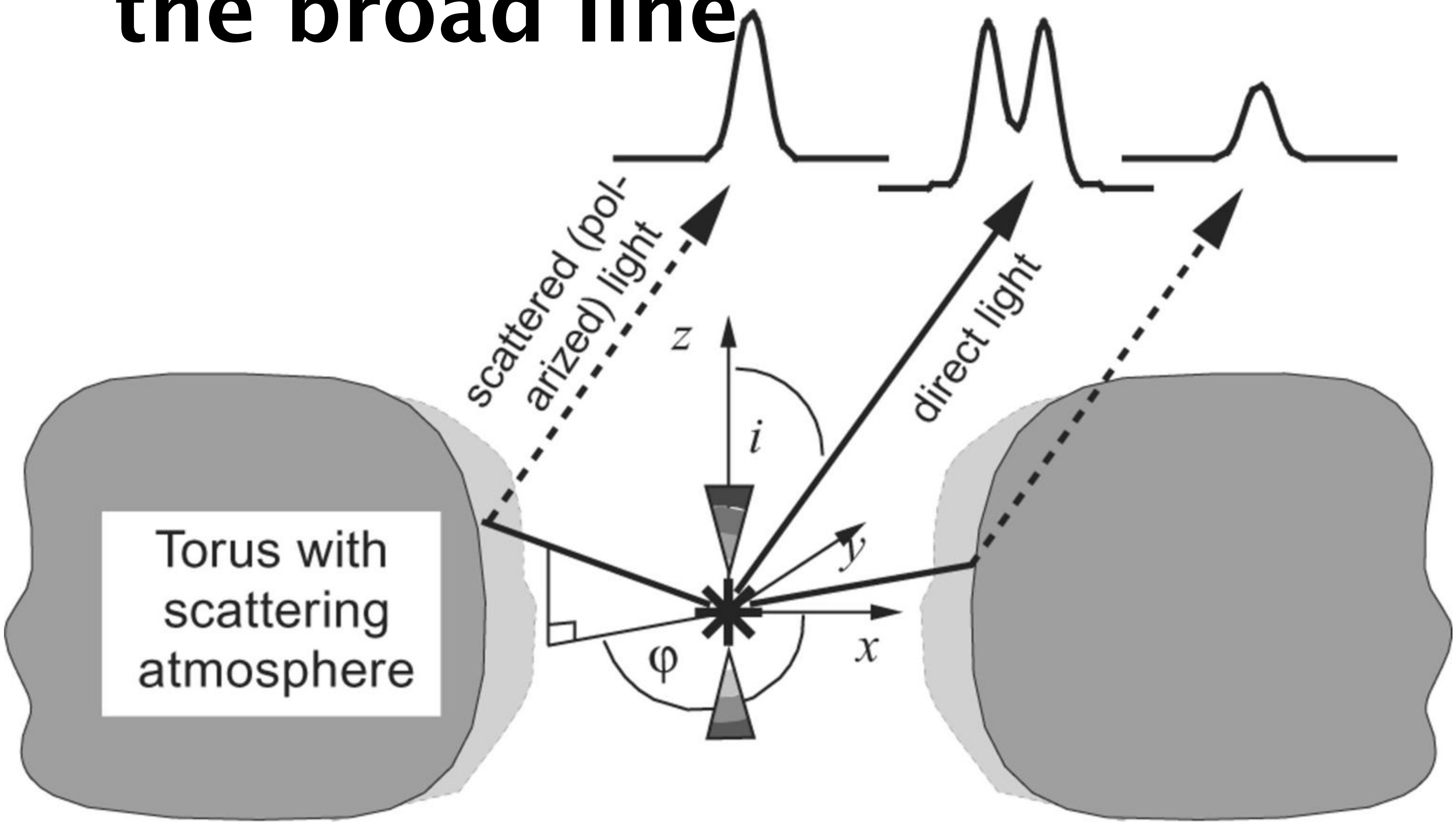

Sketch showing a possible far-field scattering geometry in which Hα photons from BLR clouds undergoing bi-polar outflow are scattered by dust or free electrons in the inner wall of a surrounding torus.

Corbett E A et al. MNRAS 2000;319:685-699

Resolving the BLR of AGNs using polarization!

- BLR characteristics
- measuring SMBH masses in AGNs

(Afanasiev & Popovic 2015)

Type 1 AGN: Equatorial polarization in broad lines (Smith et al. 2004,2005) - BLR gas motion – specific PA shapes!

Broad line P.A.

Broad line shapes

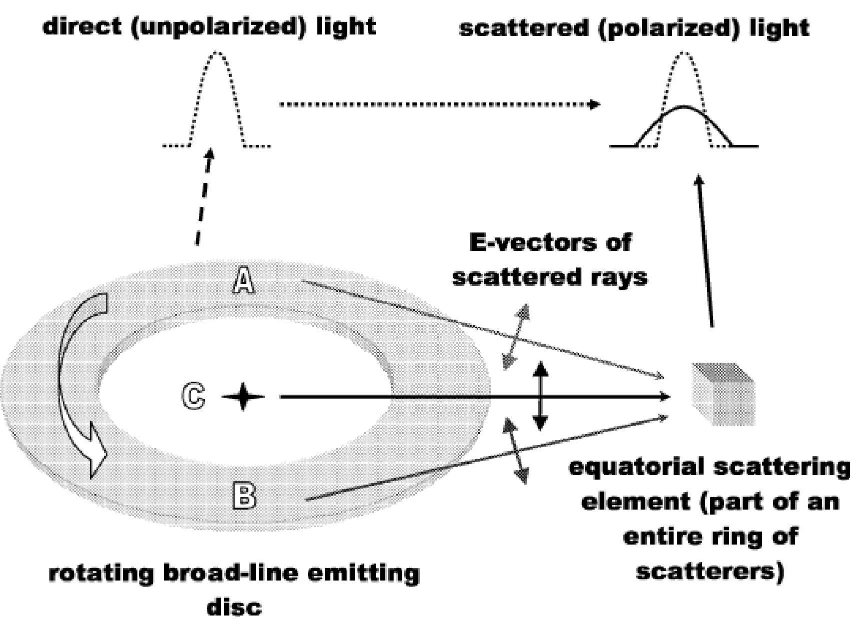

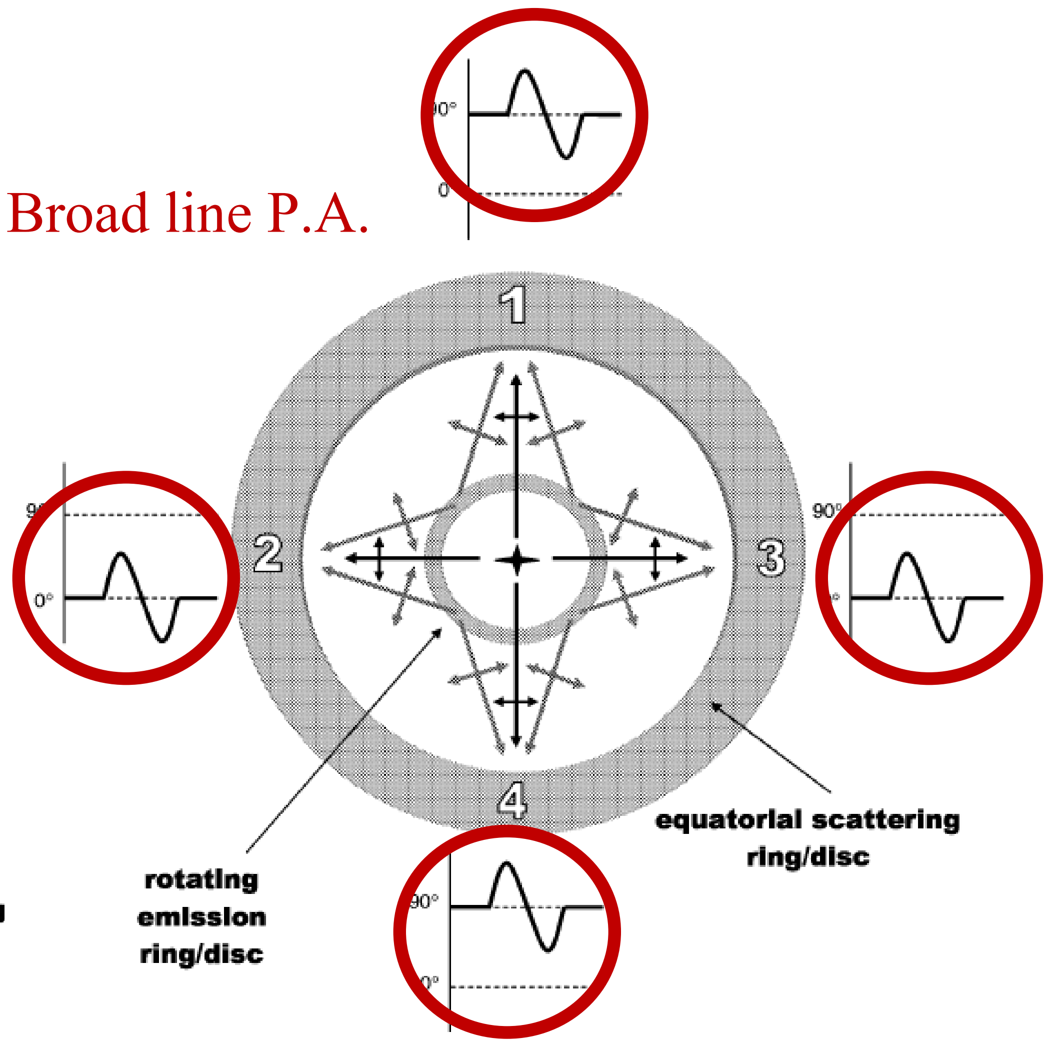

$$v_i = \sqrt{\frac{GM_{BH}}{R_i}}$$

$$R_i / Rsc = \tan(\varphi)$$

$$Rsc = const.$$

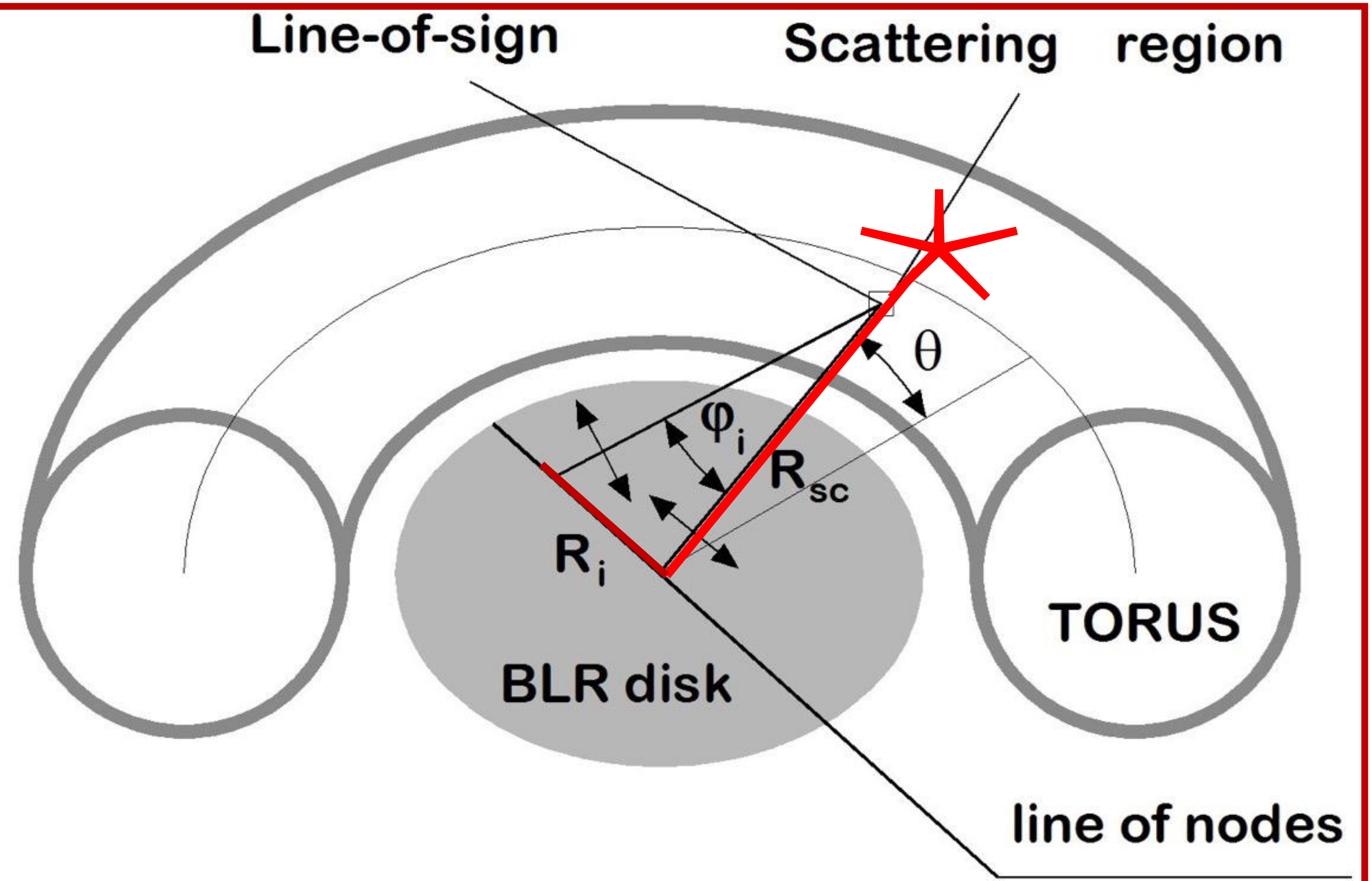

Polarization in the broad Hα (BLR). Equatorial scattering - idea

$$v_i = \sqrt{\frac{GM_{BH}}{R_{SC}\tan(\varphi_i)}},$$

$$\log(v_i) = a - b\log(\tan(\varphi_i)),$$

$$b = 0.5$$

$$a = f\left(\frac{M_{BH}}{R_{SC}}\right)$$

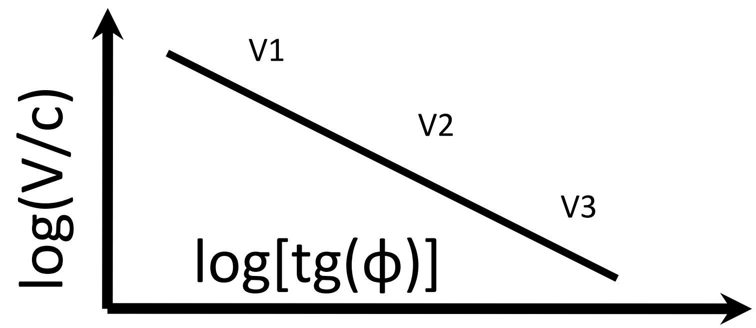

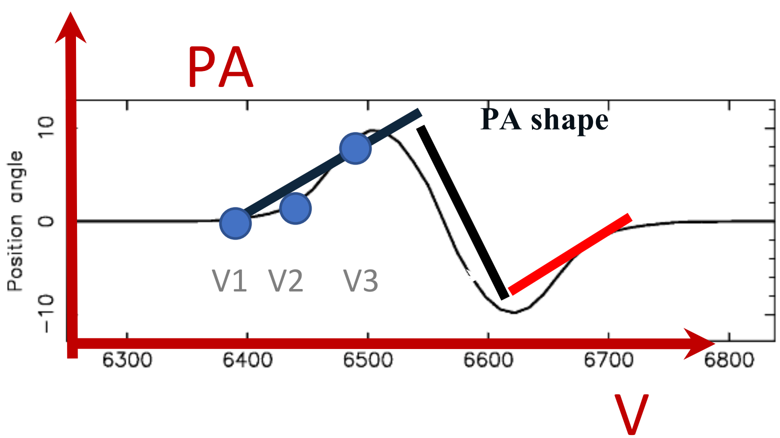

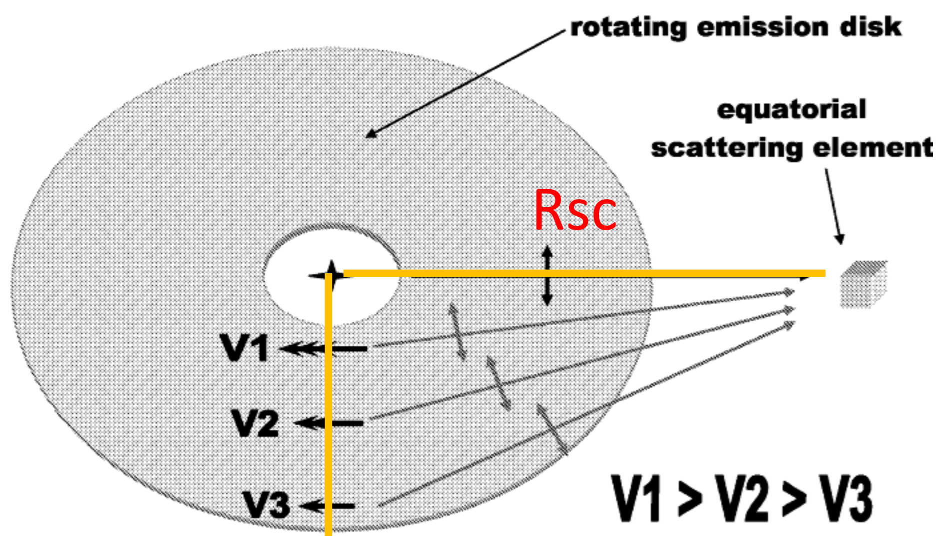

V vs. tan(ϕ) – direct evidence of Keplerian motion in the BLR of Mrk 6, Afanasiev et al. 2014

$$\boxed{\log\left(\frac{V_i}{c}\right) = a - b \cdot log(\tan(\varphi_i)),}$$

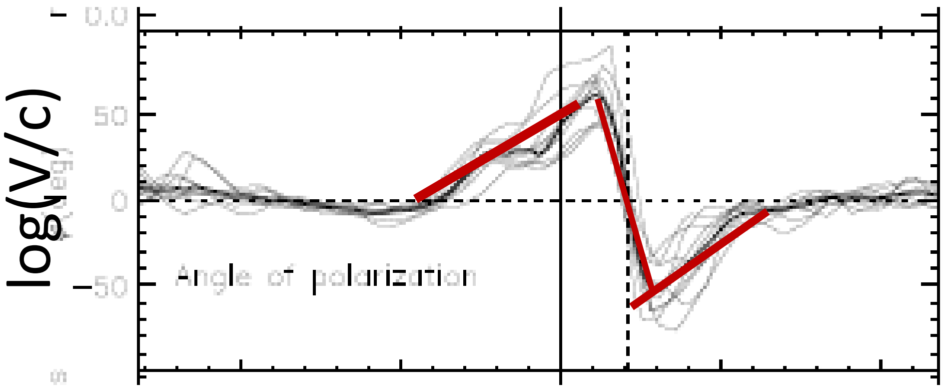

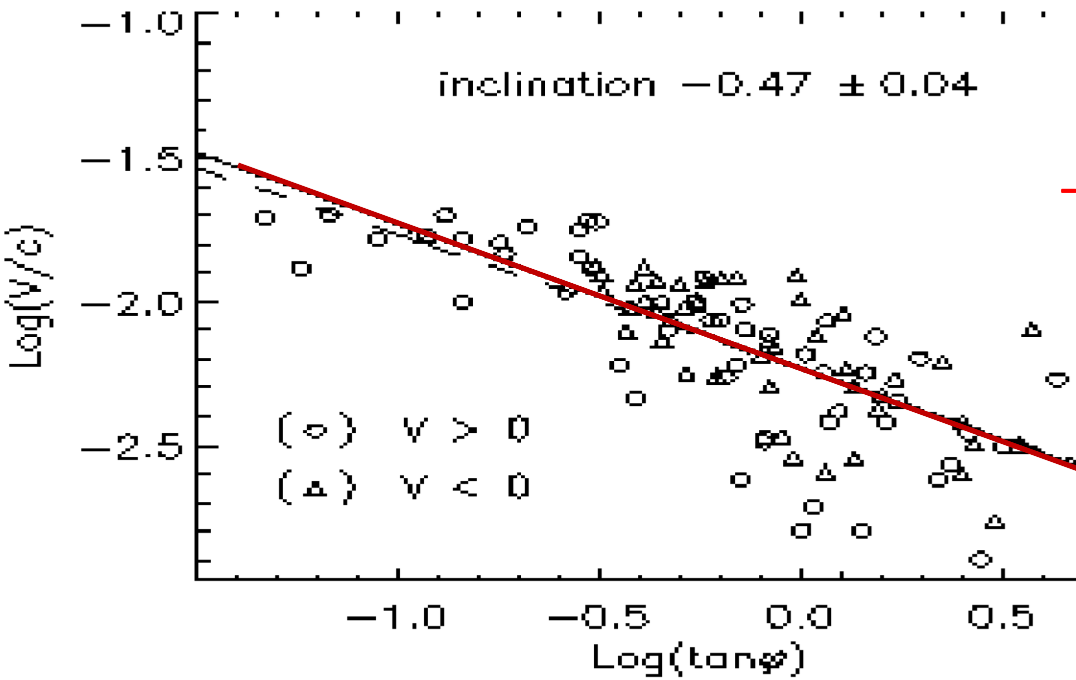

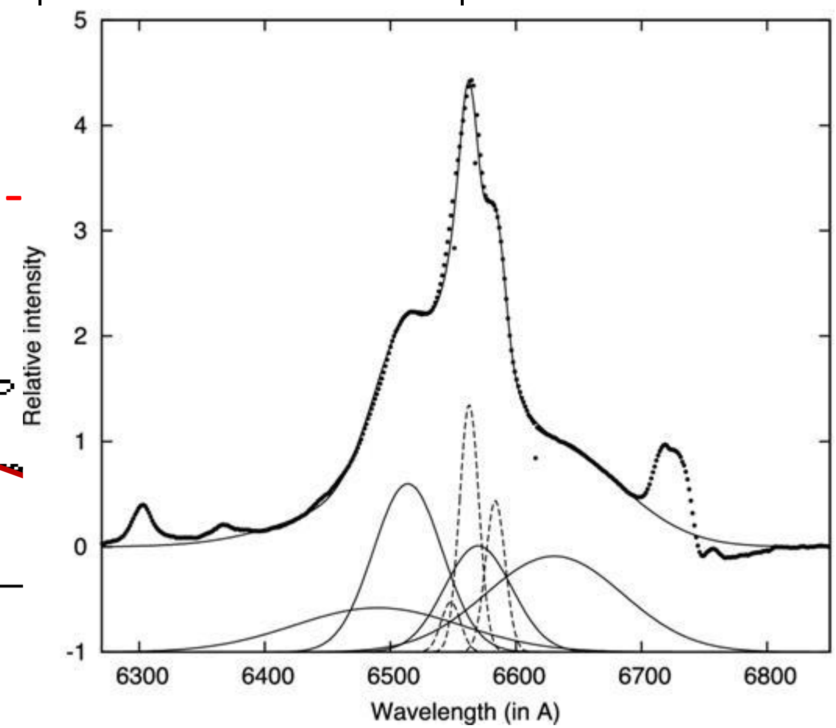

Observed P.A, Afanasiev & Popovic 2015

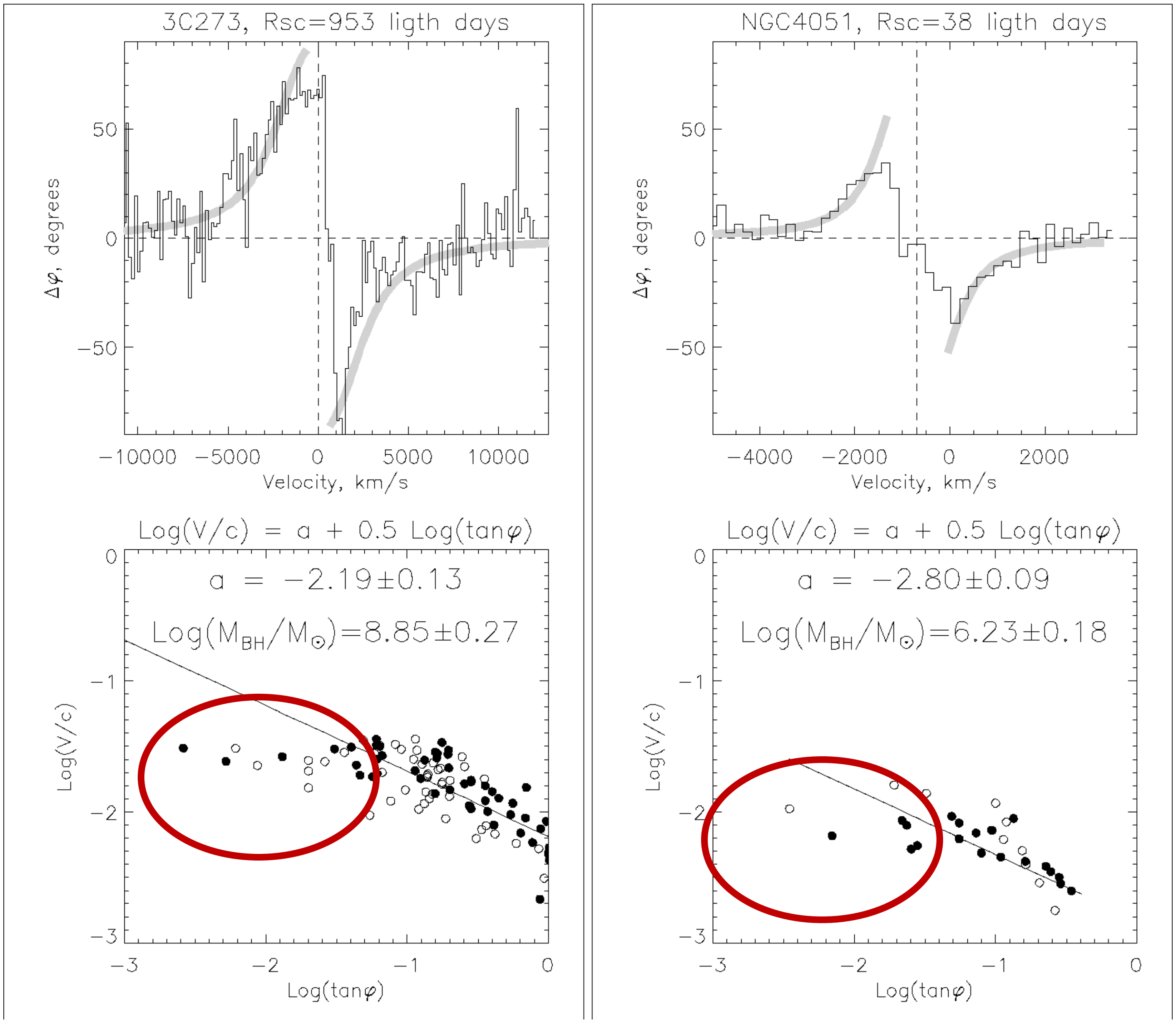

Theory vs. observations (equatorial scattering)

- Model with STOKES code (Goosmann & Gaskell 2007, Marin et al. 2012, etc)
- Savić et al. 2018, A&A, 614, 120

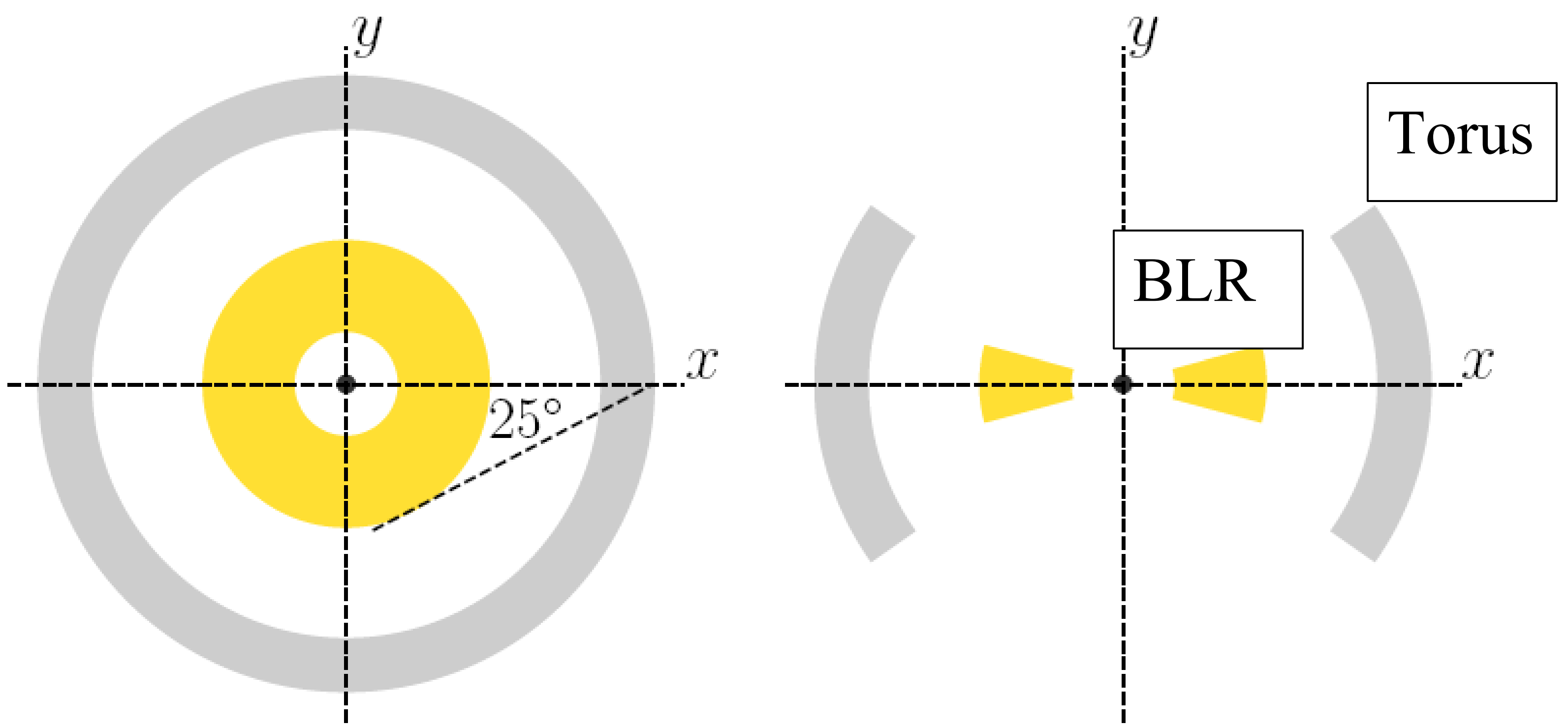

Theory vs. Observations
Savić et al. 2018

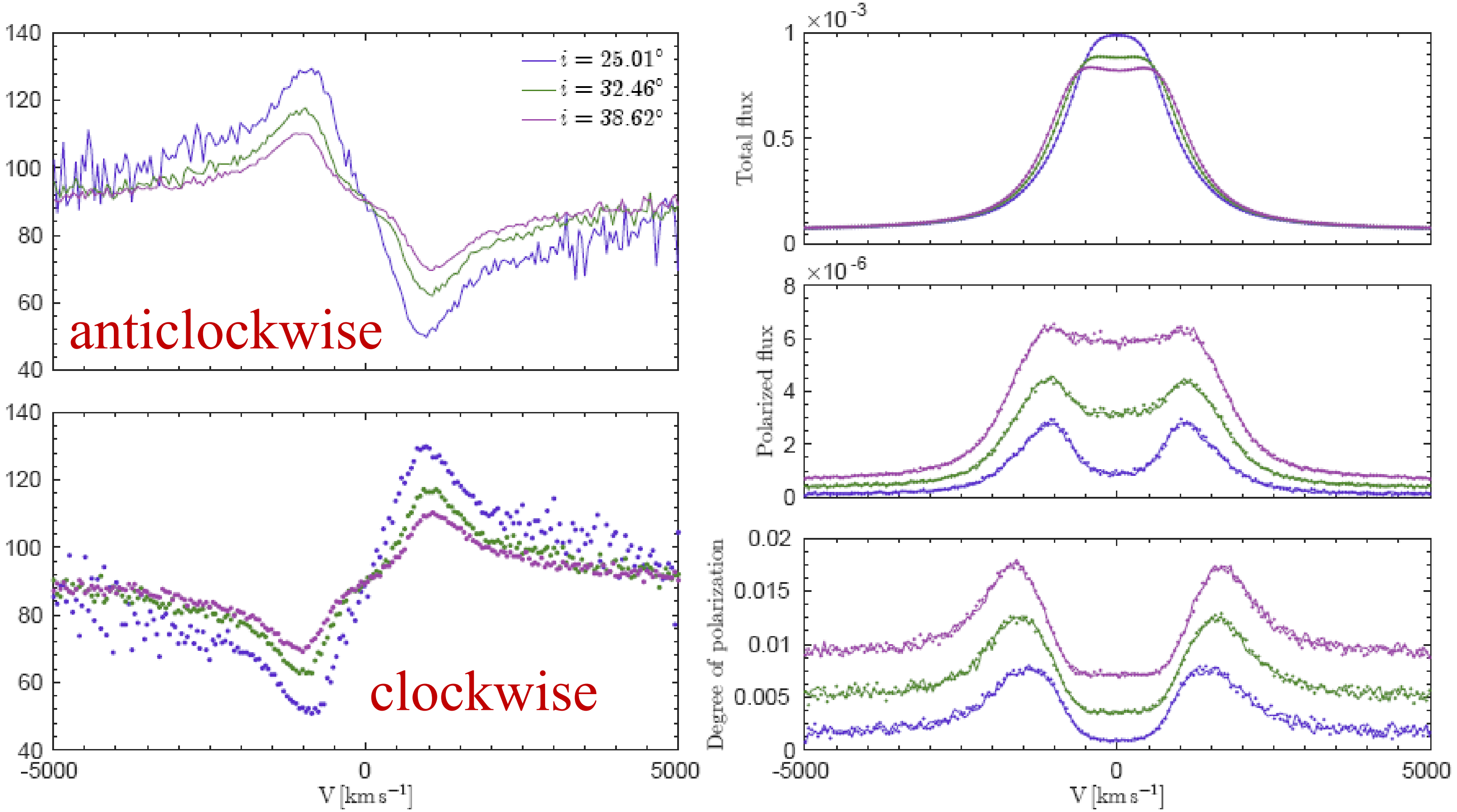

Pure Keplerian motion

Equatorial scattering for different BLR geometries (Jiang et al. 2021, MNRAS, 508, 79)

Blue wing   Line center   Red wing

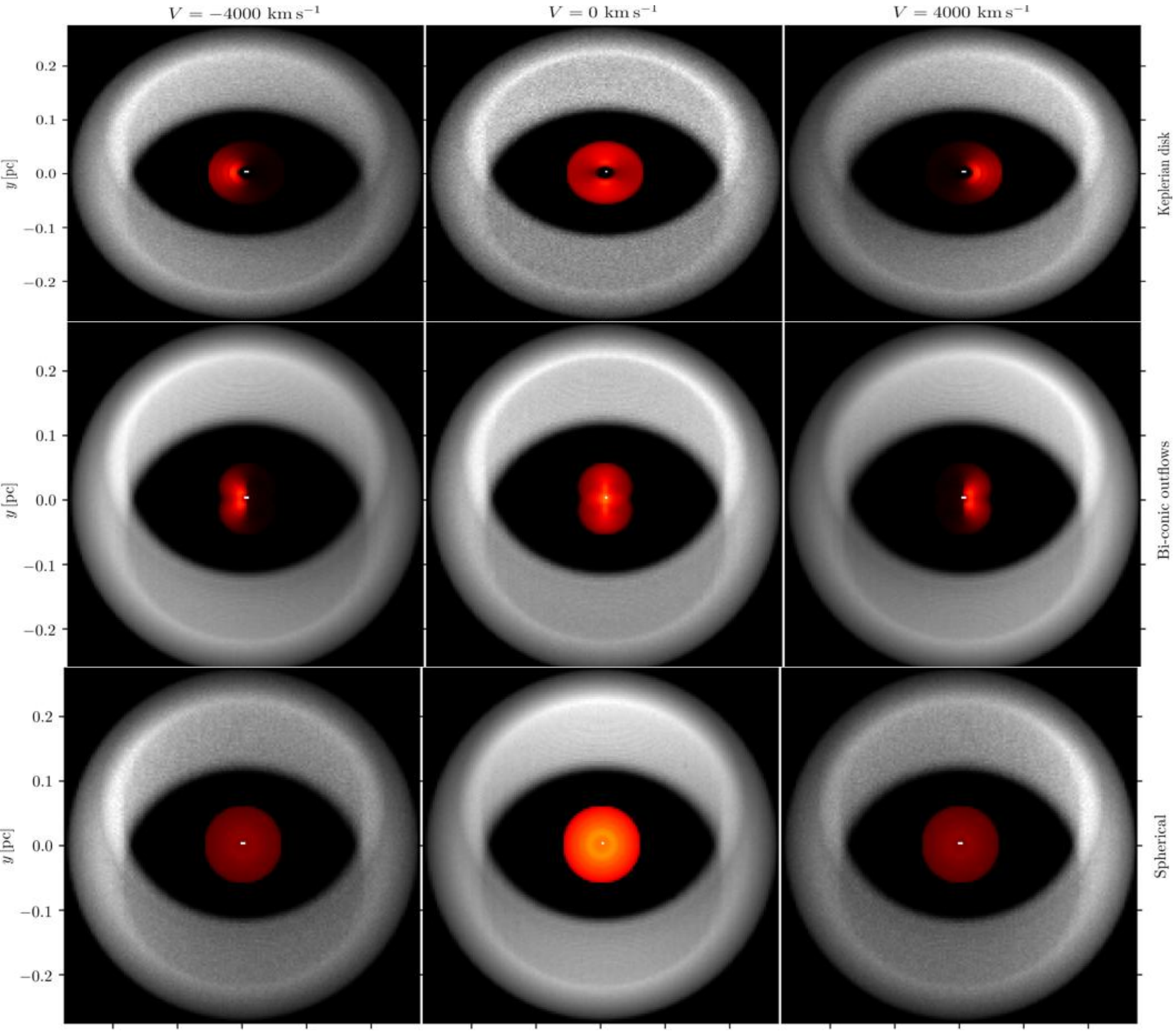

Disc - like

Otuflow

Spherical

Theory vs. Observations
Savić et al. 2018

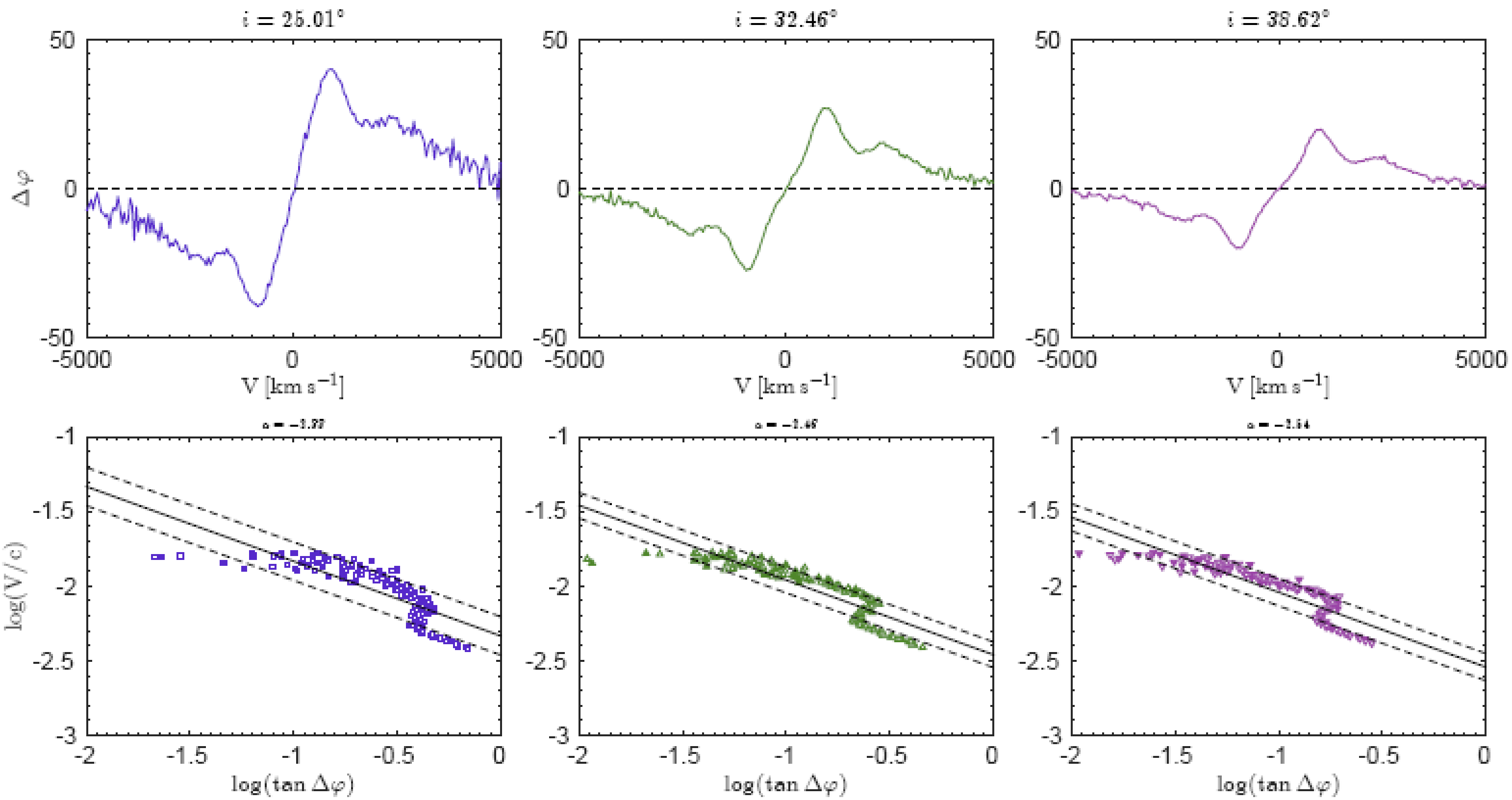

Keplerian motion + outflow -2000 km/s

Theory vs. Observations
Savic et al. 2018

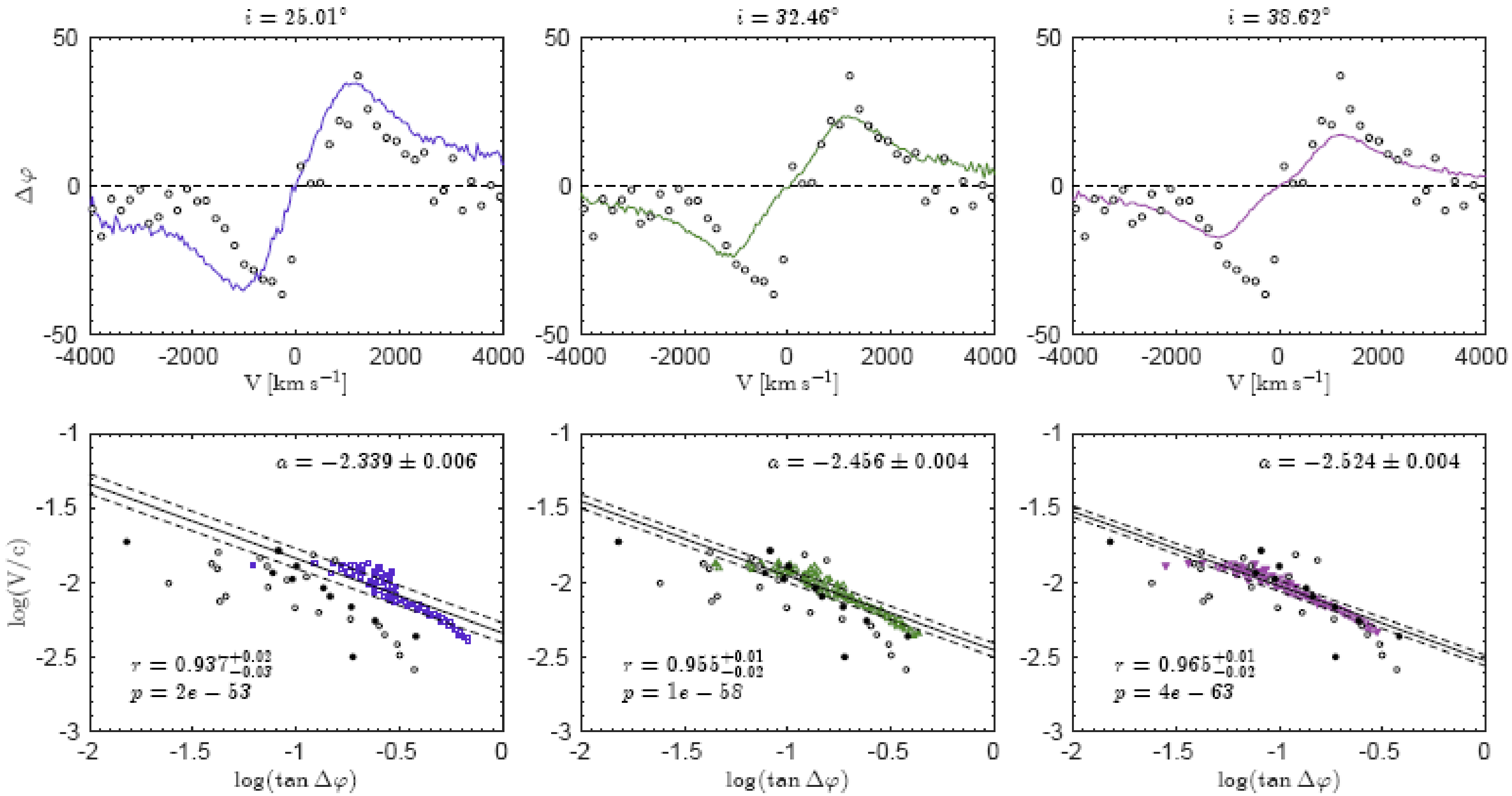

Fitted observations for NGC 4051

Black hole masses for 30 Type 1 AGNs

Afanasiev, Popović, Shapovalova 2019, MNRAS, 482, 4985

Observations with 6m telescope SAO RAS

- 6-m telescope + SCORPIO, spectral coverage 4000-8000 AA
- Different type analyzer – Savart plate, Single and Double Wollaston prisms
- Spectral resolution 5-40AA,
- Polarization measurement accuracy ~ 0.1-0.3%

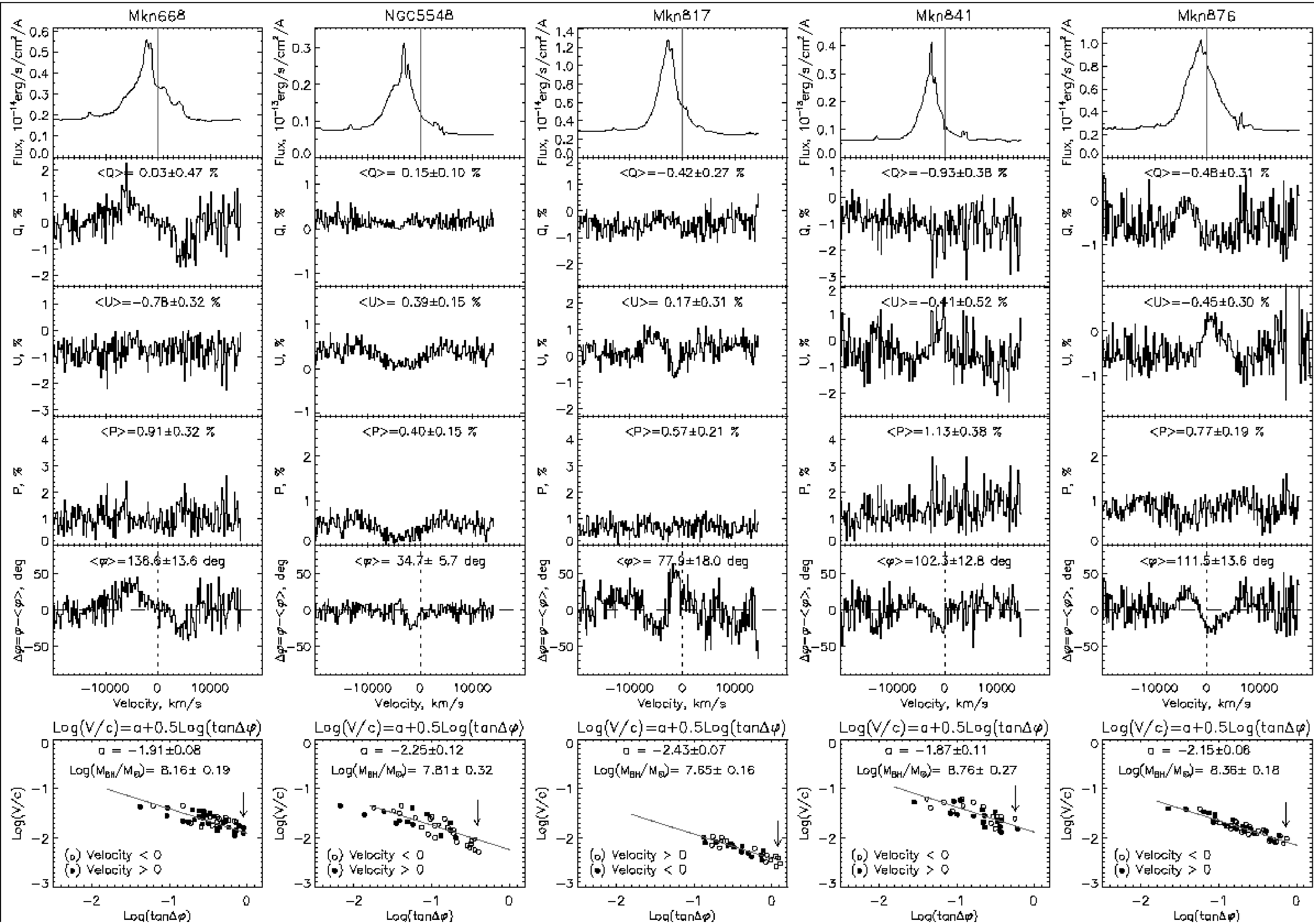

Mkn668
NGC5548
Mkn817
Mkn841
Mkn876
<Q>= 0.03±0.47 %
<Q>= 0.15±0.10 %
<Q>=−0.42±0.27 %
<Q>=−0.93±0.38 %
<Q>=−0.48±0.31 %
<U>=−0.78±0.32 %
<U>= 0.39±0.15 %
<U>= 0.17±0.31 %
<U>=−0.41±0.52 %
<U>=−0.45±0.30 %
<P>=0.91±0.32 %
<P>=0.40±0.15 %
<P>=0.57±0.21 %
<P>=1.13±0.38 %
<P>=0.77±0.19 %
<φ>=136.6±13.6 deg
<φ>= 34.7± 5.7 deg
<φ>= 77.9±18.0 deg
<φ>=102.3±12.8 deg
<φ>=111.5±13.6 deg
Velocity, km/s
Log(V/c)=a+0.5Log(tanΔφ)
a = −1.91±0.08
Log(M_BH/M_⊙)= 8.16± 0.19
a = −2.25±0.12
Log(M_BH/M_⊙)= 7.81± 0.32
a = −2.43±0.07
Log(M_BH/M_⊙)= 7.65± 0.16
a = −1.87±0.11
Log(M_BH/M_⊙)= 8.76± 0.27
a = −2.15±0.06
Log(M_BH/M_⊙)= 8.36± 0.18
(o) Velocity < 0
(•) Velocity > 0
(o) Velocity > 0
(•) Velocity < 0
Log(tanΔφ)
Log(V/c)

Black hole masses for 30 Type 1 AGNs

Afanasiev et al. 2019

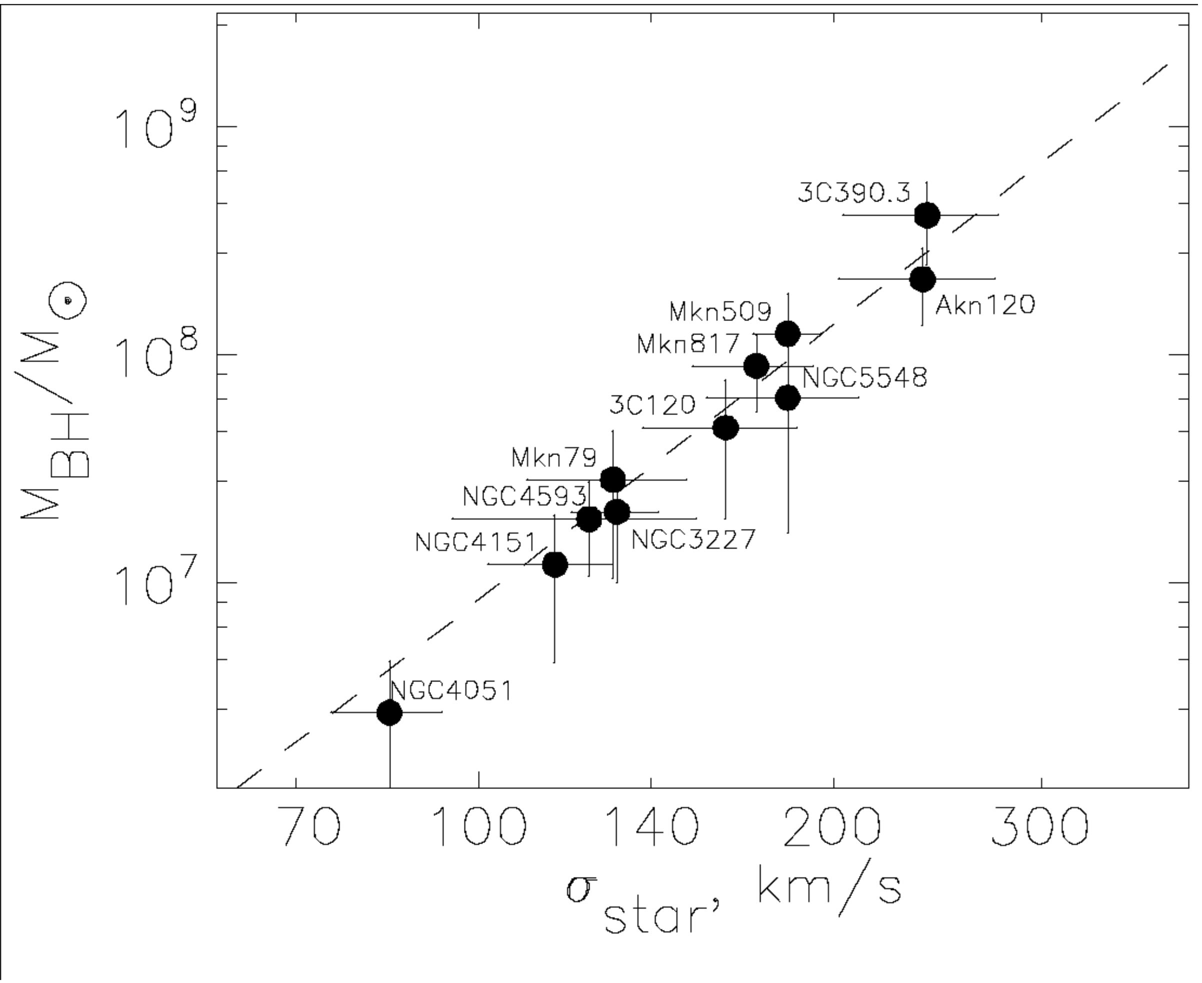

Our measurements of BH masses as a function of host galaxy bulge stellar velocity dispersion *(taken from Onken et* al. 2004). The dashed line shows the dependence of M-σ taken from Tremaine et al (2002).

BLR inclination for 30 Type 1 AGNs

Afanasiev et al. 2019

$$f = \frac{1}{\sin^2 i}$$

$$M_{BH} = f\frac{R_{BLR}v^2}{G} = f * VP$$

$$\frac{1}{f} = \frac{VP}{M_{BH}}$$

Our measurements of SMBH masses do not depend on inclination (see Afanasiev & Popovic 2015), Keplerian motion=>assumption that f depends only from BLR inclinatin!

BLR inclination for 30 Type 1 AGNs

Afanasiev et al. 2019

$$f \approx \frac{1}{\sin^2 i}$$

$$M_{BH} = f\frac{R_{BLR}v^2}{G} = f * VP$$

$$\frac{1}{f} = \frac{VP}{M_{BH}} \approx \sin^2 i$$

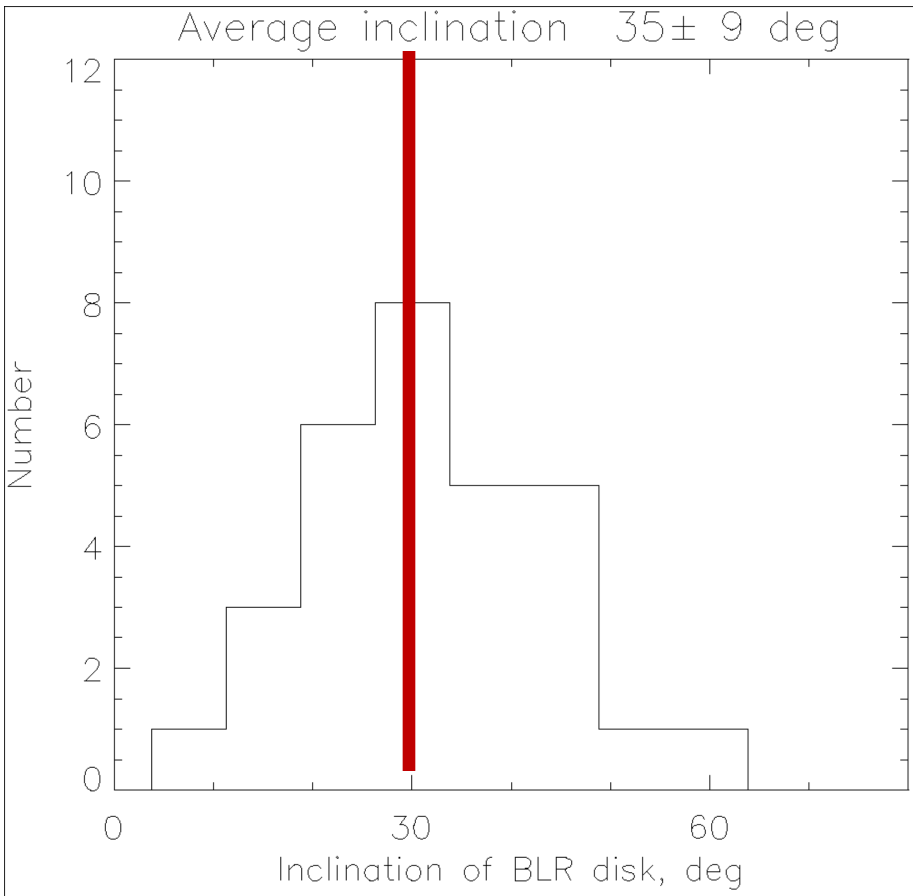

Our measurements of SMBH masses do not depend on inclination (see Afanasiev & Popovic 2015), Keplerian motion=>assumption that f depends only from BLR inclinatin!

Dimensions of the BLR

$$R_{max} = R_{sc} \tan(\varphi_{max})$$

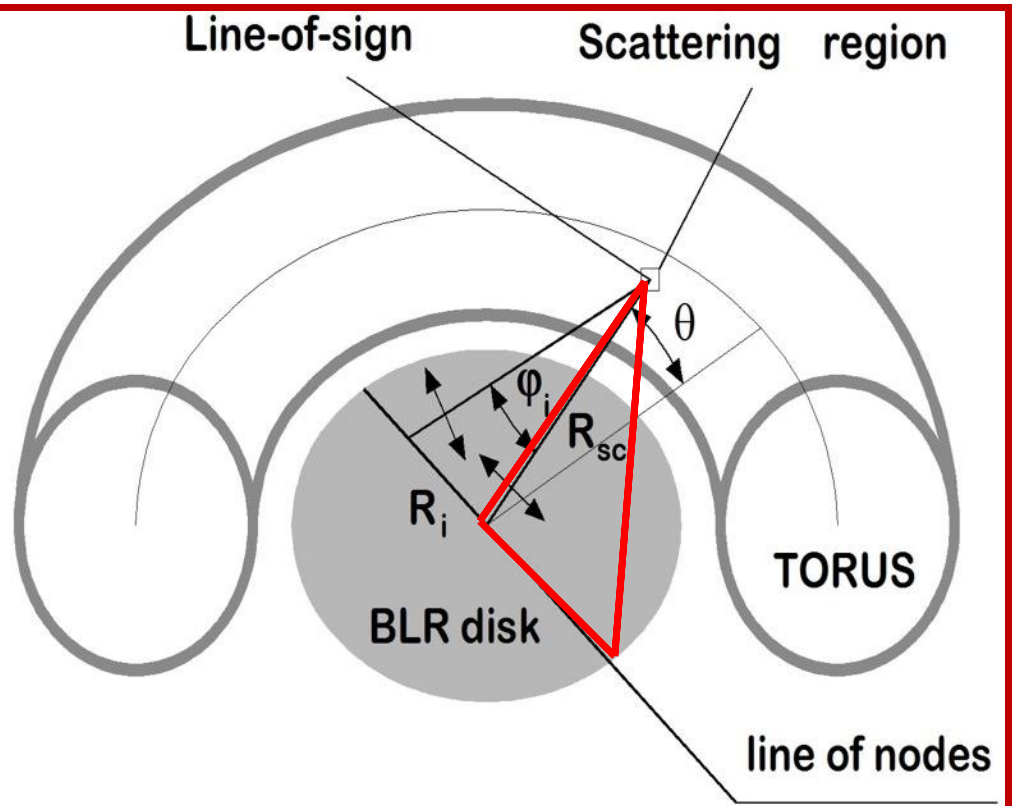

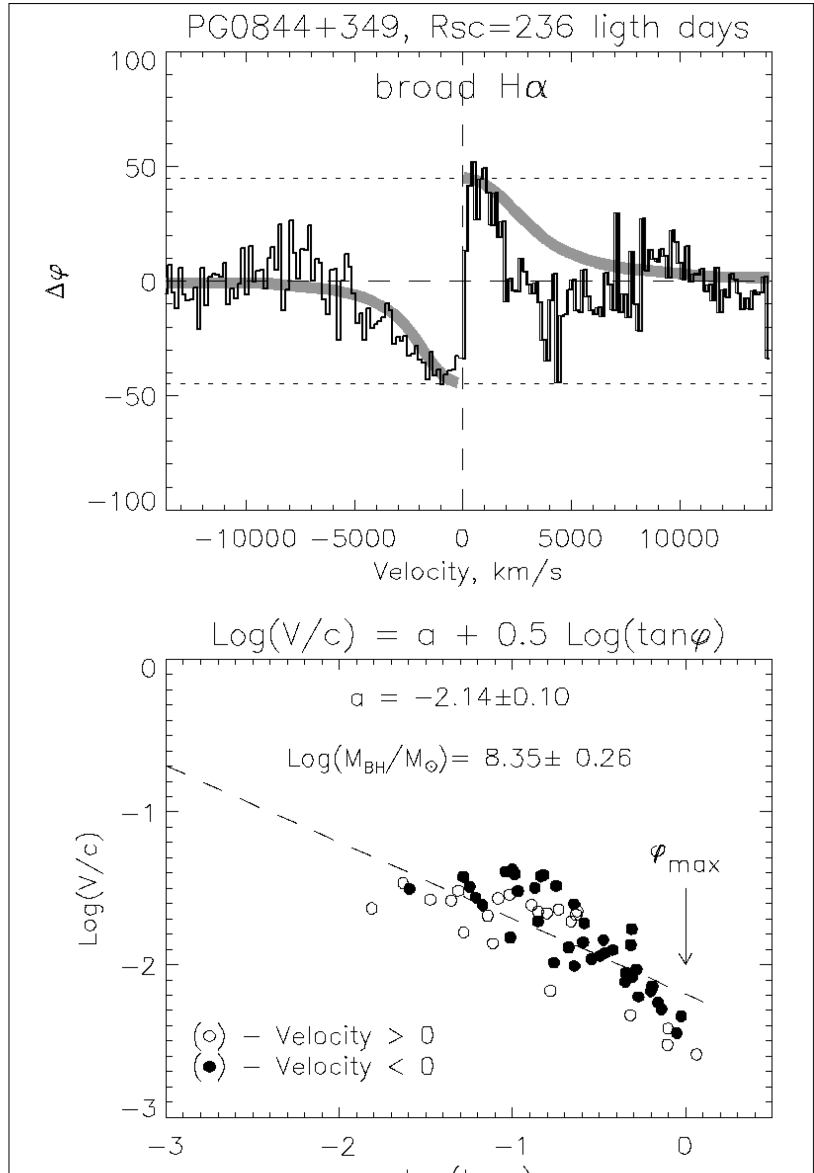

Dimensions of the BLR Afanasiev et el. 2019

The maximal (*Rmax*) *vs* *photometric BLR* (*R_{BLR}*) *r*adius. The solid line represents the best fit

R_{BLR} = (0.31 ± 0.17)Rmax

Relation between Rsc and R_{BLR}

Rsc = (1.72 ± 0.48) R_{BLR}

.

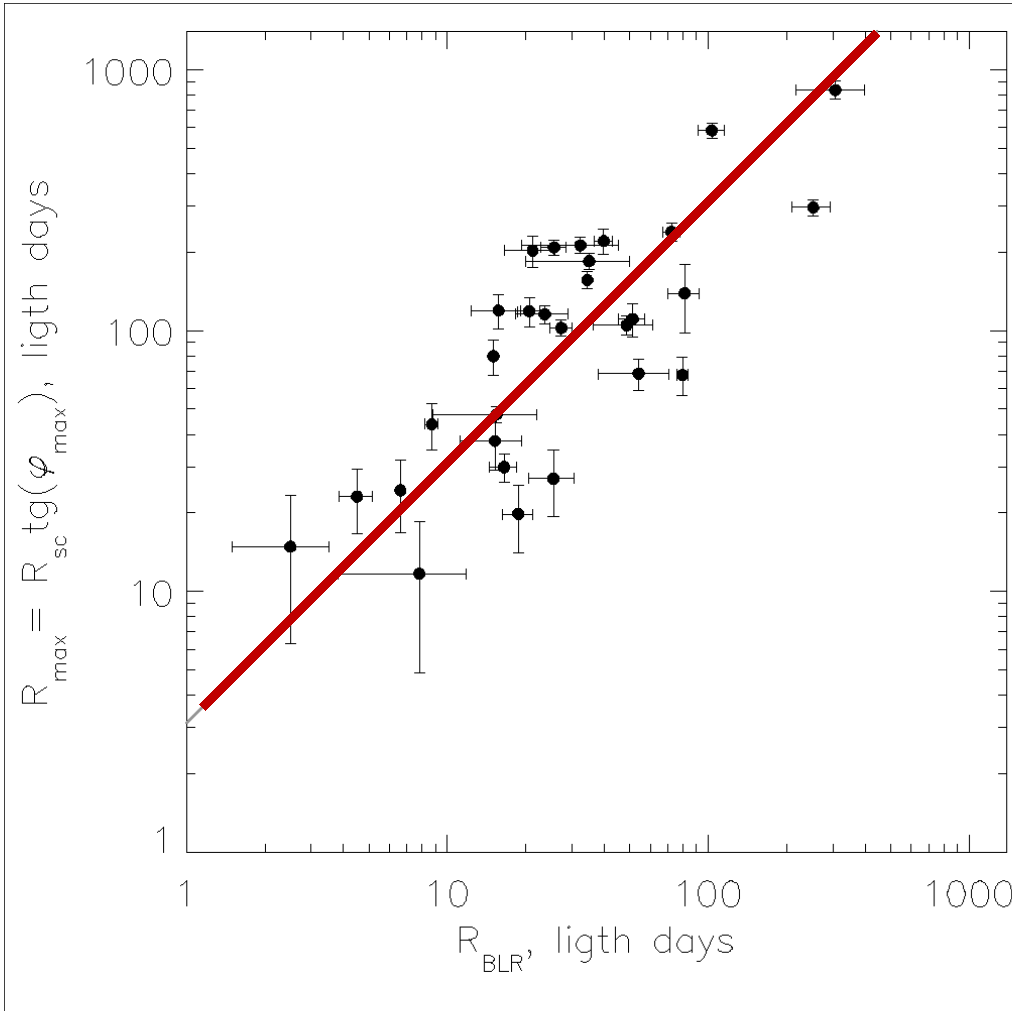

Shablovinskaya *et al* 2020 *ApJ* **892** 118

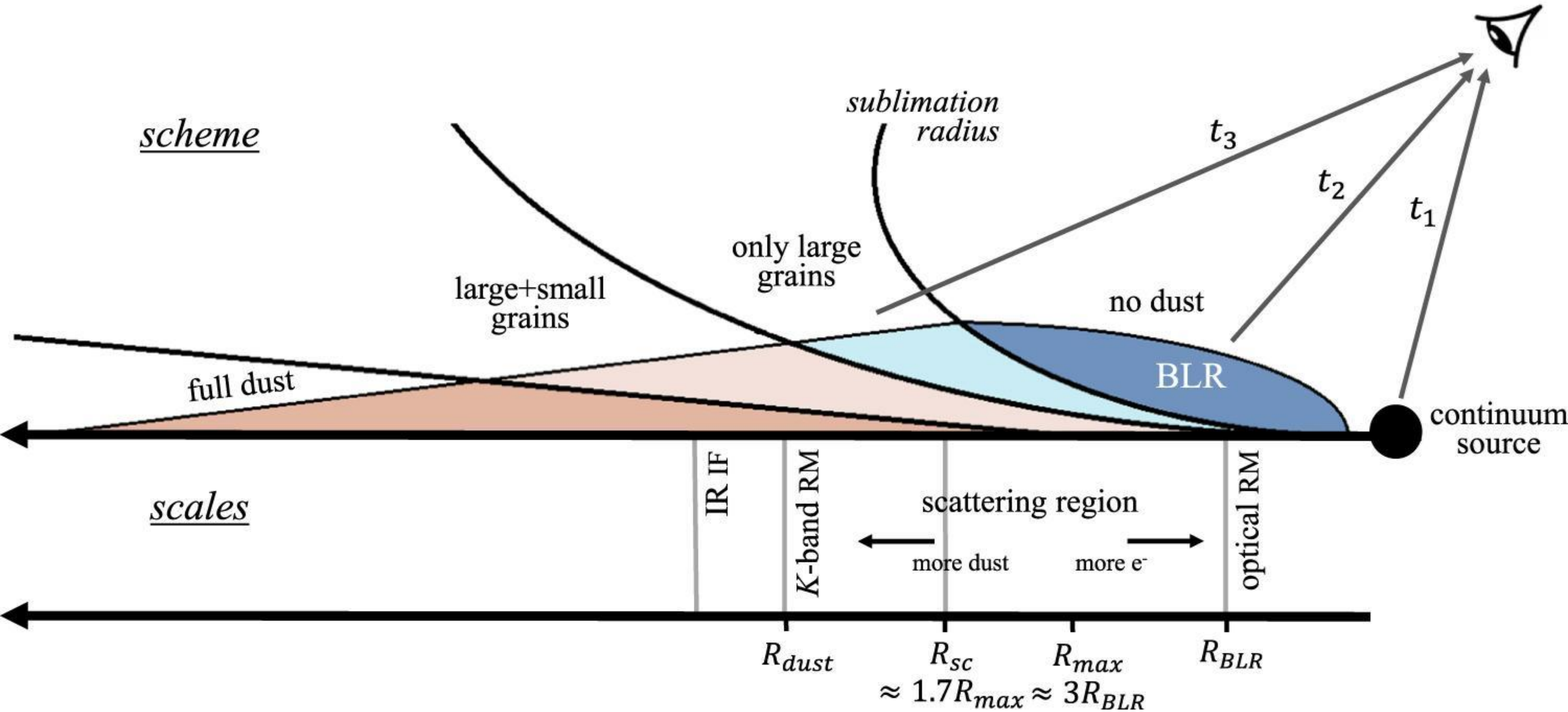

Dust sublimation region in AGN => reverberation in broad line polarization

2 *Shablovinskaya, Afanasiev, Popović*

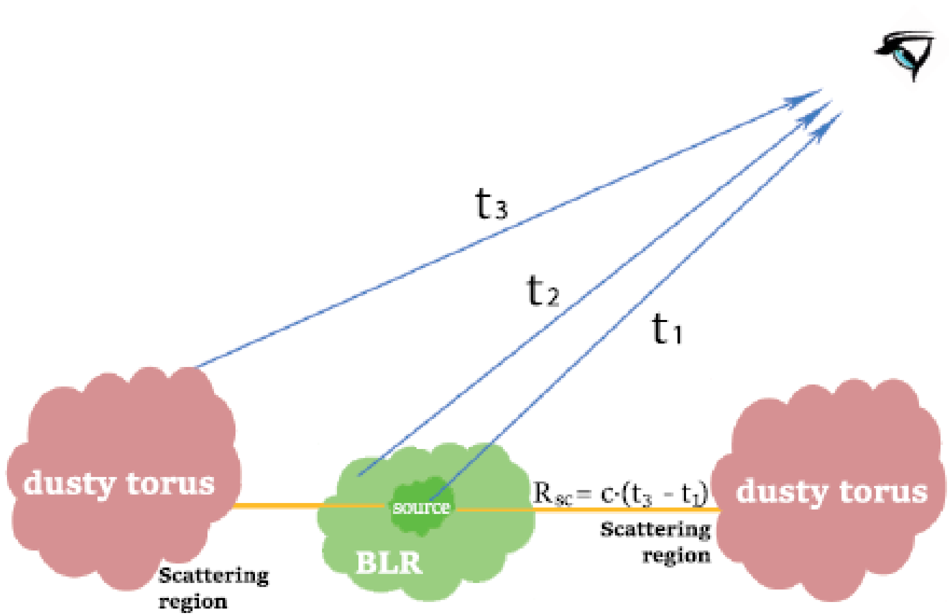

Figure 1. The scheme of the continuum emitting and line scattering region in AGN.

$$R_{\mathrm{BLR}} = c\Delta\tau_{12} = c \cdot (t_2 - t_1)$$

$$R_{\mathrm{SC}} = c\Delta\tau_{13} = c \cdot (t_3 - t_1)$$

Shablovinskaya et al. 2020

What is with other lines, as e.g. Mg II BLR – seems to be complex (Popovic et al. 2020, MNRAS, 484, 3180)

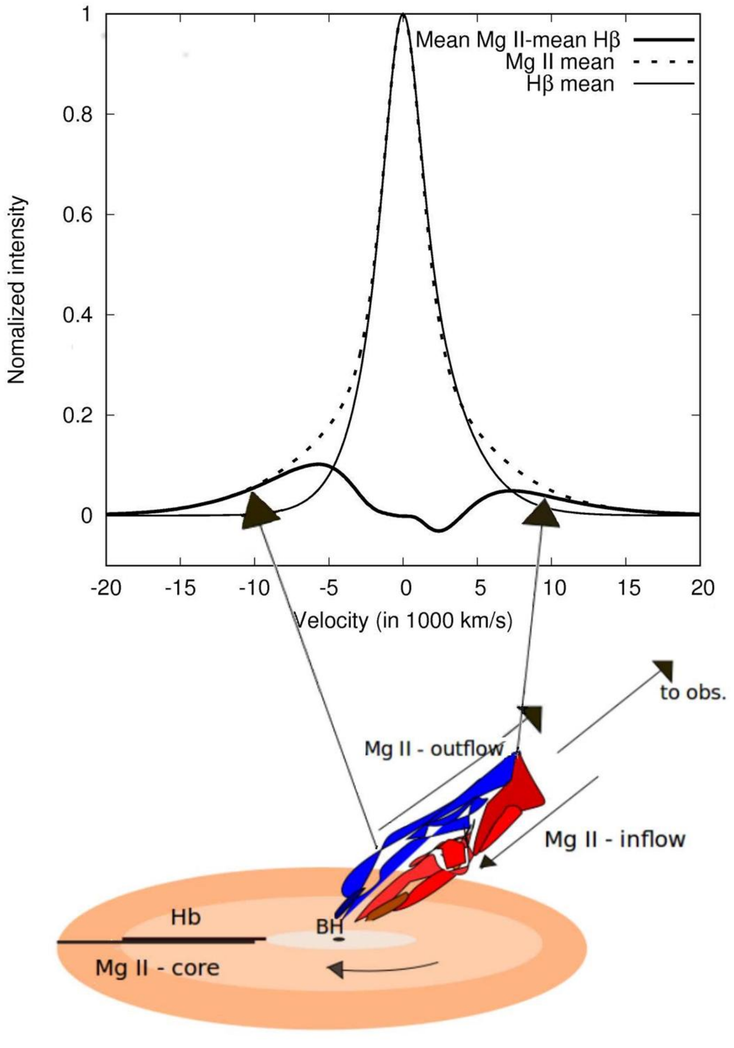

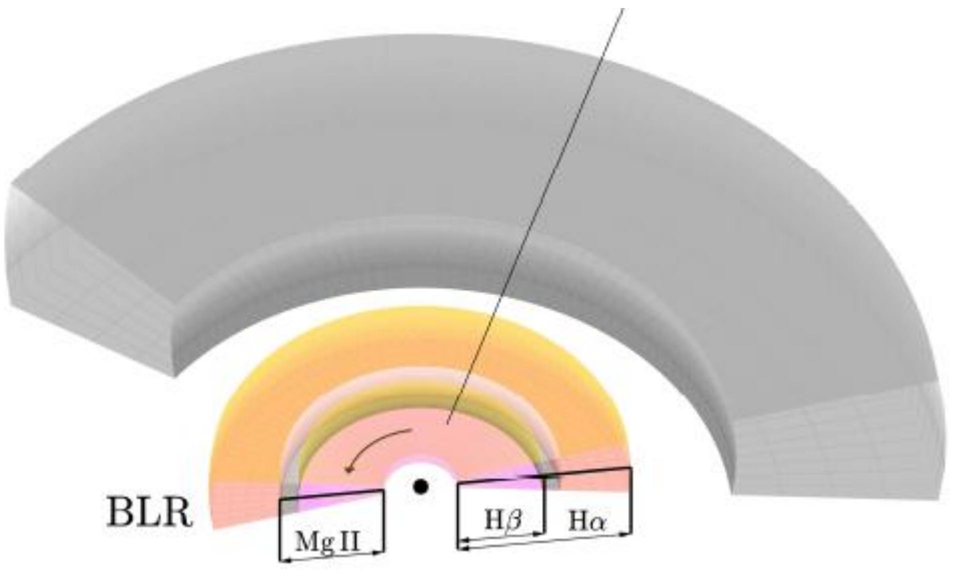

Savic et al. 2020, MNRAS, 497, 3947 – model, BLR with outflows/inflows

Śniegowska, M., et al.: A&A 678, A63 (2023)

Rola of different BLR and SR geometries

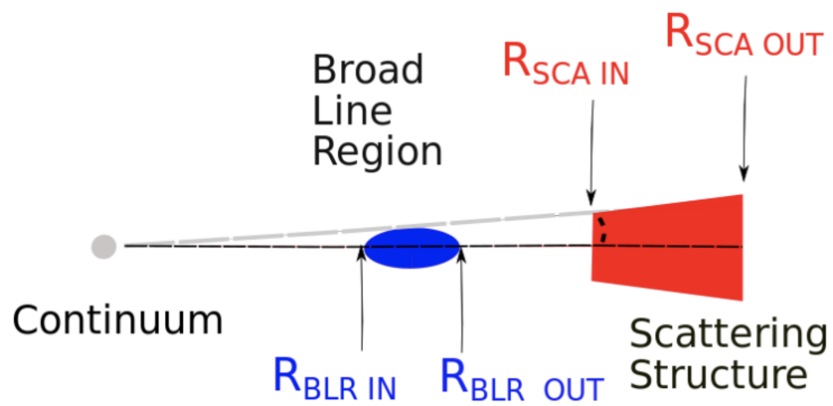

Fig. 4. Schematic view of the models with the equatorial scatterer. The continuum source is marked in gray, the BLR is marked in blue, and the equatorial scattering region is marked in red. We marked the half-opening angle of the scattering structure with a dashed curve between y and black dashed lines.

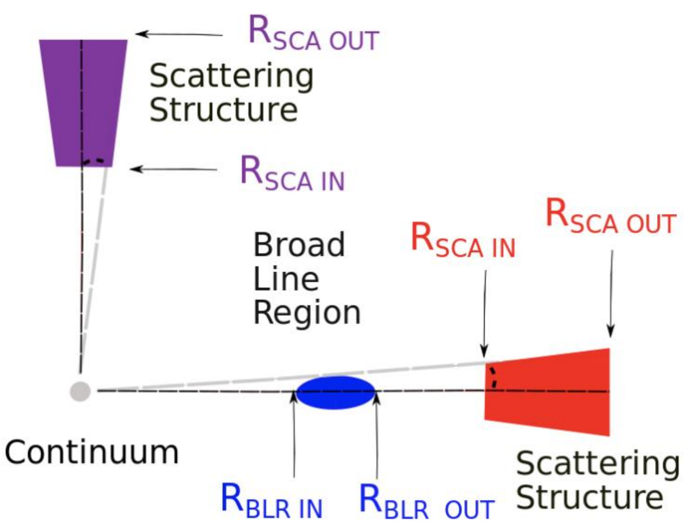

Fig. 5. Schematic view of the models with two scatterers: polar and equatorial. The various components are colored identically to Fig. 4. The polar scattering region is marked in purple.

Quasar SBS 1419+538, spectroploarometric observations of Mg II (Savic, Popovic, Shablovinskaya 2021, ApJL, 921, 21)

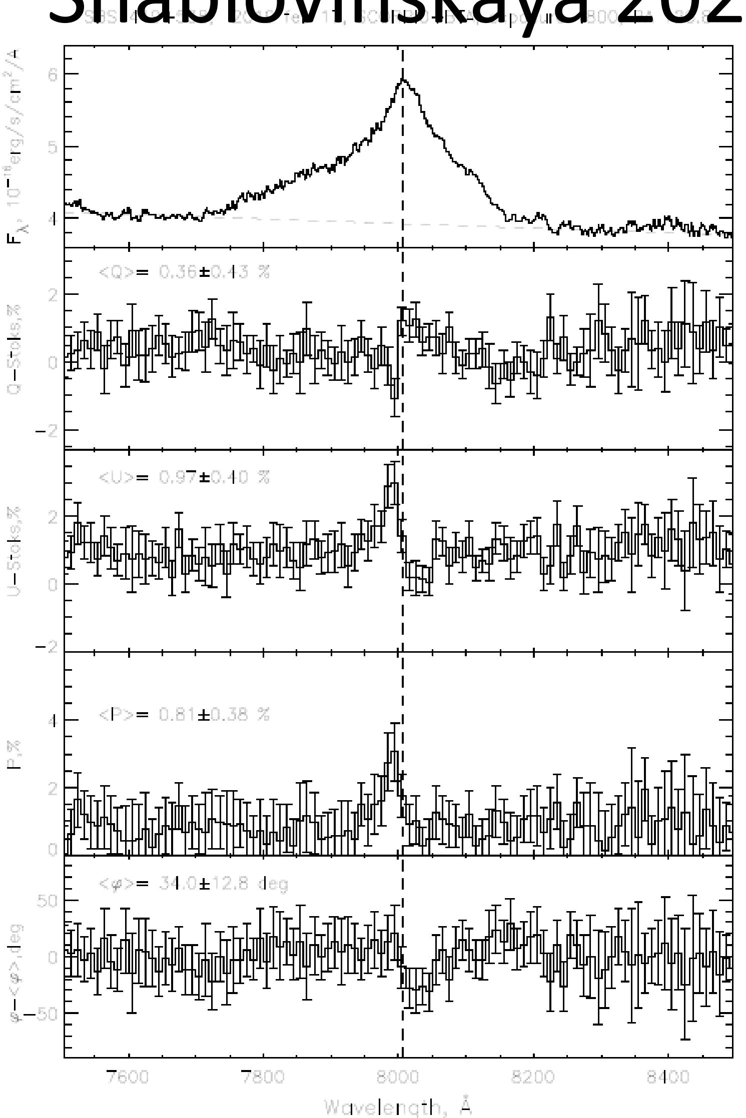

Fig. 5: The Mg II spectral region (1st panel), the Q and U Stokes

SBS1419+538 was observed with the 6-m telescope BTA of SAO RAS with the focal reducer SCORPIO-2 (Afanasiev & Moiseev 2011)

Quasar SBS 1419+538, spectroploarometric observations of Mg II (Savic, et al. 2021)

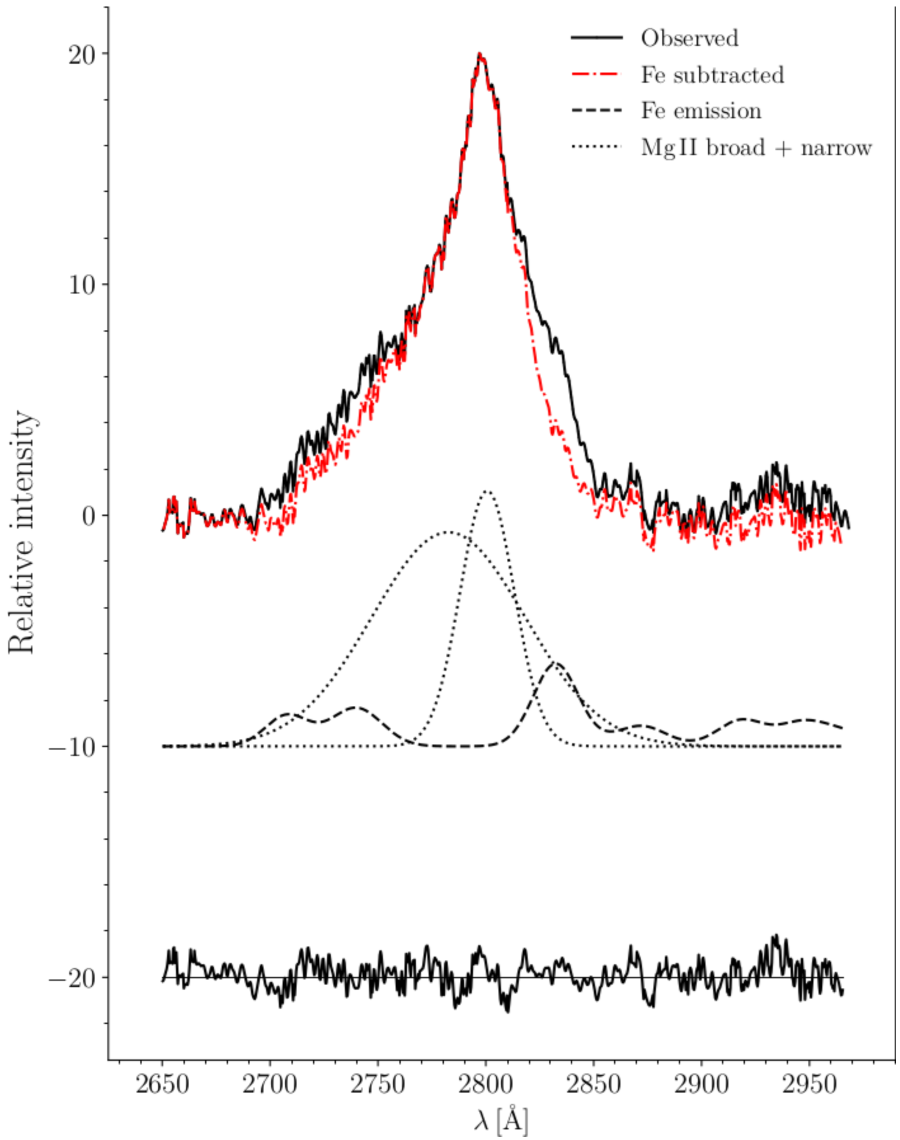

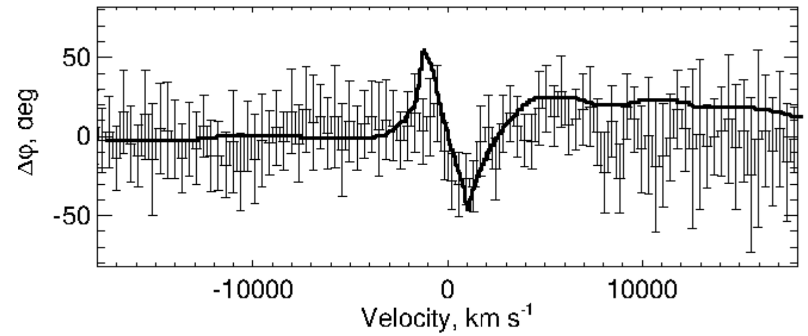

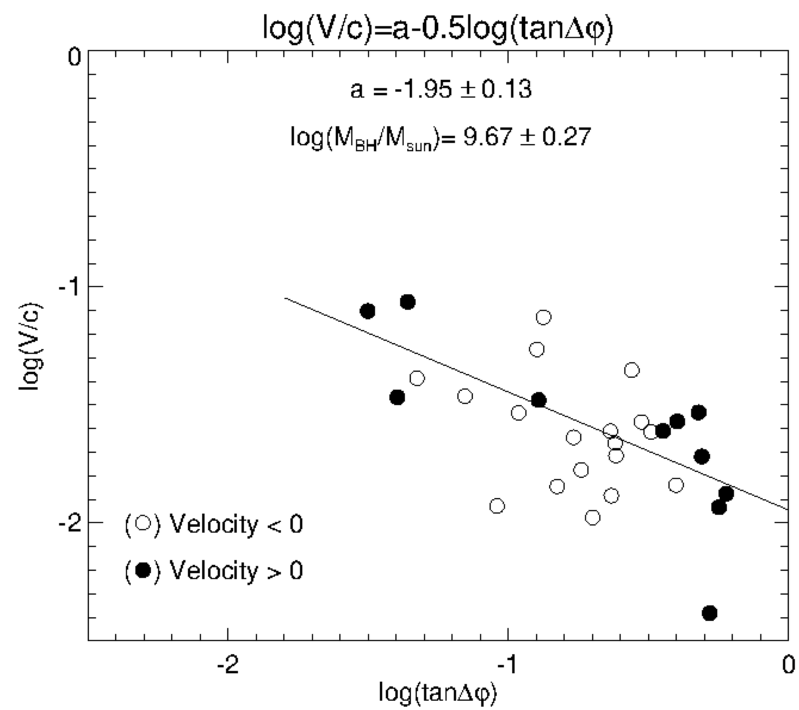

Changing look AGNs
e.g. NGC 3516
Shapovalaova et al. 2019,
Popovic et al. 2023

Polarization in Broad lines
can help?

Marin & Hutsemékers
2020, A&A, 636A, 23
Hutsemékers et al. 2026,
A&A,707, id.A17
Marin et al. 2026,
arXiv260401872

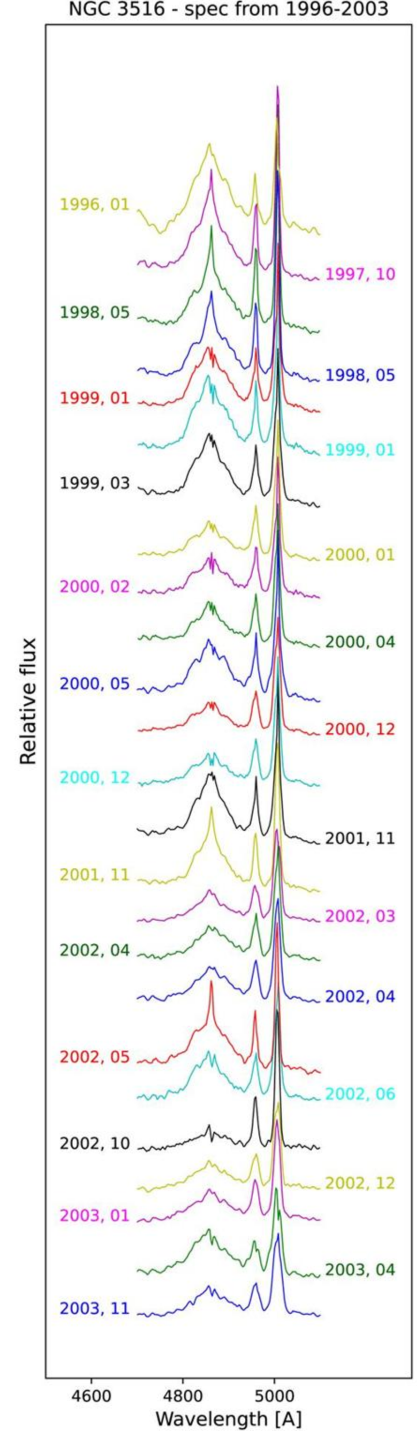

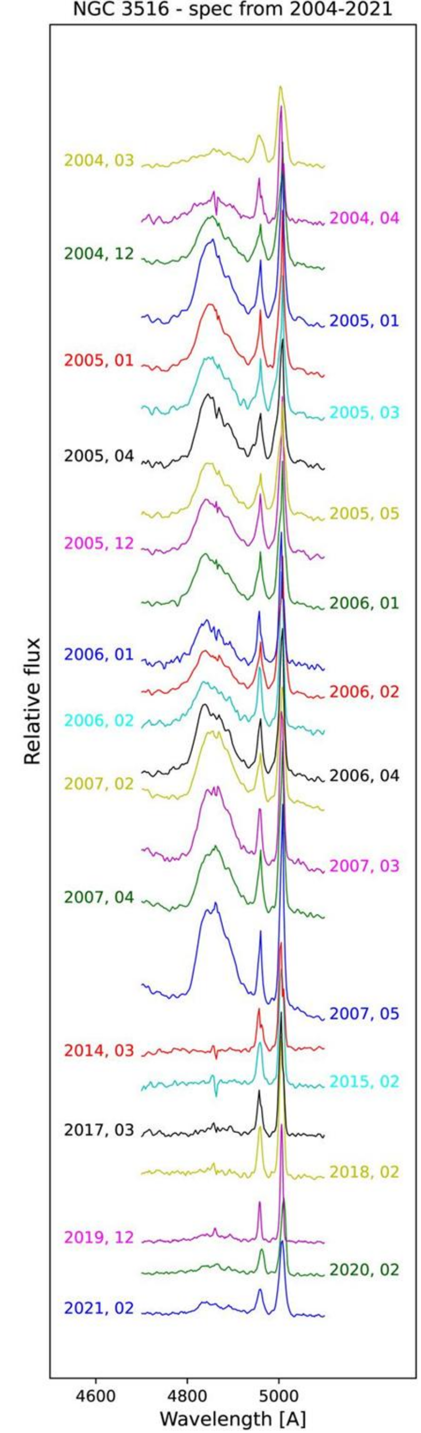

Changing look AGNs

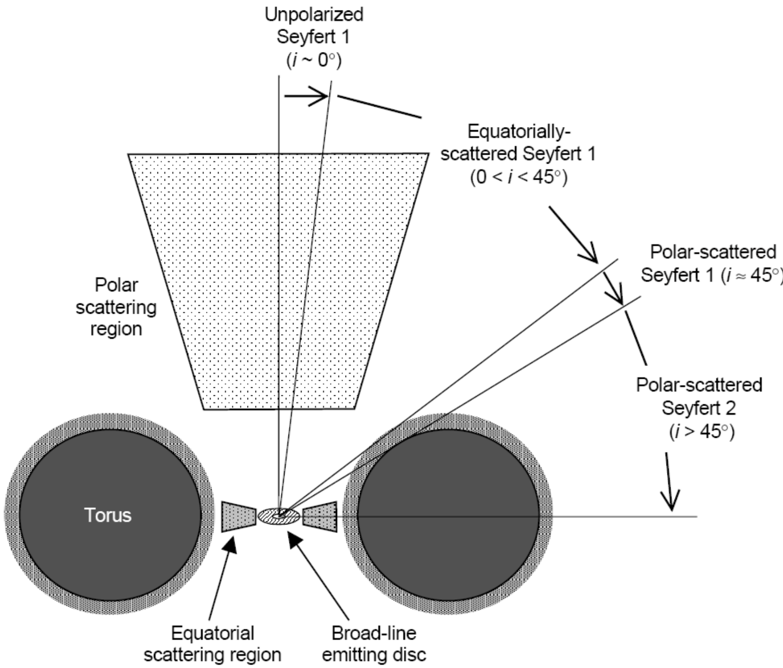

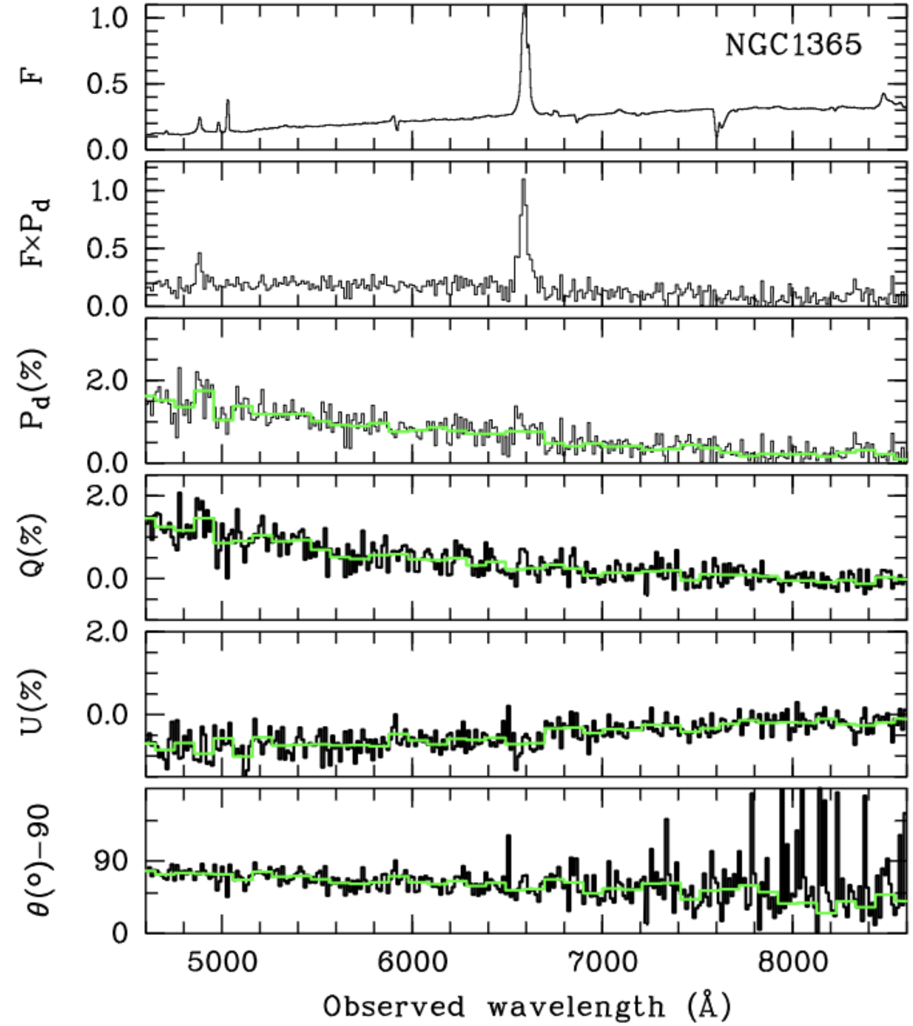

Fig. 3. Spectropolarimetry of NGC 1365N. From top to bottom: Direct and polarized fluxes in arbitrary units, debiased polarization degree in percent, normalized Stokes parameters q and u in percent, and polarization position angle in degrees (from which 90° were subtracted for clarity of the plot). The spectra in green were binned over 30 spectral

Hutsemékers et al., A&A, 707, A17 (2026)

NGC 3516, Savic et al.

Reverberation in IR?

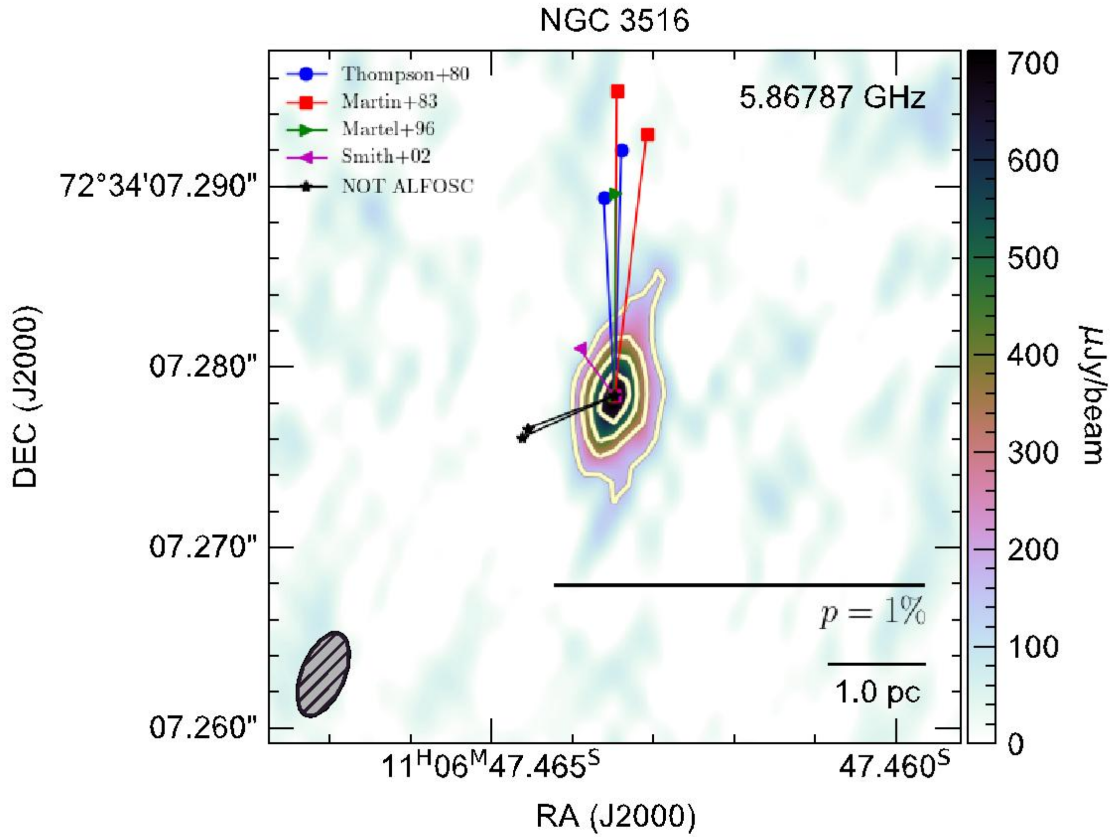

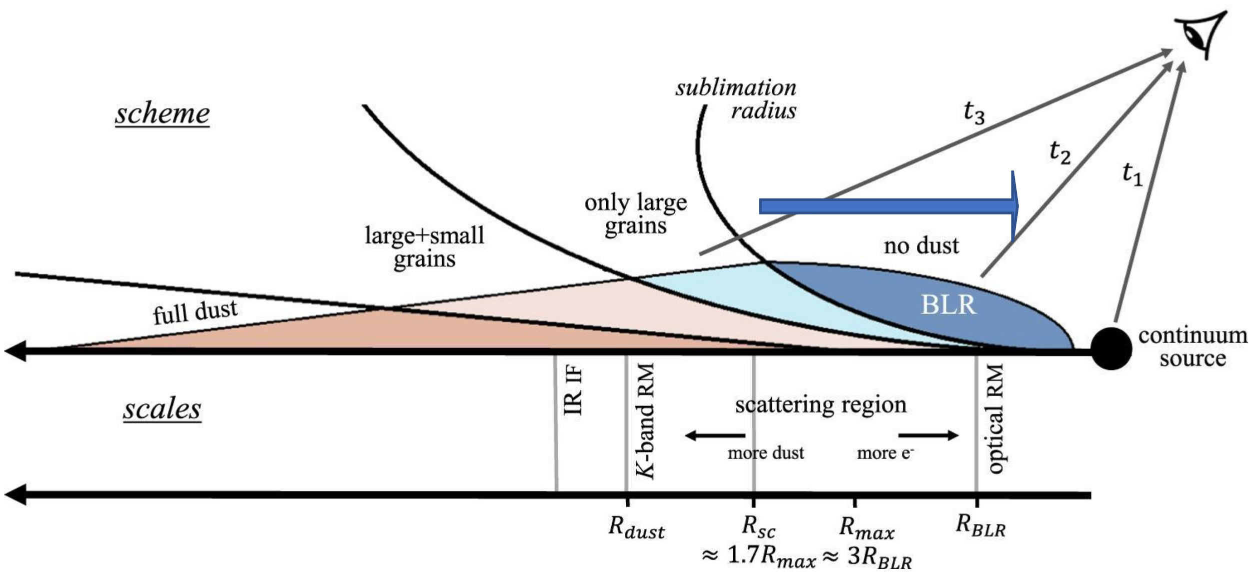

Reverberation in IR?

Supermassive binary black holes & polarization

Popović et al. 2021, MNRAS, 505, 51

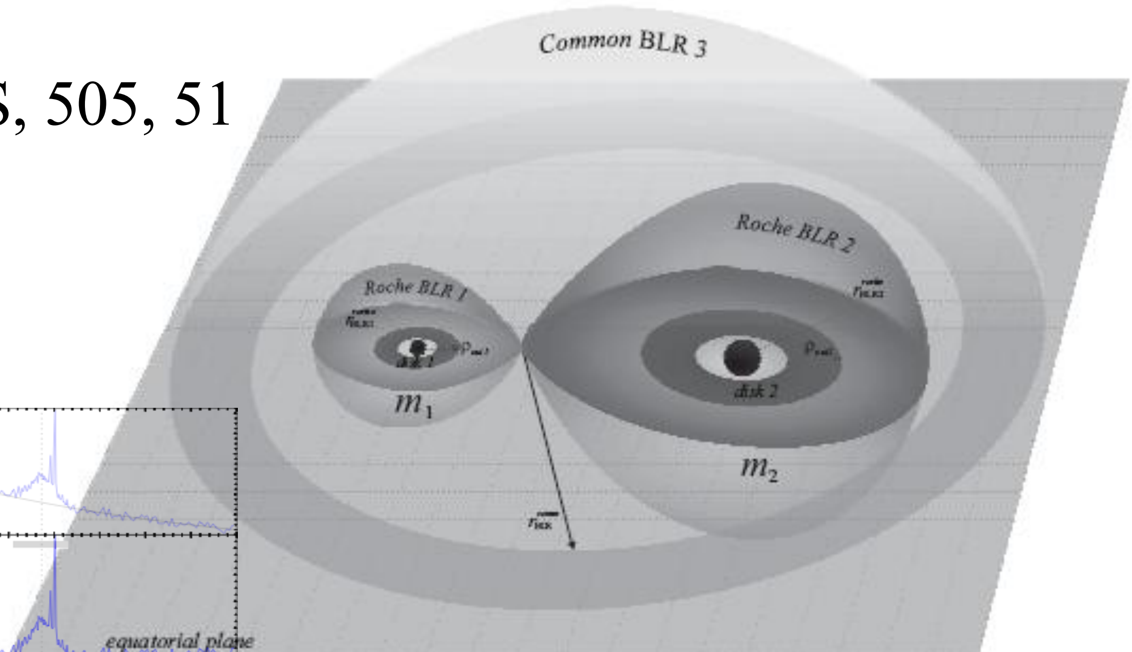

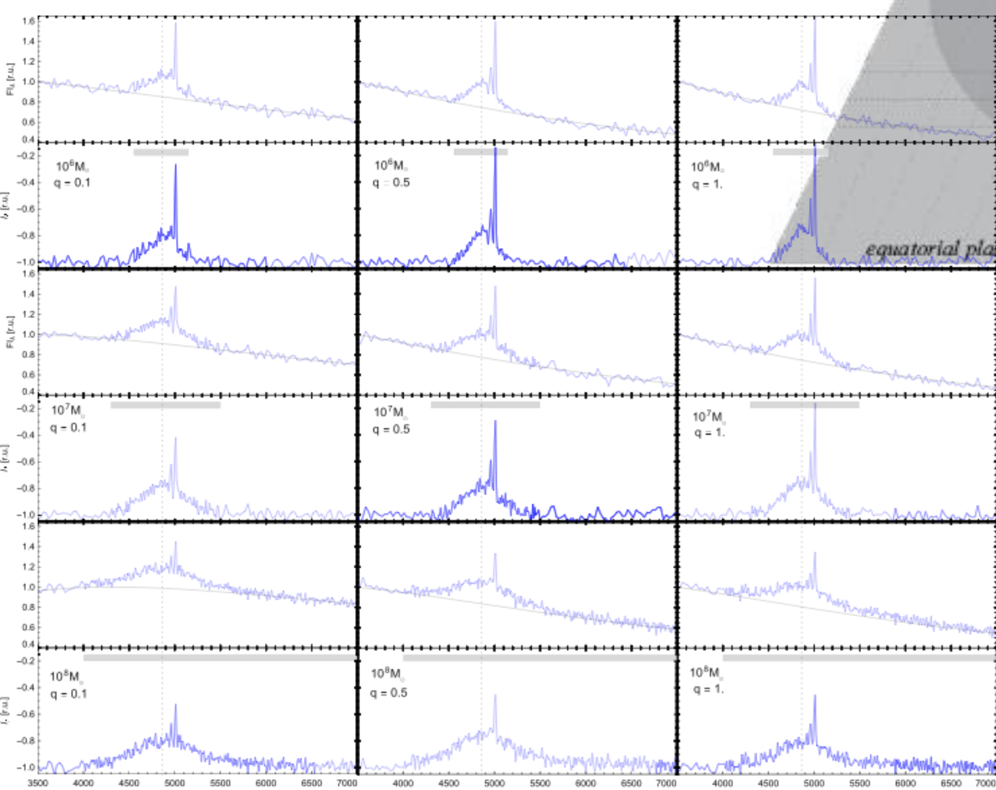

SMBBHs – polarization in broad lines, see Savić, Marin & Popović 2019, A&A,623, 56

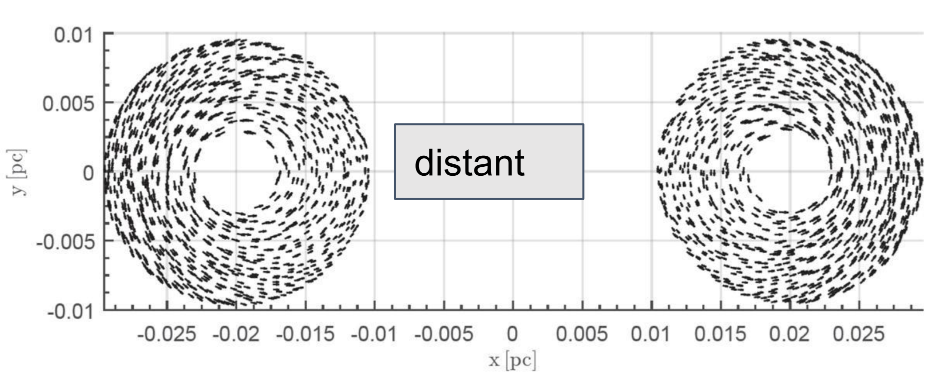

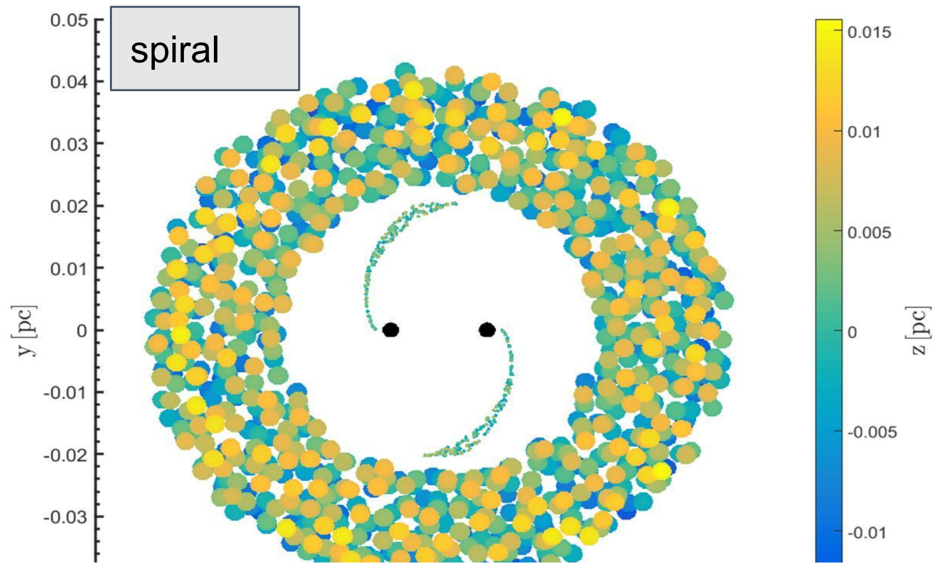

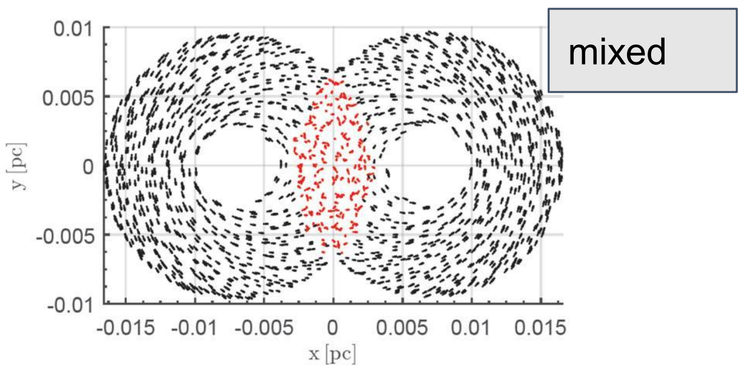

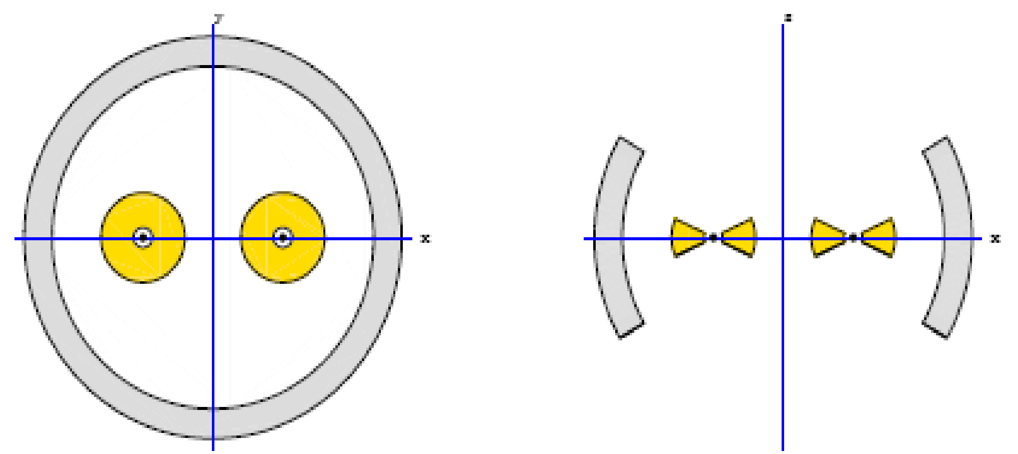

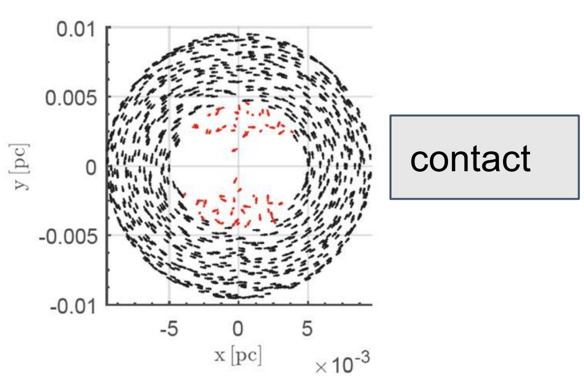

See detailed discussion in Savić et al. 2019

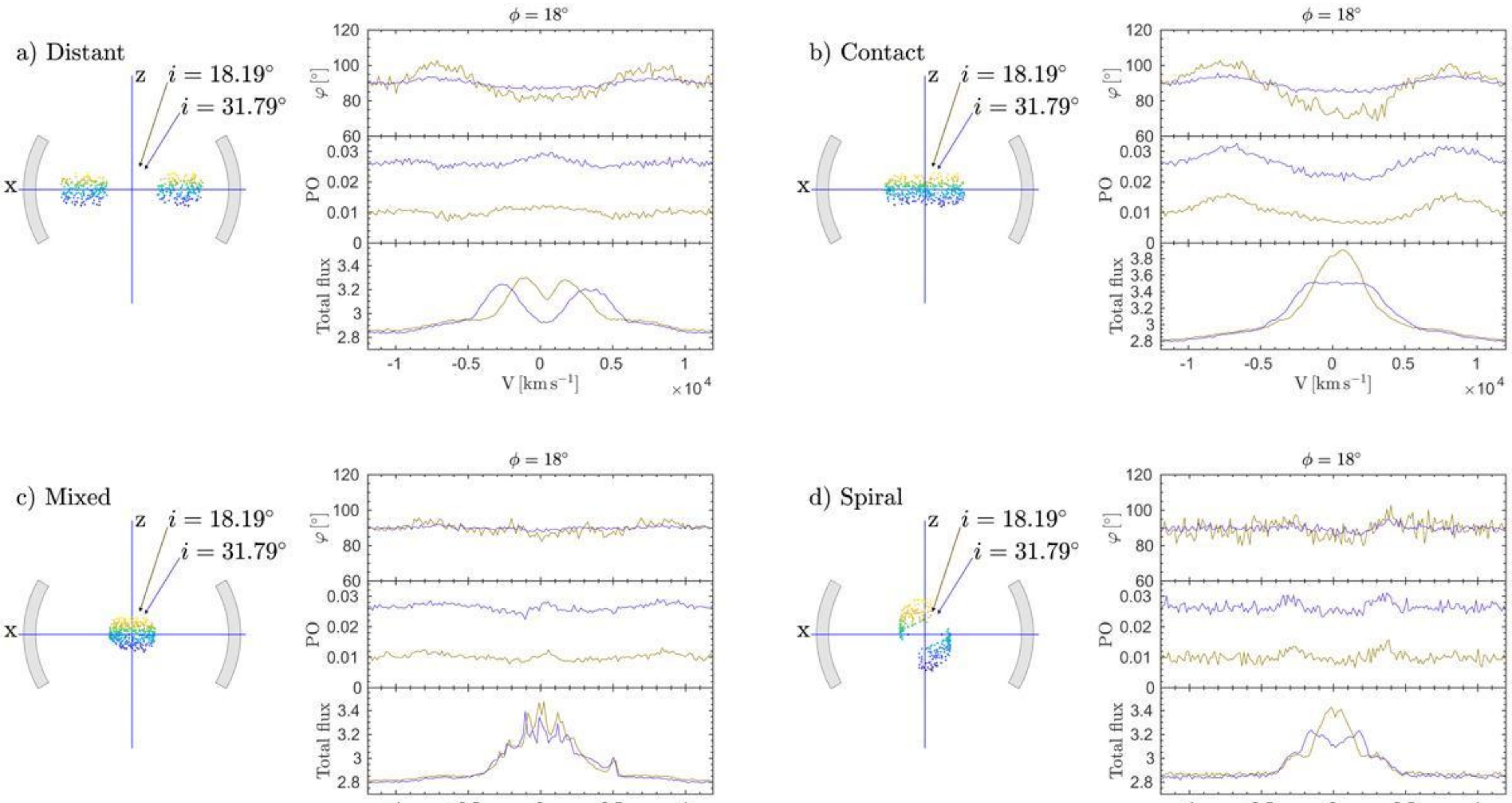

Observations case of NGC 1566 (Marin et al. 2026, arXiv260401872)

- Changing look, but candidate for SMBBH – very hard to find specific polarization sign

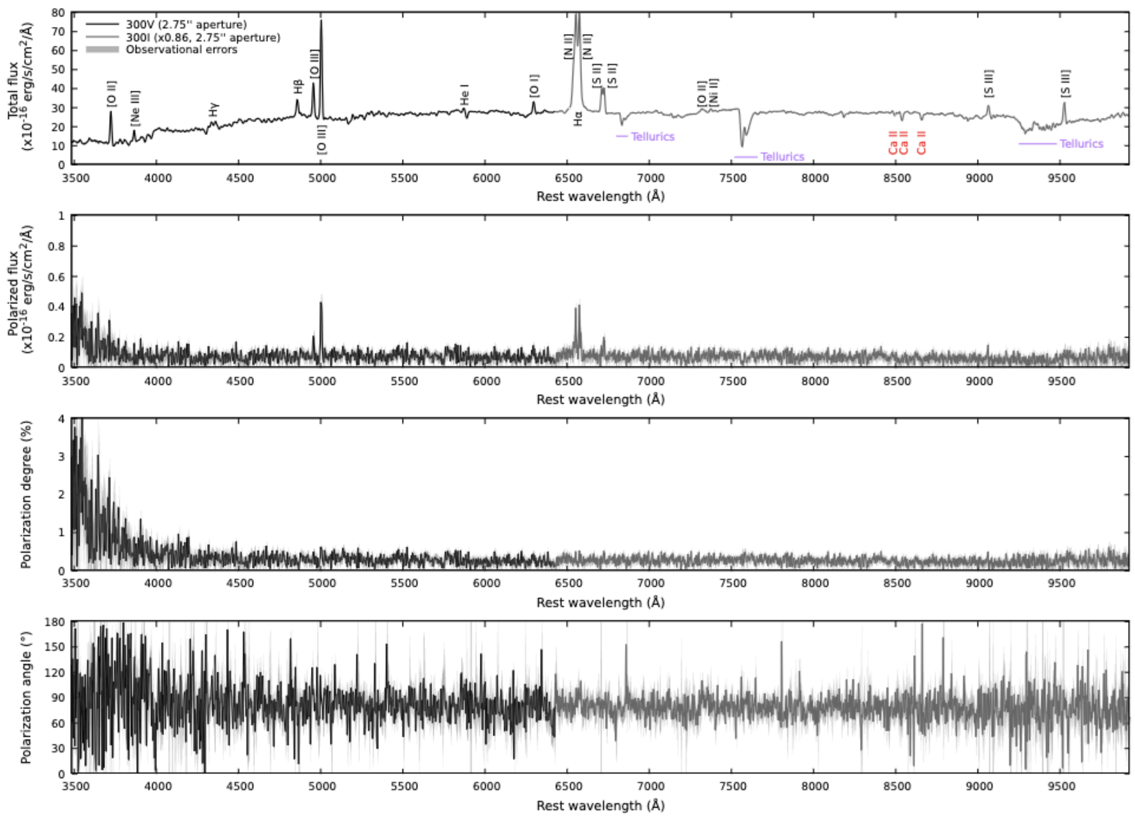

Fig. 4. VLT/FORS2 spectropolarimetry of NGC 1566. Top panel: Total flux spectrum (in 10^{-16} erg s^{-1} cm^{-2} Å^{-1}). The most prominent telluric absorption lines are indicated in purple, the calcium triplet absorption lines resulting from host starlight are indicated in red, and the most prominent emission lines are labeled in black. The 300I spectrum has been offset to match the 300V spectrum by applying a correction factor of 0.86 to account for the different observing conditions and grisms. Second panel: Polarized flux; that is, the multiplication of the total flux with the polarization degree, P. Third panel: Linear polarization degree, P. Bottom panel: Polarization position angle, θ. Spectra are shown at native spectral resolution (no binning). Observational errors are indicated in transparent gray for each spectral bin.

• Gravitational microlensing – amplification of an image

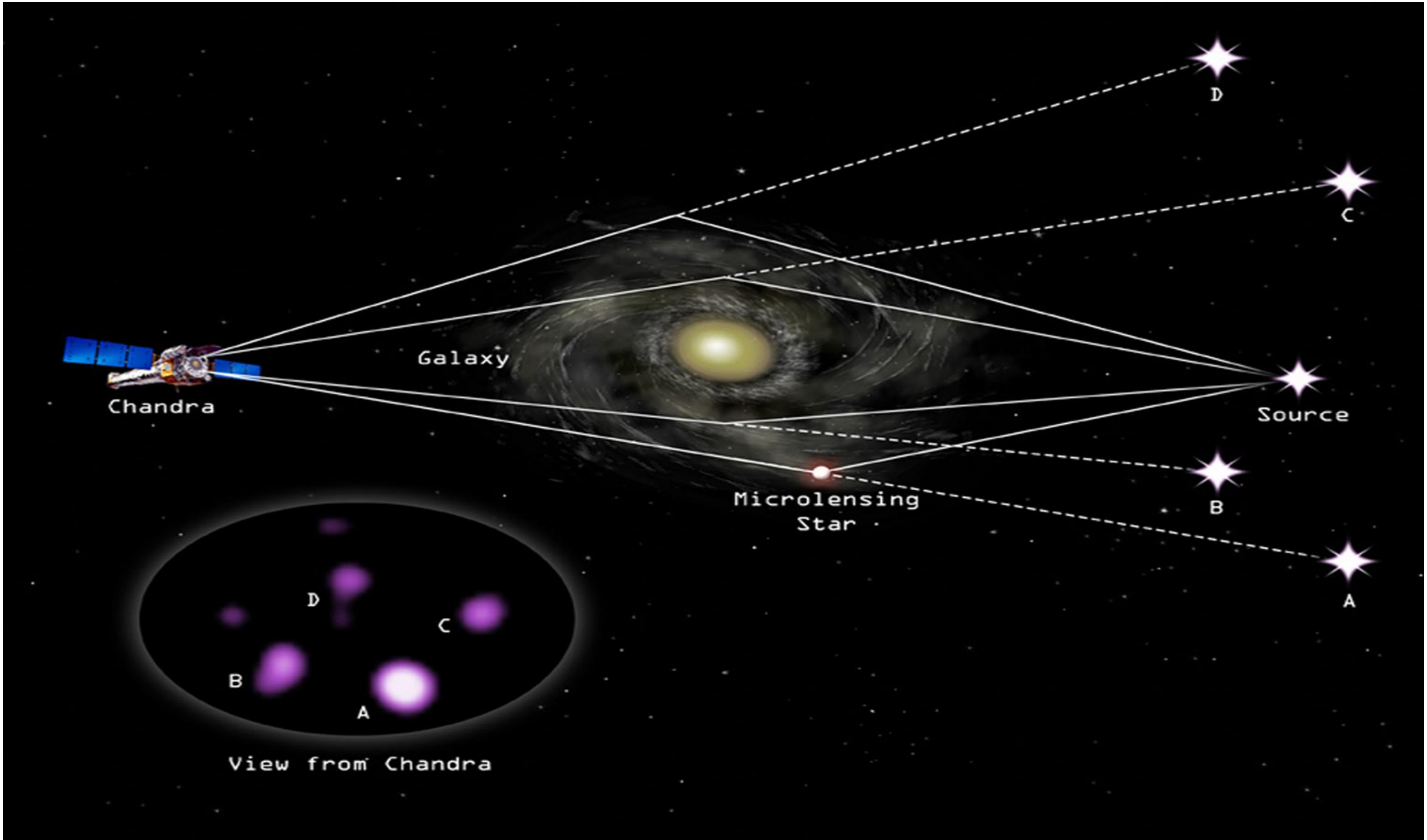

• IDEA:

- Combination microlensing structure (star surface density in lens galaxy) and qusar structure; micorolens=>scanner for the quasar inner structure

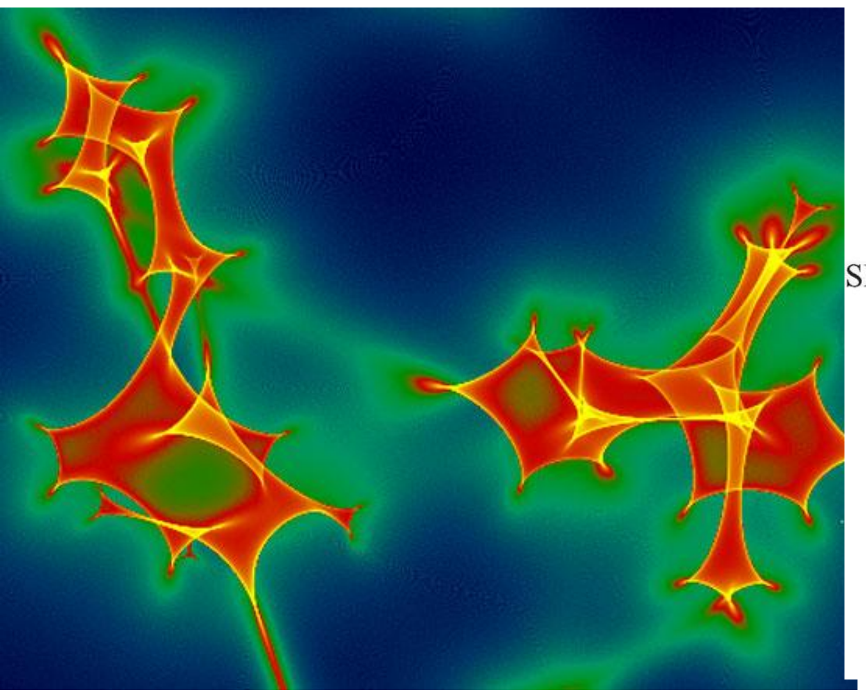

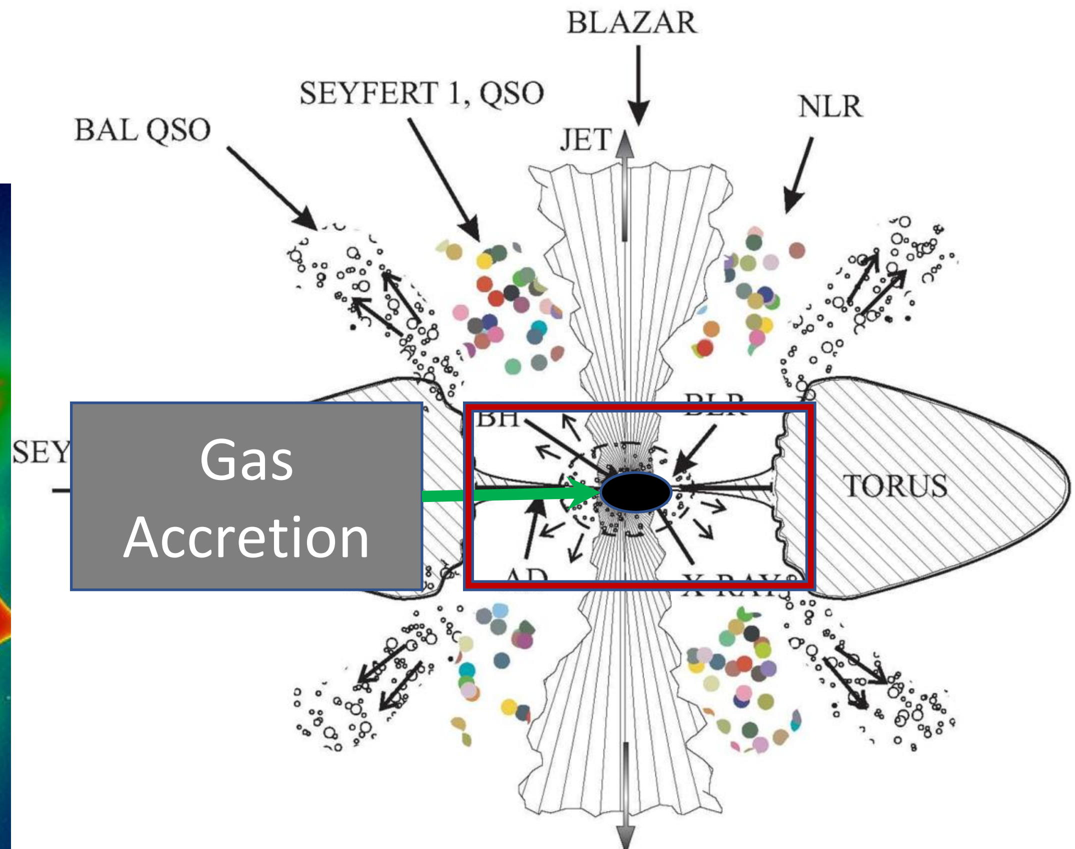

- AGN central part and ERR of microlensing, e.g. Millilensing (1000 - 10000 stars)

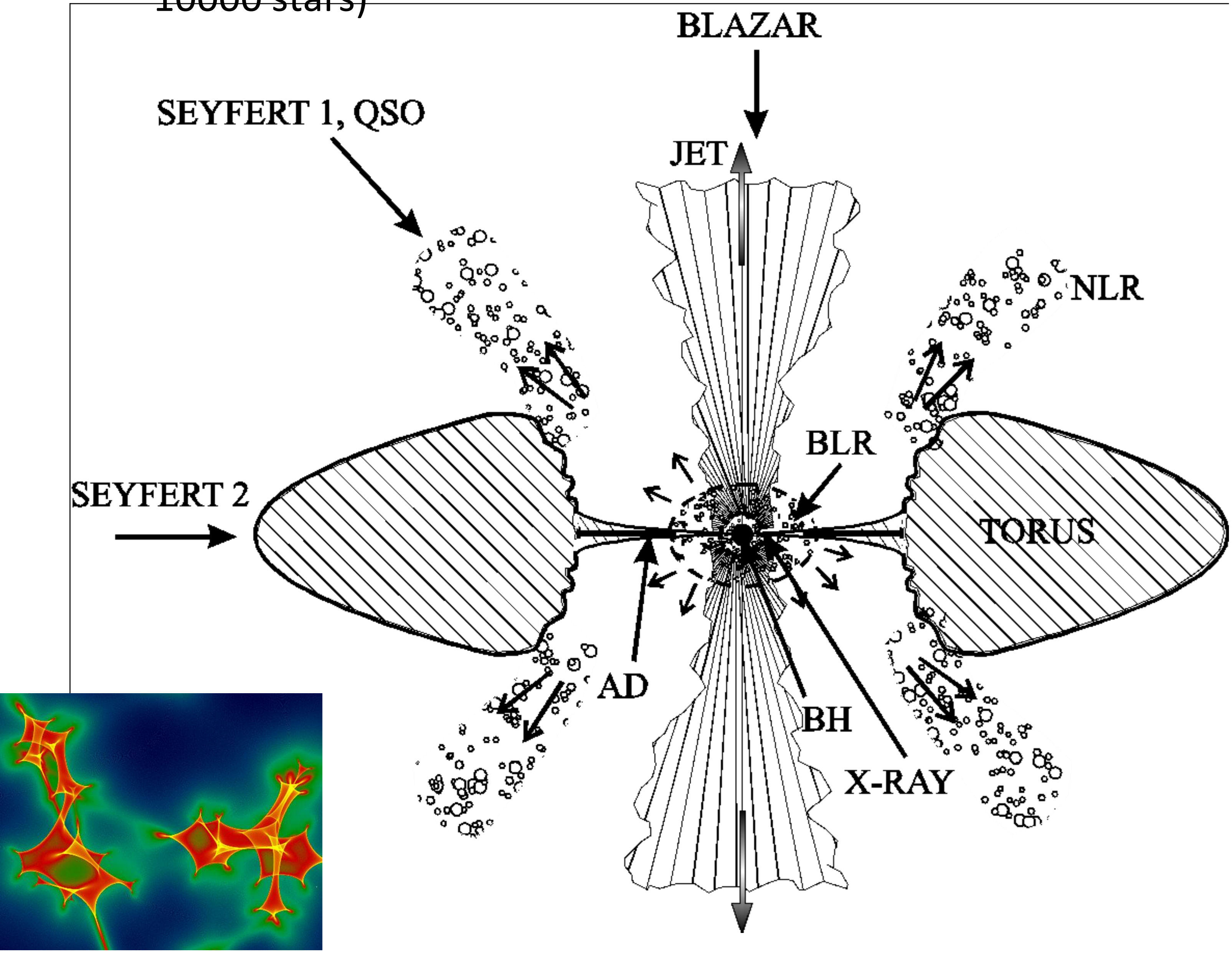

- AGN central part and ERR of microlensing, e.g. microlensing (several sul-like stars)

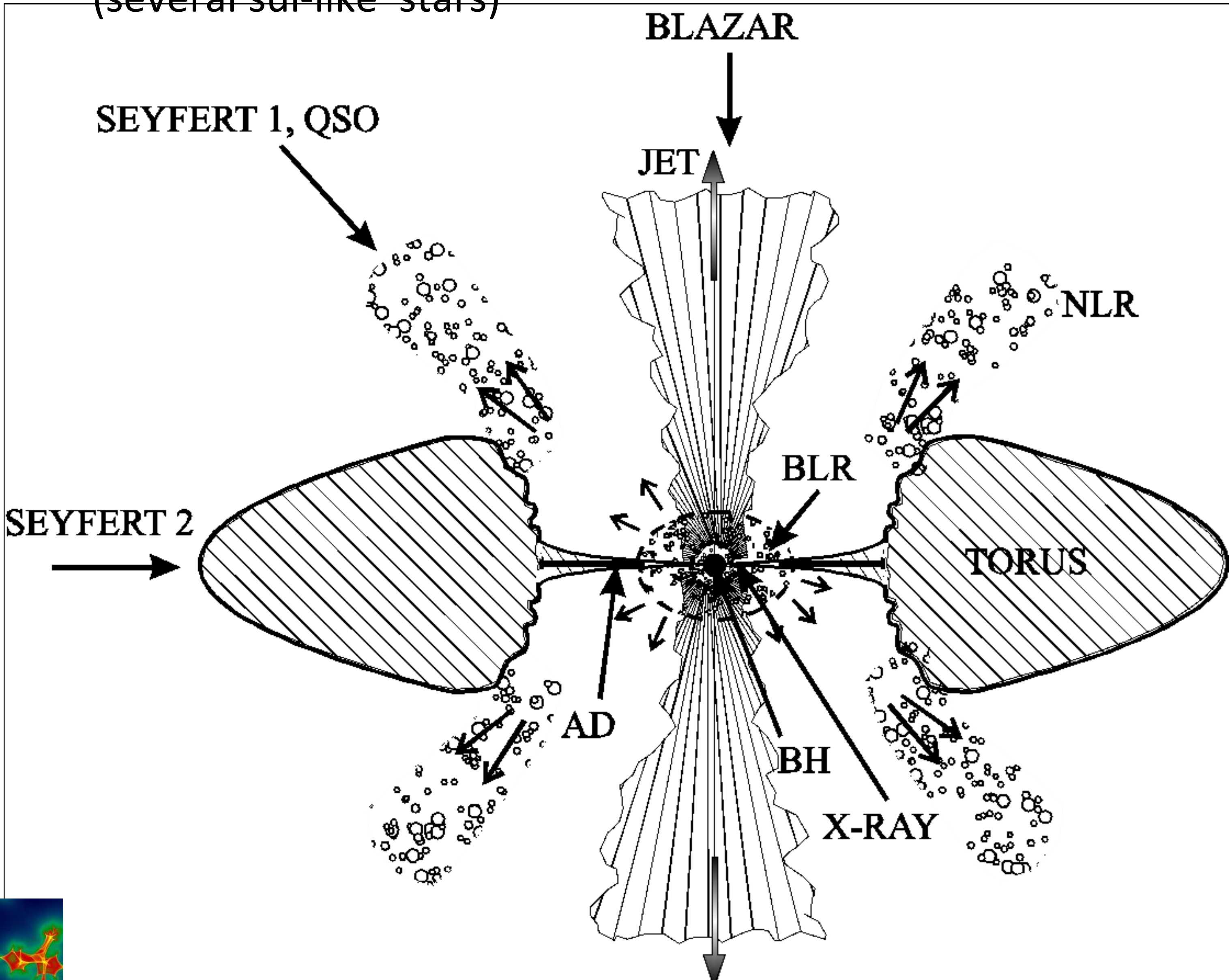

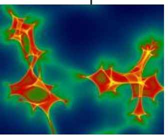

- Task: Investigate quasar structure using micorlensing effects

(observations with 6 m SAO telescope – spectroscopical and polarometric mode)

- **Polarization of SDSS J1004+4112, Popovic, Afanasive et al. 2020, A&A, 634, 27**
- Problem enhancement in the blue wing of component A (only): Richards et al. 2014, ApJ, 610, 647

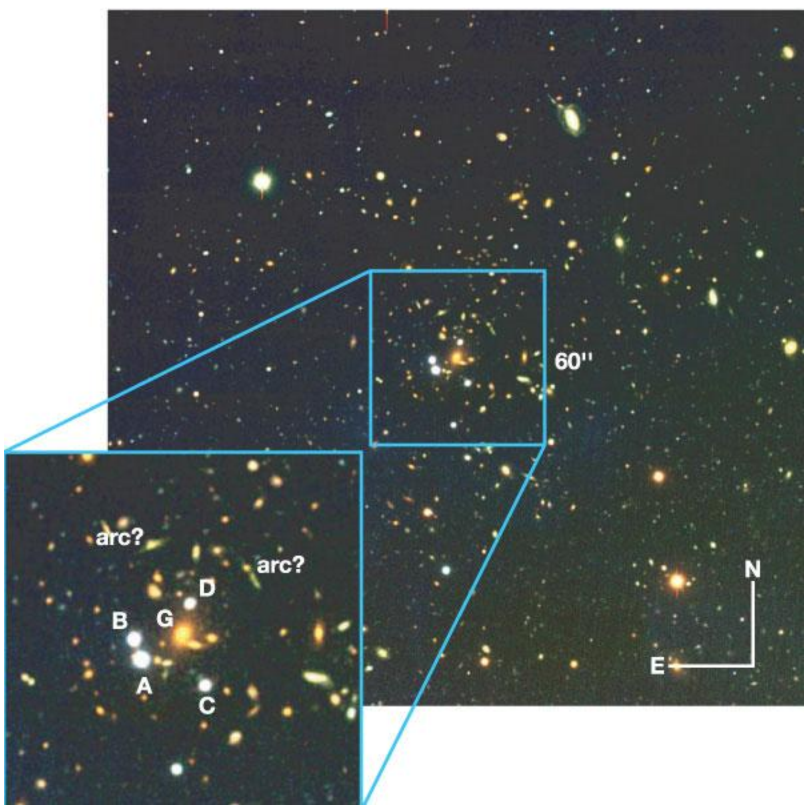

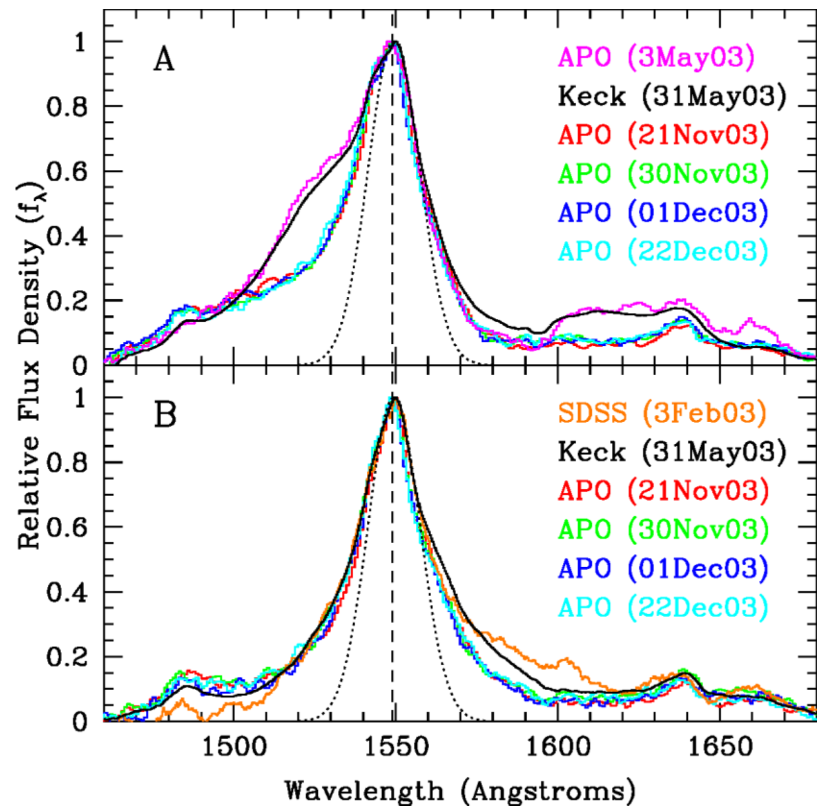

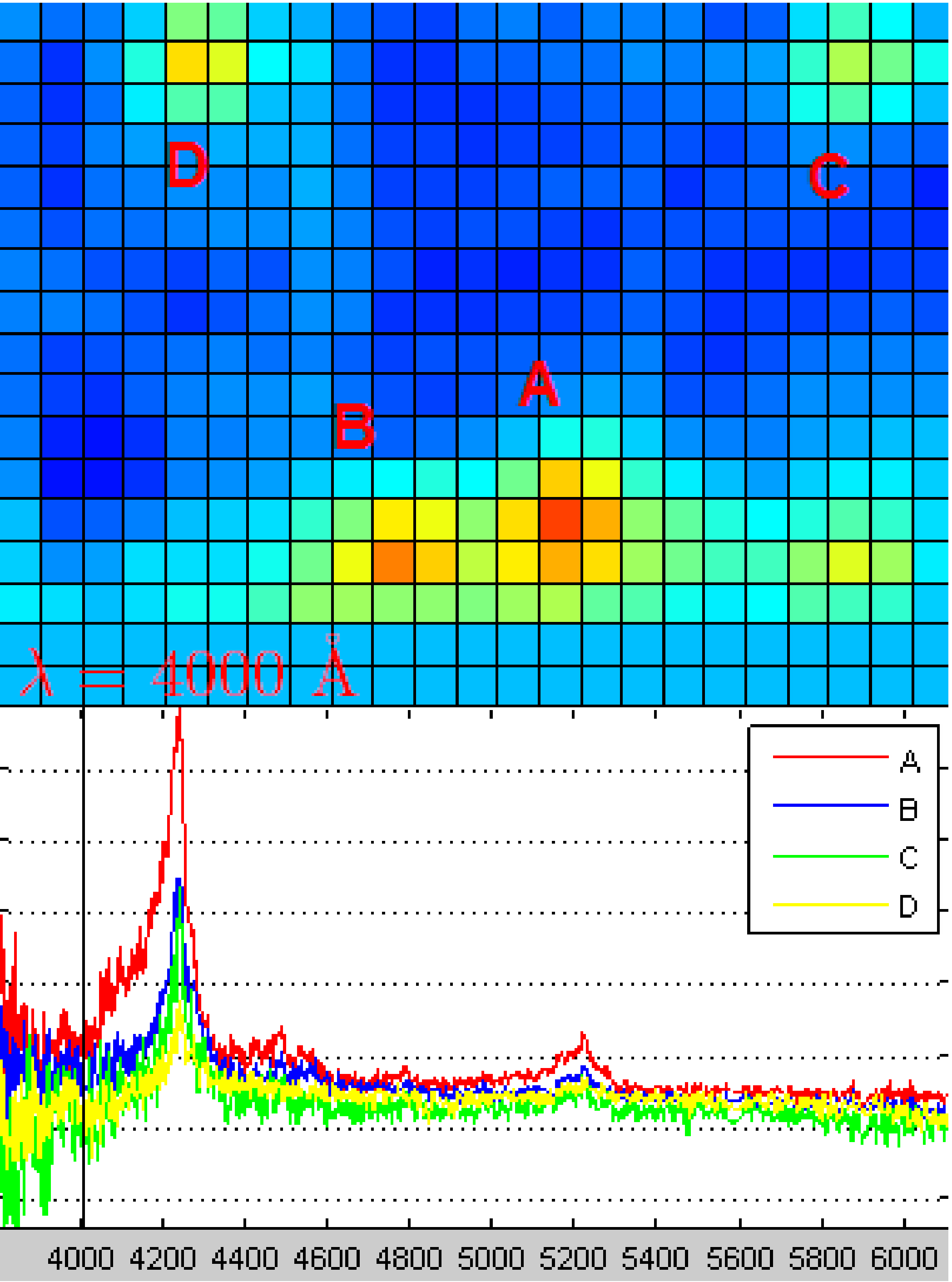

- Observations with 6m SAO telescope

Spectra

- MPFS 2007
- SCORPIO 2008
- SCORPIO-2 2018
- polarization observations

Polarization observations (2014 - 2017)

- A – component, blue wing!

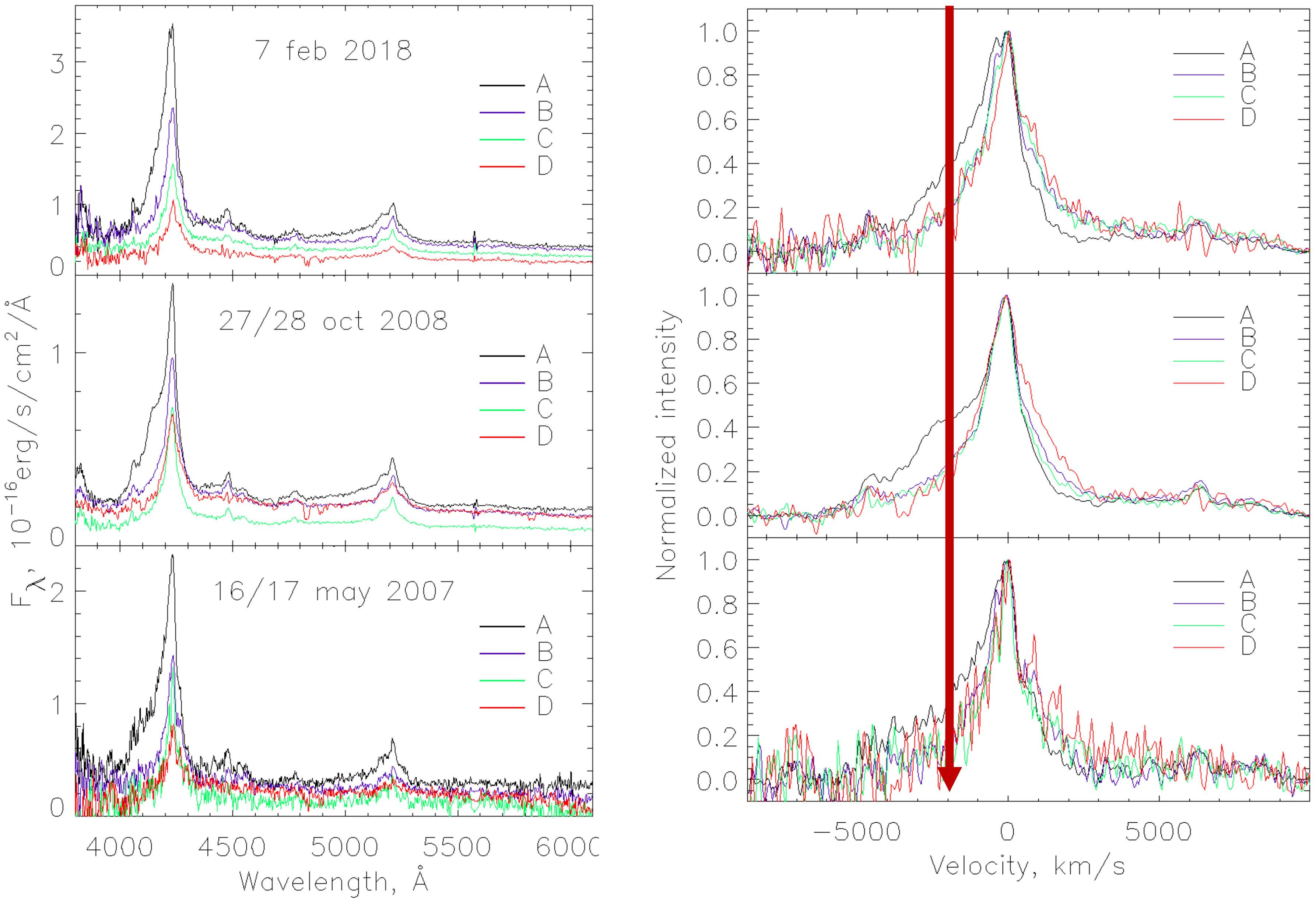

- Possible explanation
- BLR is too big to be microlensed
- In quasars C IV has (usually) a blue asymmetry
- Outflow!

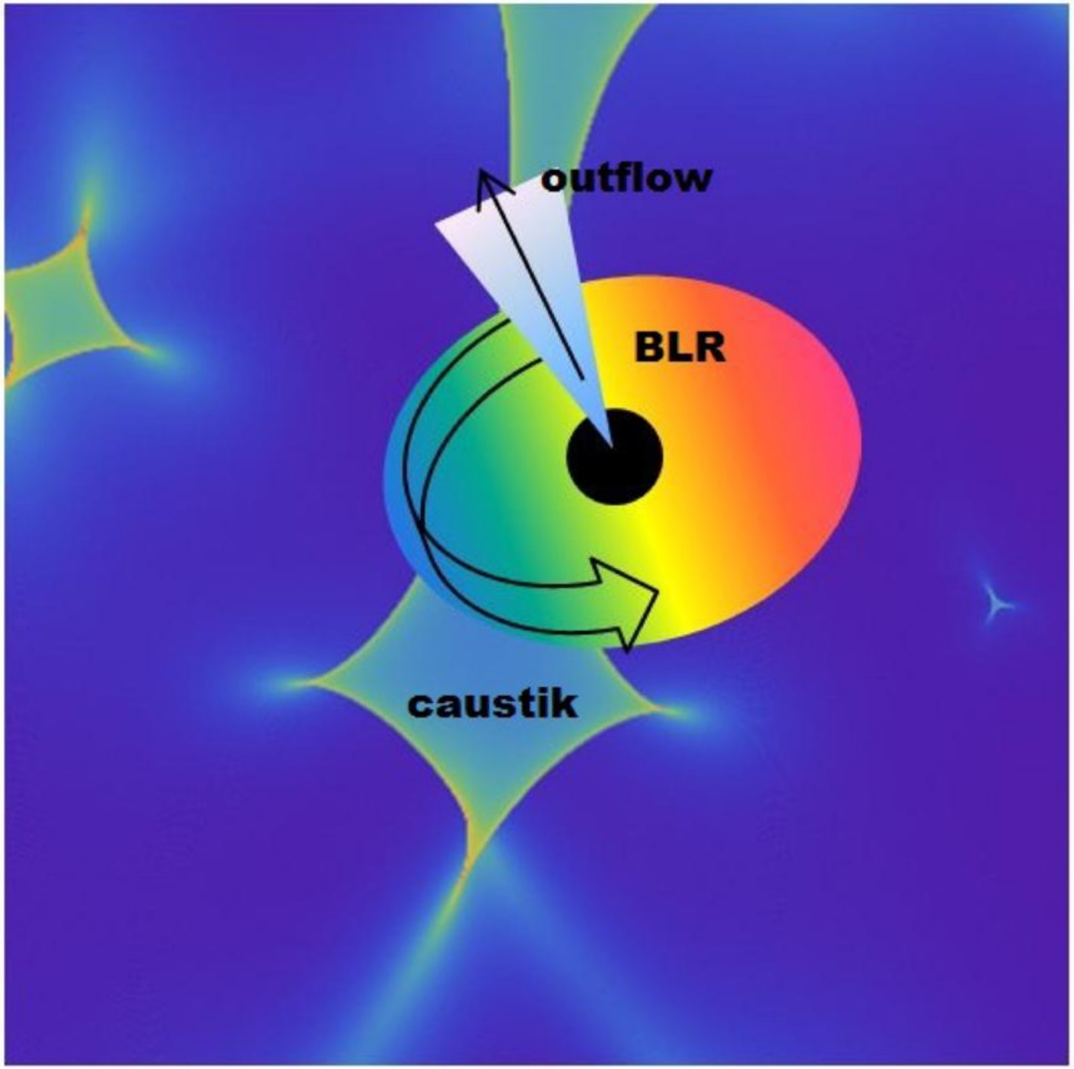

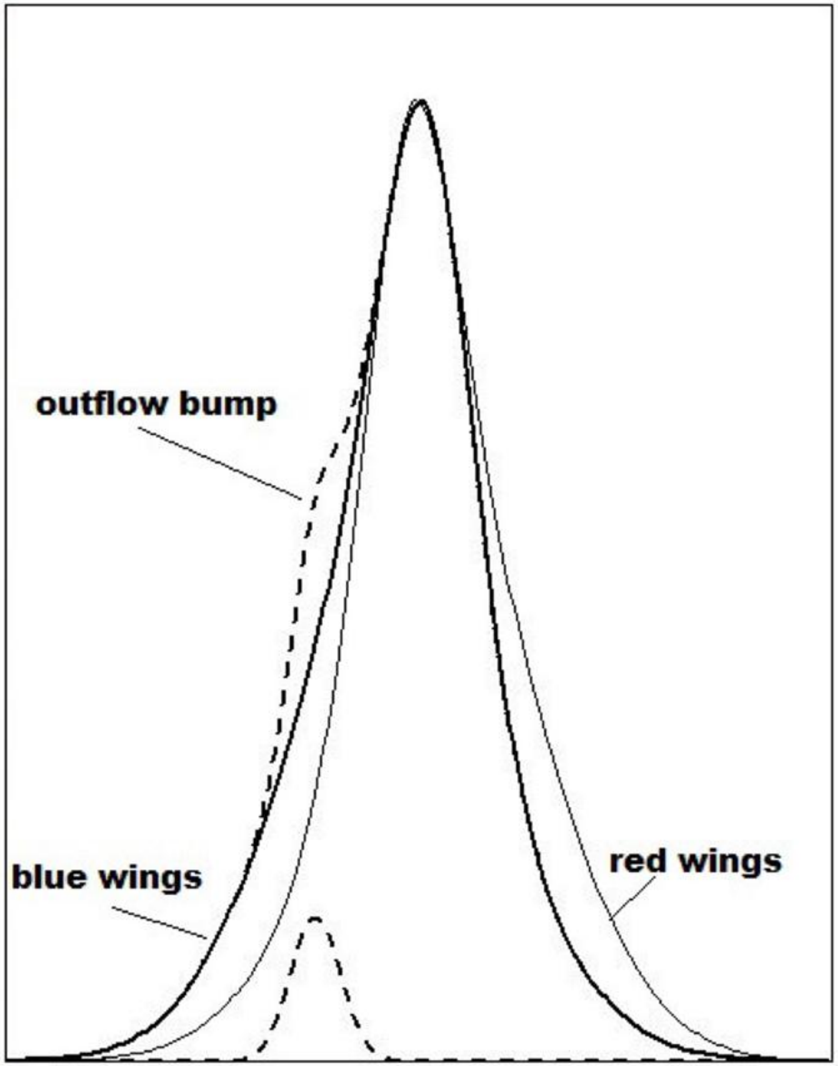

- Polarization – D seems to change polarization parameters

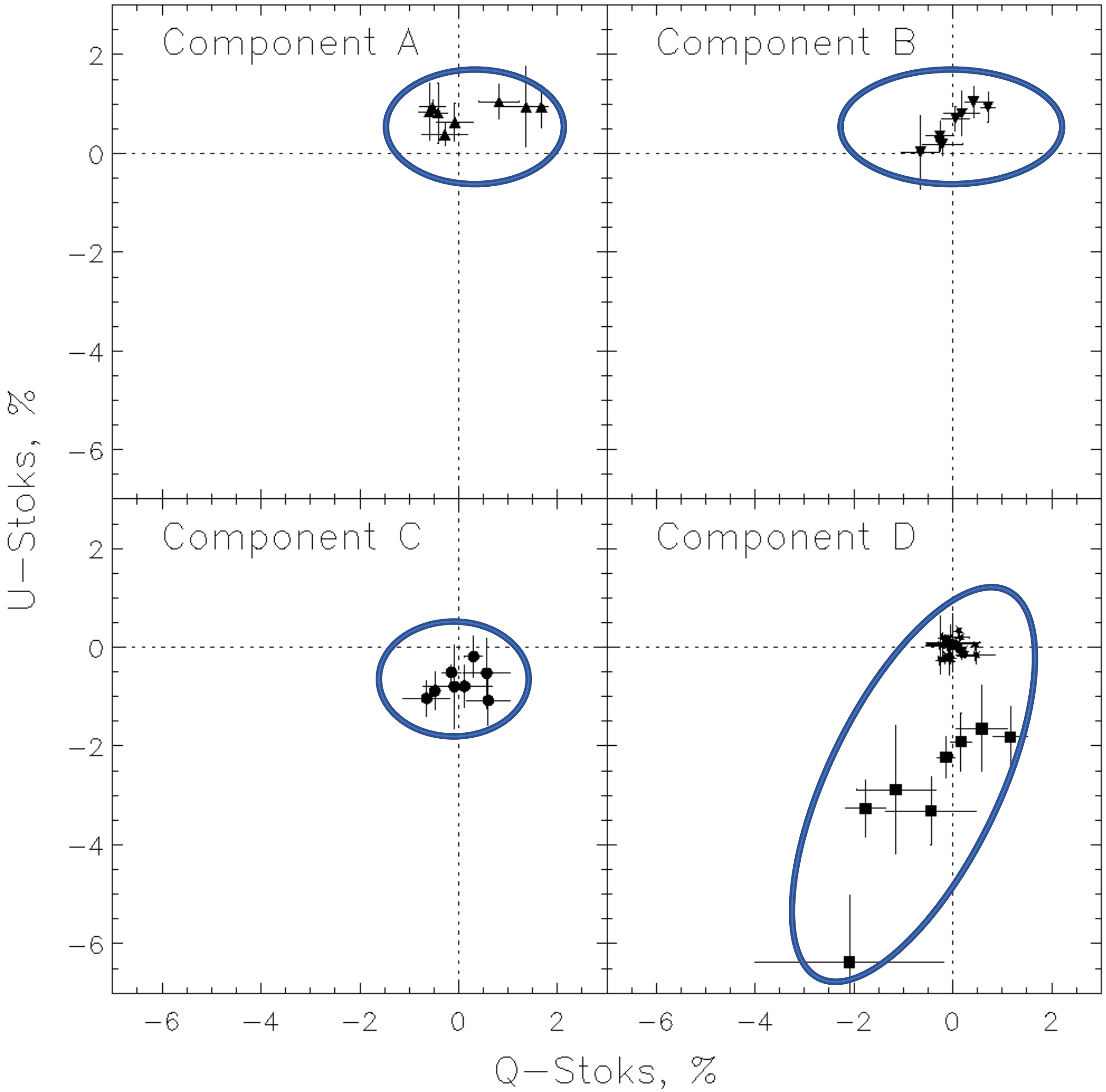

- AGN ccretion disc lensing, and Fe Kα line

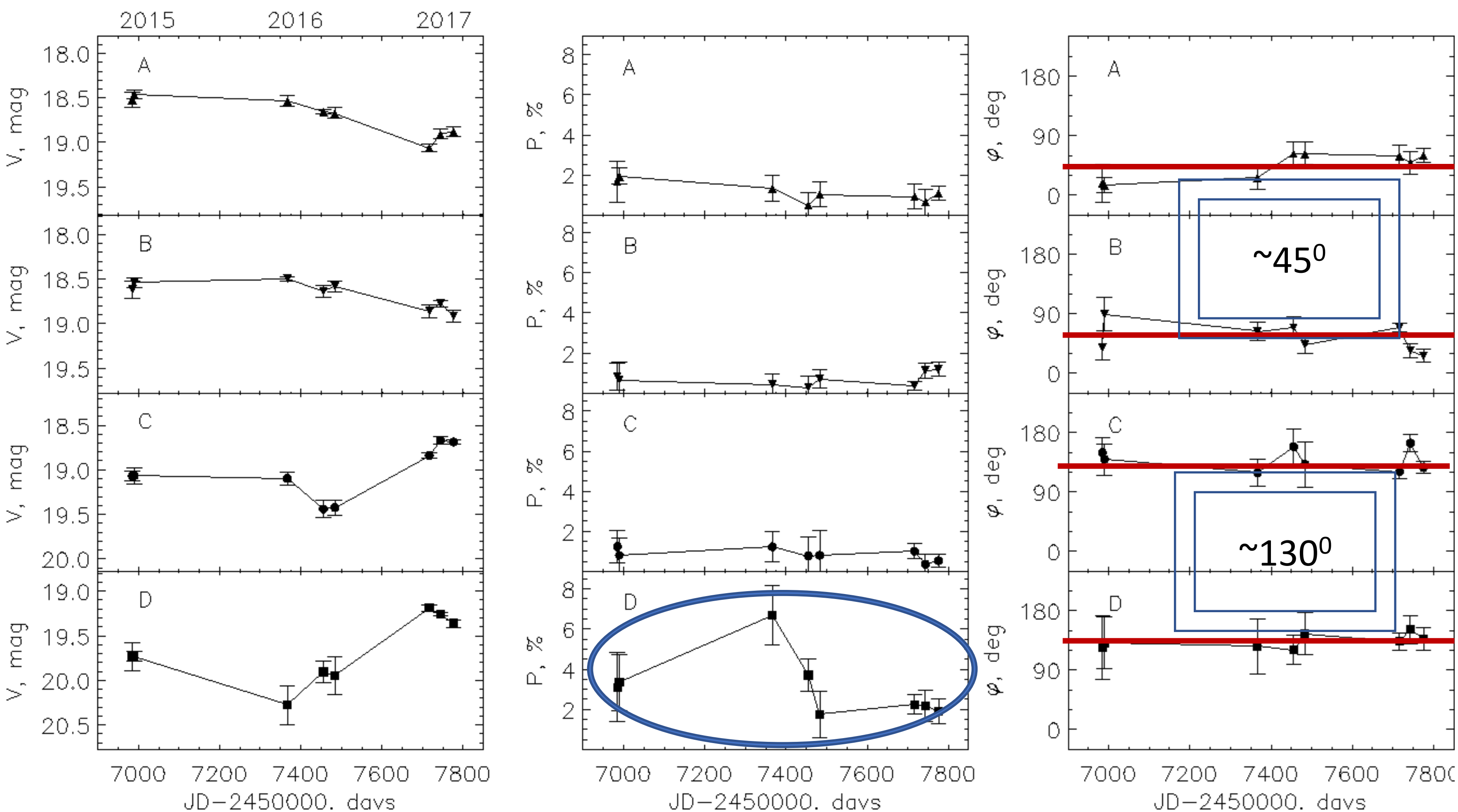

- Nature of polarization – gravitational lensing
- Type 1 AGN (with broad lines)=> equatorial polarization (dust in the inner part of a torus)
- Macro or microlensing

  - Model (see Savic et al. 2018, A&A, 614, 112). Equatorial scattering in the inner part of the torus

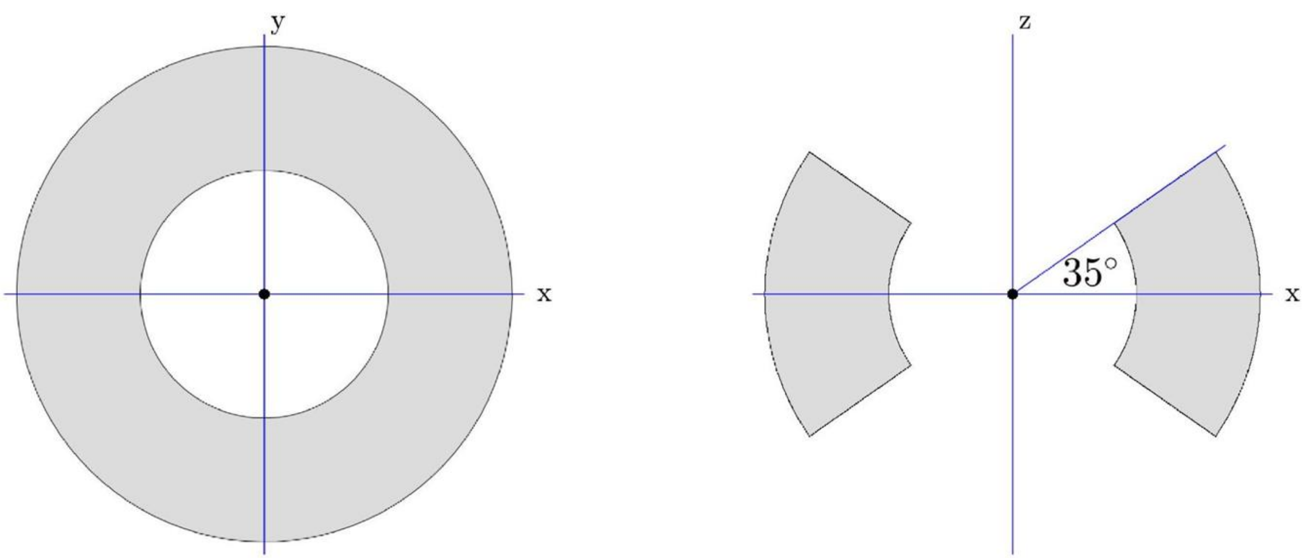

- Polarized picture of the central part of SDSS J1004+4112

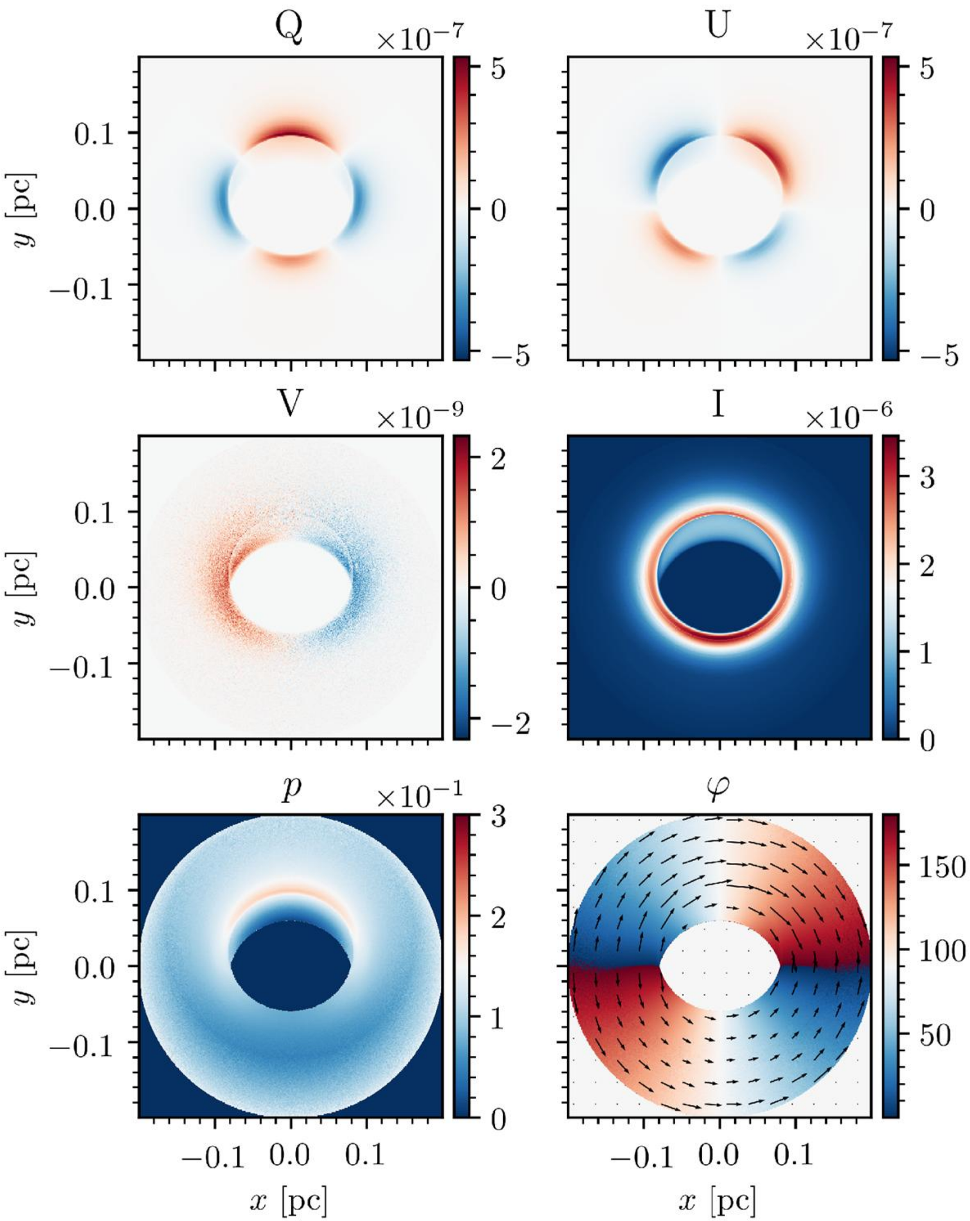

• Macrolensing – model shows that changes in the D cannot be due to macrolensing (see paper)!

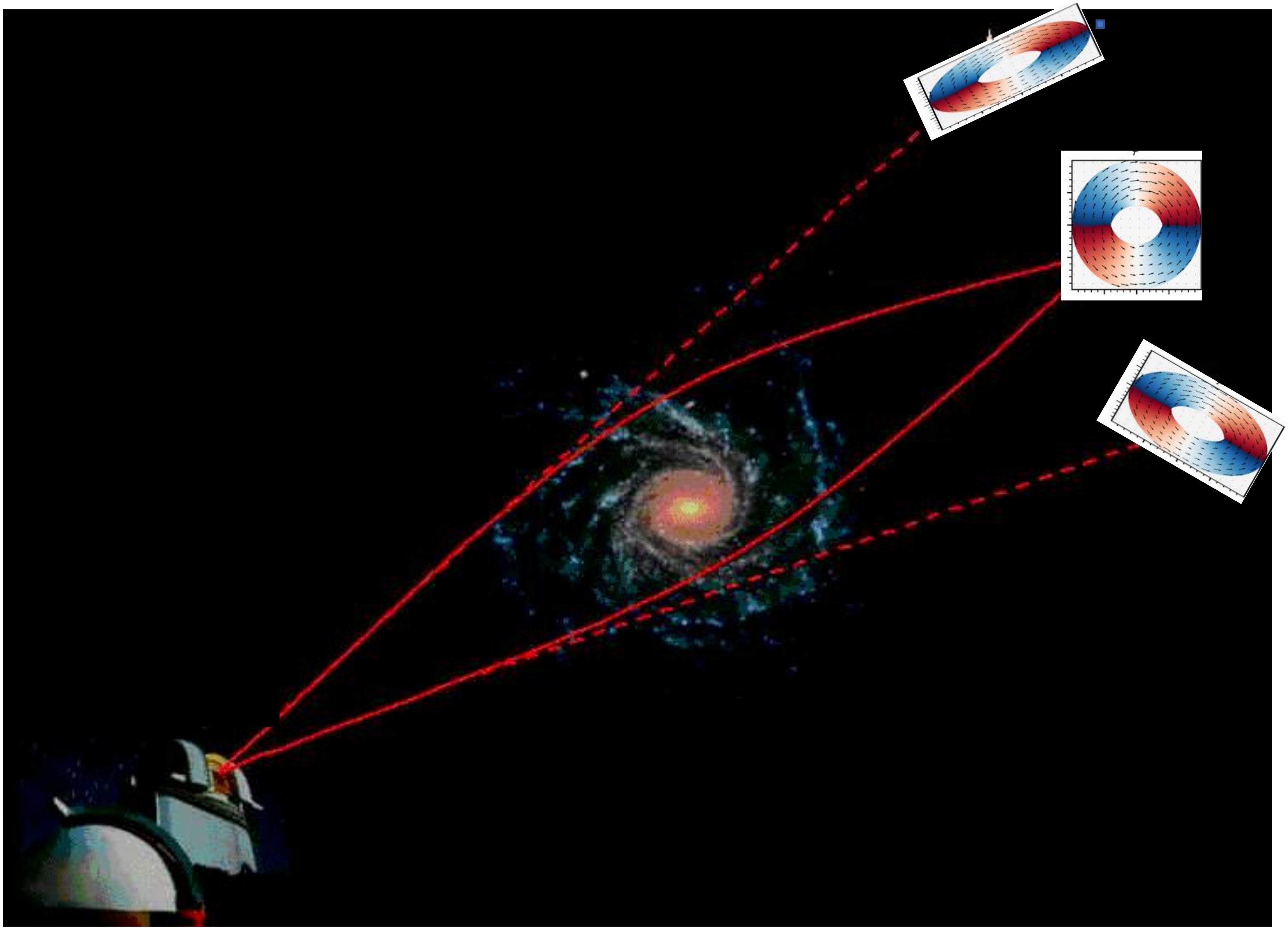

- Polarization – macrolensing => position on the UQ plane

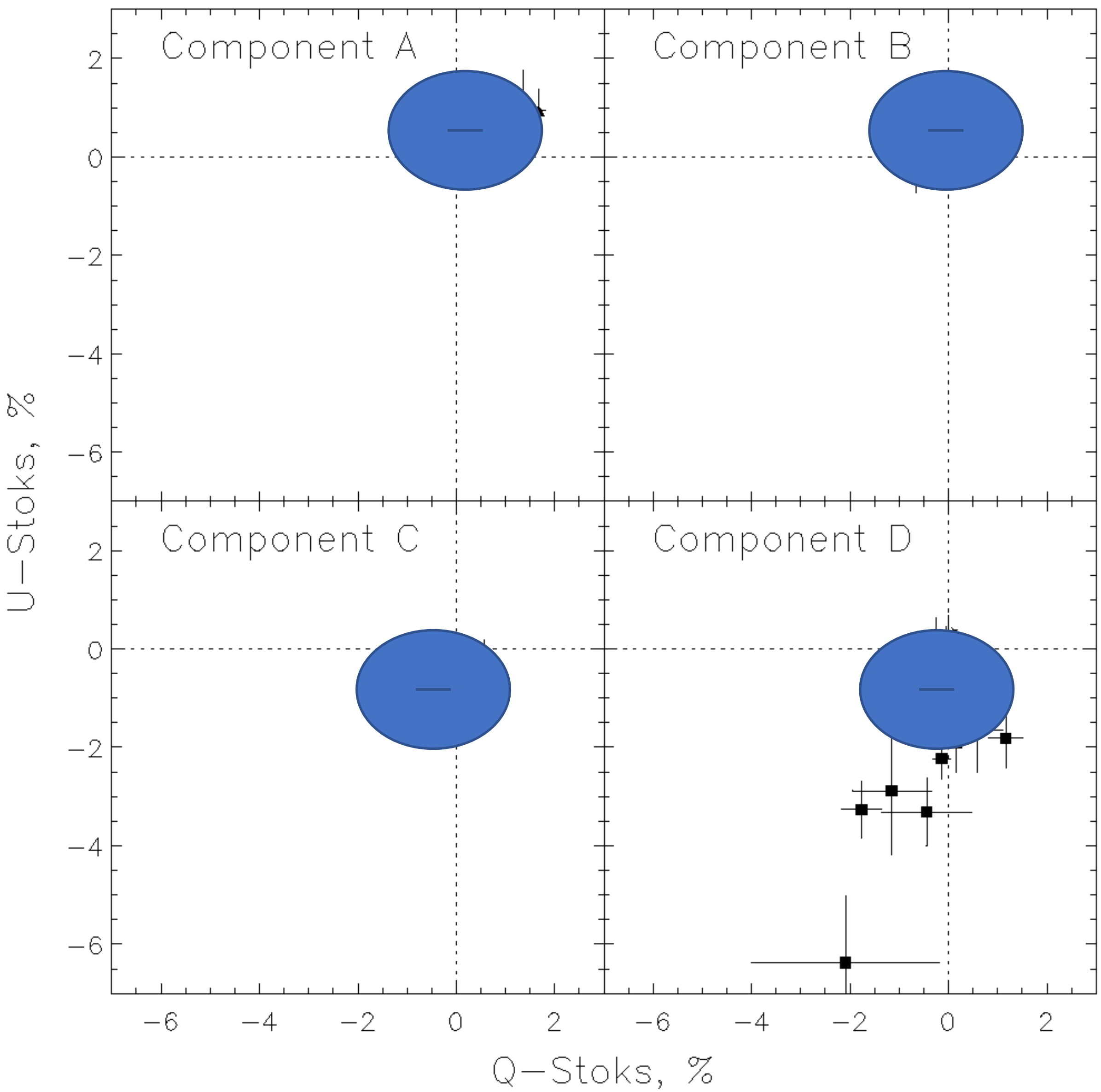

- Microlensing (maps)

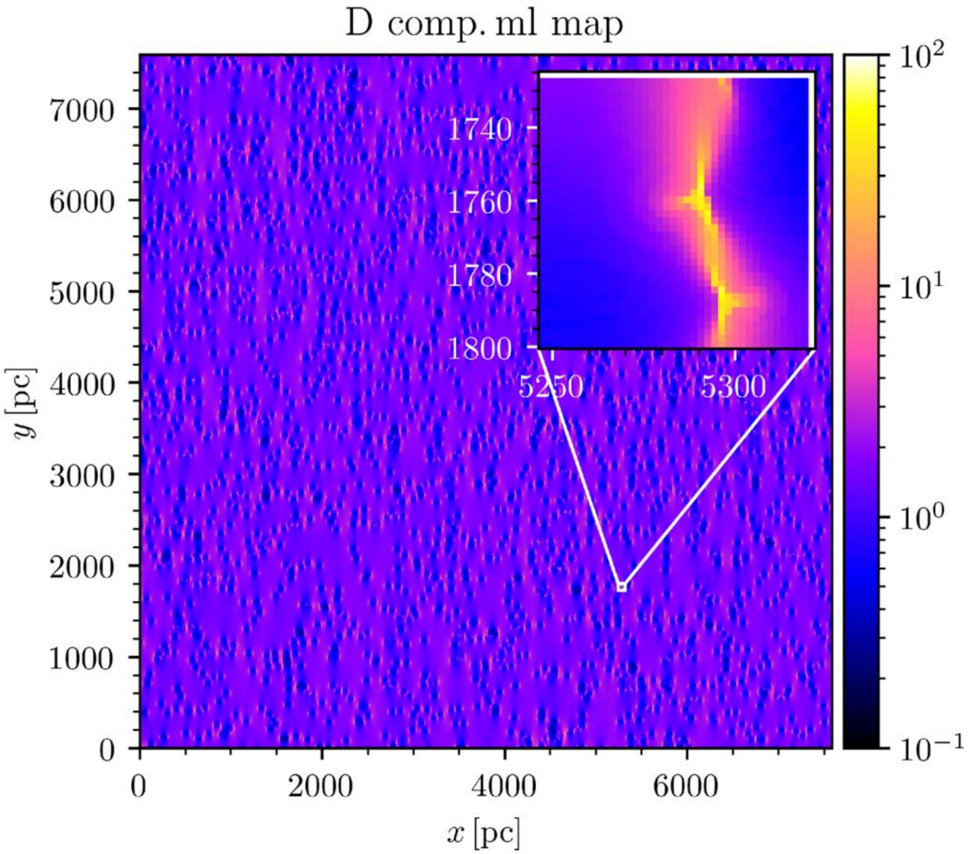

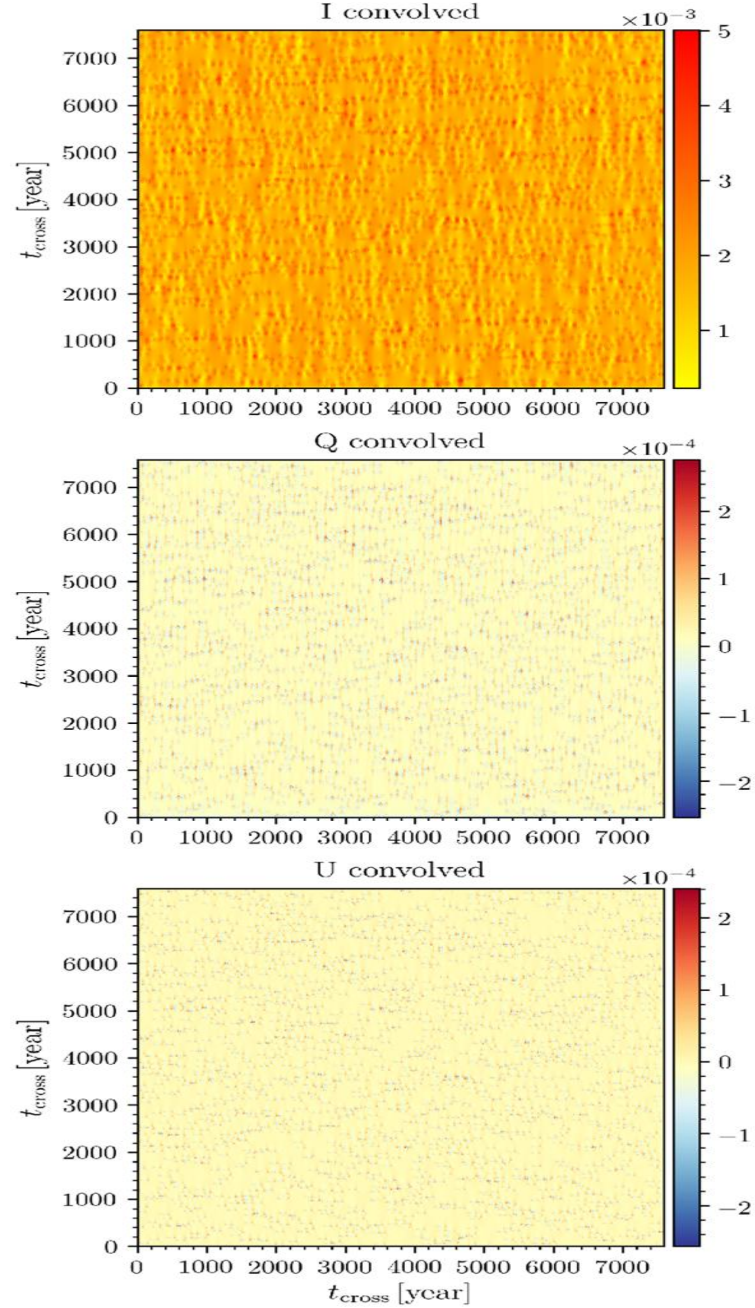

• Model – microlensing the inner part of the torus (dust sublimation region)

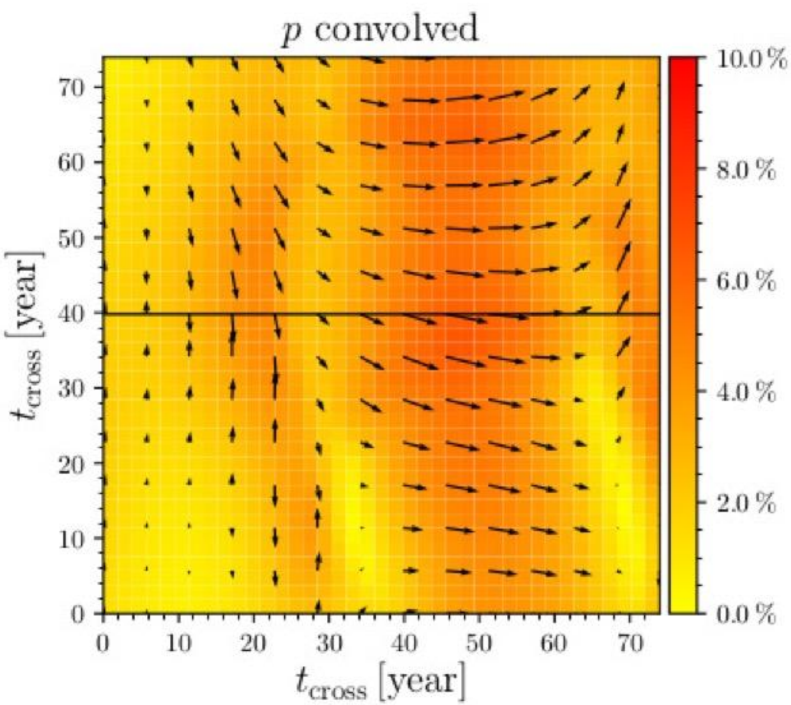

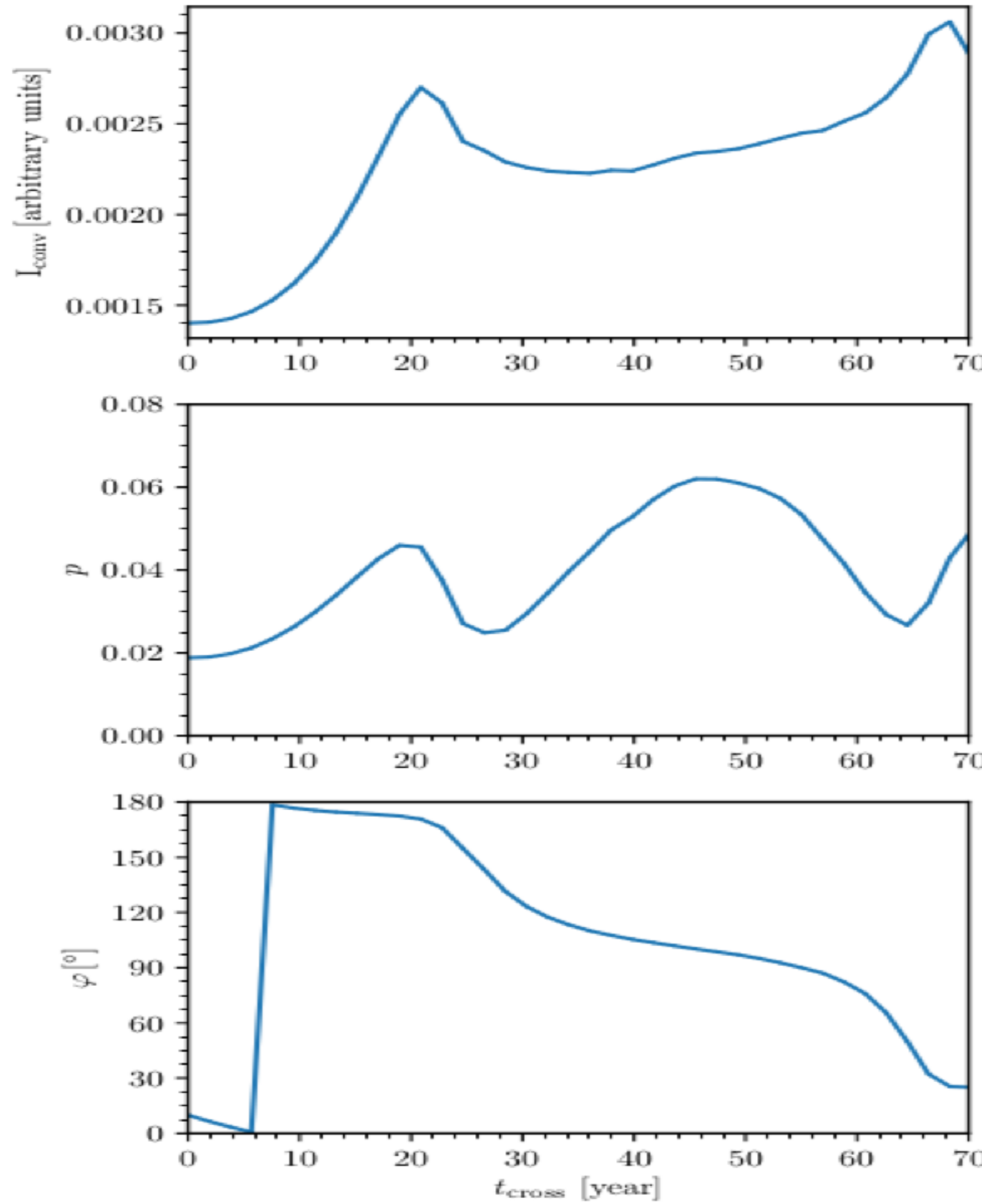

A&A 647, A98 (2021)
https://doi.org/10.1051/0004-6361/202039914

Astronomy & Astrophysics

Spectroscopy and polarimetry of the gravitationally lensed quasar Q0957+561

L. Č. Popović[1,2], V. L. Afanasiev[3,†], E. S. Shablovinskaya[3], V. I. Ardilanov[3], and Dj. Savić[1]

[1] Astronomical Observatory, Volgina 7, 11000 Belgrade, Serbia
e-mail: lpopovic@aob.rs
[2] Department of Astronomy, Faculty of Mathematics, University of Belgrade, Studentski trg 16, Belgrade 11000, Serbia
e-mail: lpopovic@matf.bg.ac.rs
[3] Special Astrophysical Observatory of the Russian AS, Nizhnij Arkhyz, Karachaevo-Cherkesia 369167, Russia
e-mail: vafan@sao.ru

Received 15 November 2020 / Accepted 18 January 2021

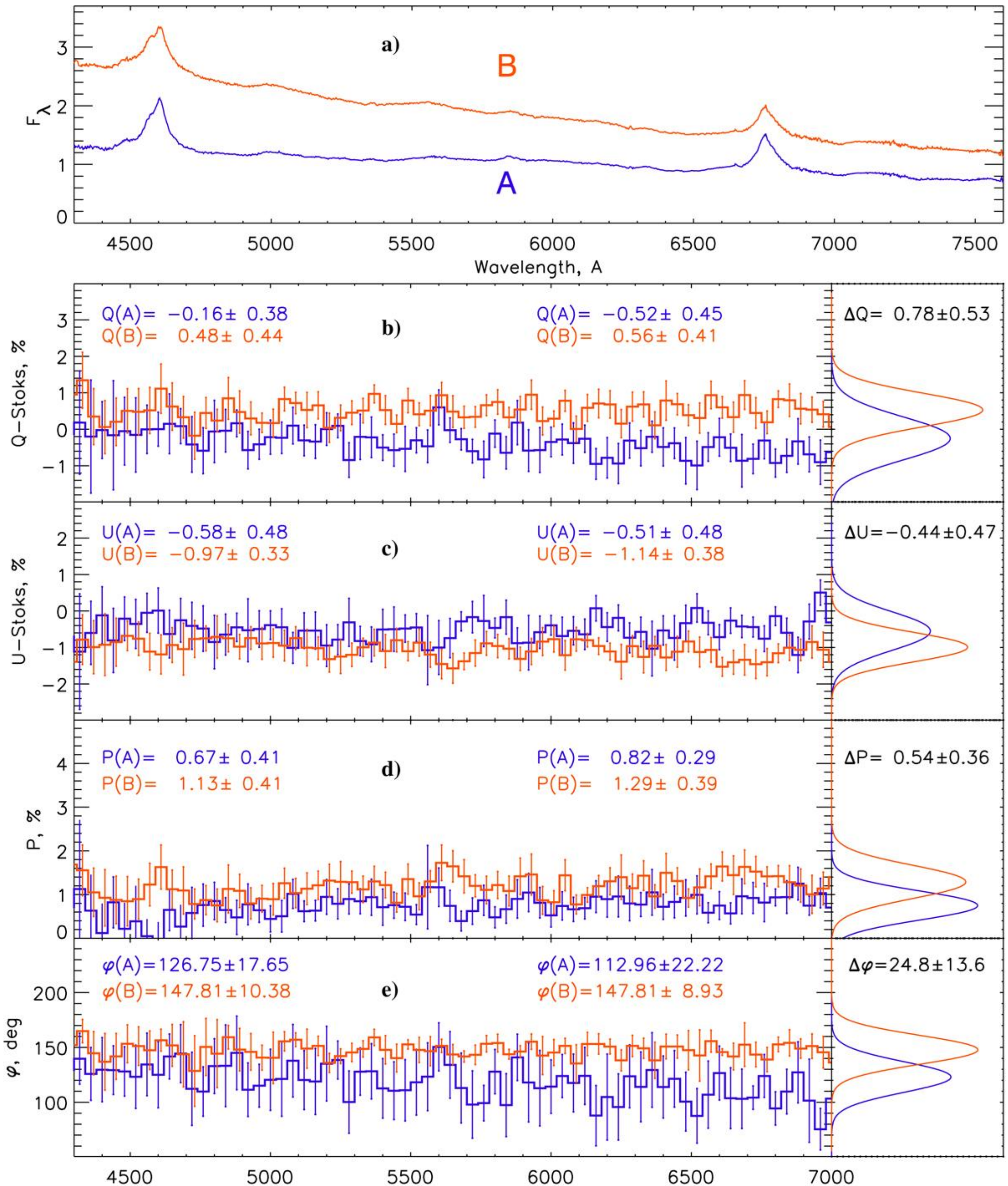

a)
B
A
F λ
Wavelength, A
b)
Q(A)= −0.16± 0.38
Q(B)= 0.48± 0.44
Q(A)= −0.52± 0.45
Q(B)= 0.56± 0.41
ΔQ= 0.78±0.53
Q−Stoks, %
c)
U(A)= −0.58± 0.48
U(B)= −0.97± 0.33
U(A)= −0.51± 0.48
U(B)= −1.14± 0.38
ΔU=−0.44±0.47
U−Stoks, %
d)
P(A)= 0.67± 0.41
P(B)= 1.13± 0.41
P(A)= 0.82± 0.29
P(B)= 1.29± 0.39
ΔP= 0.54±0.36
P, %
e)
φ(A)=126.75±17.65
φ(B)=147.81±10.38
φ(A)=112.96±22.22
φ(B)=147.81± 8.93
Δφ=24.8±13.6
φ, deg

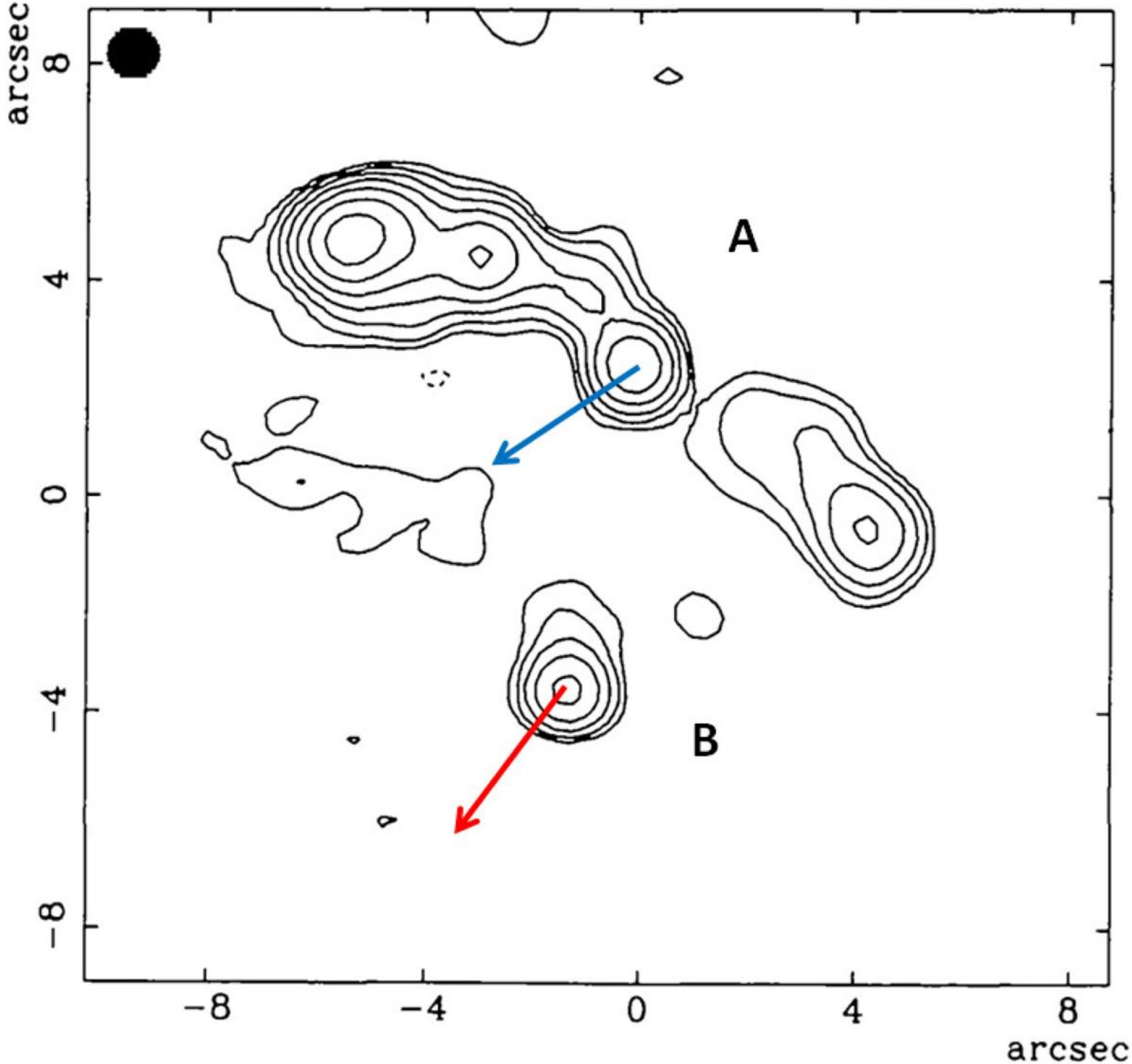

arcsec
8
4
0
−4
−8
A
B
−8
−4
0
4
8
arcsec

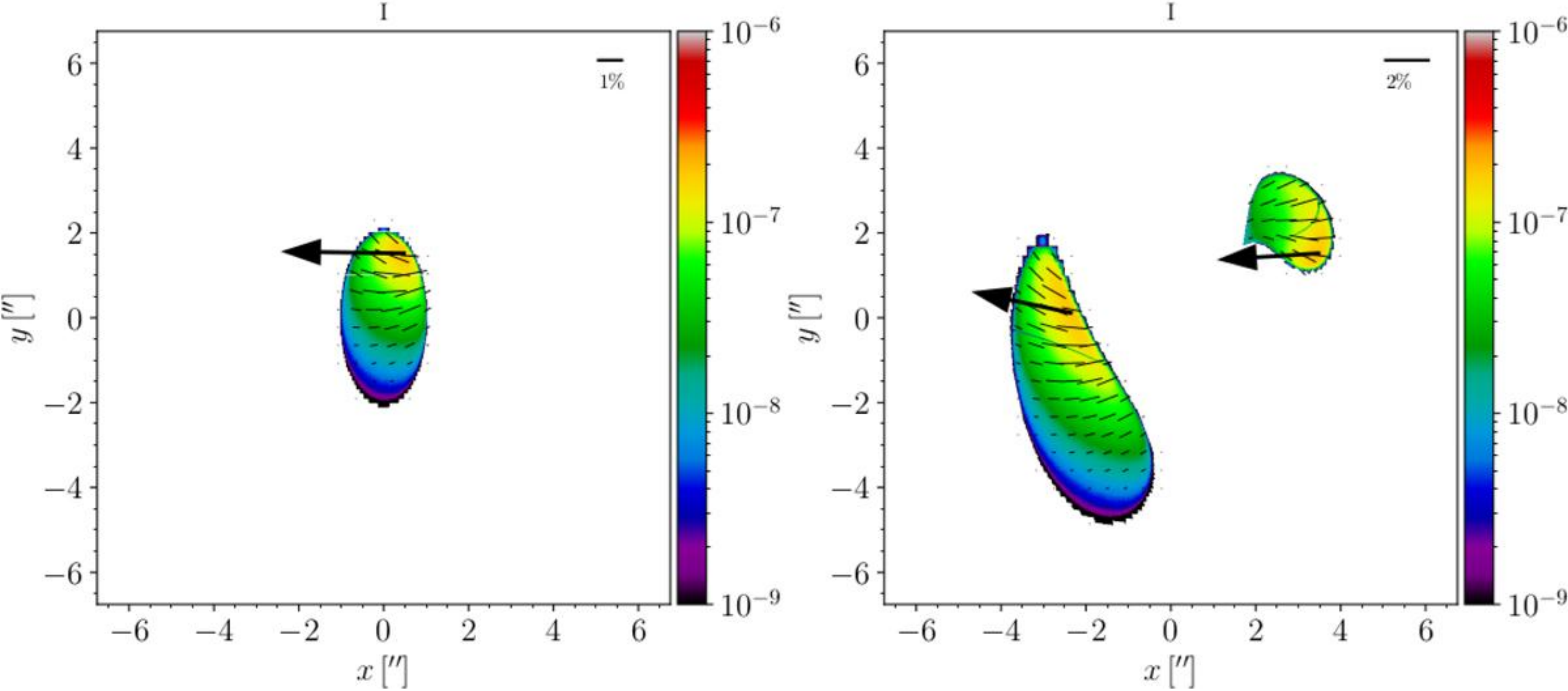
I
1%
10^{-6}
10^{-7}
10^{-8}
10^{-9}
y ['']
x ['']
I
2%
10^{-6}
10^{-7}
10^{-8}
10^{-9}
y ['']
x ['']

Conclusions

- Equatorial polarization in Type 1 AGNs seems to be dominant
- Keplerian motion in BLR is dominant, but outflows can affect PA shape, but it still be used for SMBH mass estimates
- Polarization of GL - new information abut GL effects
-

Thank you for your attention